

Tutor/s

Ricard Torres

*Department of Chemical
Engineering*



Master in Chemical Engineering

Final Master's Work

Design of a solar thermal installation for the production of domestic hot water.

Diseño de una instalación solar térmica para la producción de agua caliente sanitaria.

Roger Rovira Mora

September 2020



UNIVERSITAT DE
BARCELONA

Dos campus d'excel·lència internacional

B:KC Barcelona
Knowledge
Campus

HUB^c Health Universitat
de Barcelona
Campus

This work is subject to the license of Attribution-Non
Commercial-Without Derivative Works



<http://creativecommons.org/licenses/by-nc-nd/3.0/es/>

REPORT

Content

1. Summary.....	1
Resumen.....	2
2. Objectives	3
3. Introduction.....	3
3.1. Solar energy	3
3.2. Solar thermal energy in the world	4
3.3. Solar thermal applications	5
3.4. Parts of a solar thermal installation	6
3.4.1. Capturing system	6
3.4.2. Accumulation system.....	11
3.4.3. Exchange system	11
3.4.4. Distribution system.....	13
3.4.5. Support system	15
3.4.6. Control system.....	15
4. Initial data	16
4.1. Geographical data.....	16
4.2. Climatic data	16
4.3. Heat transfer fluid.....	20
5. Energy demand	21
5.1. Initial data	21
5.2. Calculation of DHW energy demand	24
6. Consumption mass flow rate.....	26
7. Minimum solar contribution.	27
8. Selection of the collector.	27
9. Calculation of the catchment area	28
9.1. Heuristic method	29
9.2. Thermal resistance and energy balance method.....	31
9.2.1. Loss-free DHW installations	31

9.2.2.	Installation of DHW with losses.....	36
9.2.3.	Calculation of the catchment area with losses.....	59
10.	Comparison of methods.....	62
11.	Lost due to shadows, orientation and inclination.....	63
12.	Sizing of the installation.....	68
12.1.	Dimensioning the support system	68
12.1.1.	Dimensioning of the DHW storage tank.....	68
12.1.2.	Dimensioning of the auxiliary boiler	72
12.2.	Dimensioning of pipes	73
12.2.1.	Method of sizing the pipes	73
12.2.2.	Sizing of pipes per circuit	75
12.3.	Dimensioning the pipe insulation.....	77
12.4.	Dimensioning of the solar storage tank	78
12.5.	Dimensioning of the plate heat exchanger	78
12.6.	Sizing of expansion vessels.....	82
12.7.	Dimensioning of the pumping system	87
13.	Environmental study	93
14.	Economic study.....	96
15.	Conclusions	102
16.	Appendixes	104
	Bibliography.....	128

Figure 1. Evolution of the worldwide operating capacity and energy efficiency of thermal installations.....	4
Figure 2. Comparison of the world's operating capacity and energy efficiency of the most used renewable energies.	5
Figure 3. Global solar thermal applications.	5
Figure 4. Parts of a conventional flat-plate thermal collector.	6
Figure 5. Operation of a solar thermal collector.....	7
Figure 6. Connection of thermal collectors in series.	8
Figure 7. Balancing with flow control valves.	9
Figure 8. Balancing with inverted return.	10
Figure 9. Mixed connection.	10
Figure 10. Stratification of an accumulator to obtain DHW.	11
Figure 11. On the right side, exchanger by coil. On the left is the double-shell exchanger.....	12
Figure 12. External plate heat exchanger.....	12
Figure 13. Circulation by thermo siphon effect.....	13
Figure 14. Components of a closed expansion vessel.....	14
Figure 15. Monthly solar intensity values (MJ/m ²).....	20
Figure 16. Freezing temperature of water as a function of propylene glycol concentration.....	20
Figure 17. Monthly DHW demand.....	25
Figure 18. Comparison of properties of commercially available thermal collectors.....	28
Figure 20. Monthly solar coverage as a function of demand and solar energy produced.....	31
Figure 21. DHW system on which the processes will be performed.....	33
Figure 22. Representation of the stratification temperatures in the solar accumulator.....	34
Figure 23. Diagram of thermal resistances in the upper part of the collector.	49
Figure 24. Diagram of the solar storage and heat losses.....	53
Figure 25. Piping diagram.....	57
Figure 26. Energy balance in collectors with wind losses.	59
Figure 27. Energy balance in the exchanger with system losses.....	59
Figure 28. Energy balance in the solar accumulator with losses in the system.....	60
Figure 29. Evolution of monthly system temperatures (°C).....	62
Figure 30. Monthly differences of the solar fraction of the methods used.....	63
Figure 31. Plan of the terrace. Representation of the elements of the primary circuit and engine room. Own elaboration.....	64
Figure 32. Azimuth angle and inclination of sensors.....	64
Figure 33. Percentage representation of slope and orientation losses of the collectors.	65
Figure 34. Distance between rows of sensors and nearby obstacles.....	65
Figure 35. Distance between rows of collectors and nearby obstacles taken at our facility. Own elaboration.....	66
Figure 36. Solar trajectory diagram.	67

Figure 37. Diagram of friction losses in copper pipe.....	74
Figure 38. Primary circuit diagram. Own elaboration.	75
Figure 39. Minimum insulation thicknesses for DHW pipes.	77
Figure 41. Graphical representation of the evolution of the accumulated cash flow.....	102
Figure 42. General diagram of the process. Own elaboration.	103

Table 1.Monthly average wind speed (m/s).	16
Table 2.Monthly average temperature of mains water in Barcelona (°C).	16
Table 3. Average monthly temperature of the mains water in the installation (°C).	17
Table 4.Monthly average temperature of the environment in the hours of sunshine in Barcelona (°C).	17
Table 5. Monthly average temperature of the environment in the hours of sunshine in the installation (°C). ...	17
Table 6.Daily Sun Hours (h)	17
Table 7.Monthly daily global irradiation on horizontal surface (MJ/m2).	17
Table 8.k-values for latitude 41	18
Table 9.k-values for latitude 42.....	18
Table 10.Corrected k-values (latitude 41.4).	18
Table 11.Overall useful radiation on inclined surface (MJ/m2).	19
Table 12.Daily solar intensity (W/m2).	19
Table 13. Properties of the heat transfer fluid at a reference temperature of 35°C.....	21
Table 15.Number of people according to the number of bedrooms.	22
Table 16.Number of people in the building.	22
Table 17.Centralisation factor according to the number of dwellings.	23
Table 18.Corrected monthly consumption (L/month).	24
Table 19.Monthly DHW demand (MJ).	25
Table 20.Monthly consumption mass flow rate (Kg/s).	26
Table 21.Energy collected in the collectors (MJ/m2).	29
Table 22.Calculation of the necessary collection area and solar fractions obtained.	30
Table 23.Calculation of the necessary catchment area in the system without losses.	35
Table 24.Results of simulation of the system of equations without losses in the system.	36
Table 25.Monthly convection resistances at the back of the manifold (K/W).	39
Table 26. Monthly convection resistances at the top of the manifold (K/W).	41
Table 27.Monthly sky temperatures (°K).	42
Table 28.Radiation resistance between the deck and the sky (K/W).	43
Table 29.Radiation resistance between inner cover and plate (K/W).	44
Table 30.Natural convection resistance inside the collector (K/W).	45
Table 31.Heat loss from the bottom of the collector (W).	48
Table 32. Heat loss from the top of the collector (W).	49
Table 33. Heat loss from the side of the collector (W).	50
Table 34.Average monthly water temperature inside the collector (°C).....	50
Table 35. Heat losses yielded to heat transfer fluid (W).	51
Table 36.Summary of useful heat and losses of the collector according to the manufacturer's curve.....	51
Table 37. Summary of useful heat and losses of the collector by thermal resistances.	52
Table 38. Comparison of results obtained with thermal resistance and curvature of the manufacturer.	52

Table 39. Air properties inside the engine room.	54
Table 40. Monthly convection resistance in the engine room (K/W)	55
Table 41. Monthly heat loss from solar storage tank(W).....	56
Table 42. Annual system simulation results with losses for 11 collectors.....	61
Table 43. Annual system simulation results with losses for 12 collectors.....	61
Table 44. Monthly system simulation results with losses for 12 collectors.....	61
Table 45. Comparison of results of the methods of calculation of the catchment area and annual solar fraction.	63
Table 46. Maximum allowable losses.....	63
Table 48. Azimuth and elevation angle of the right building to the nearest collector array	66
Table 49. Percentage of losses for each quadrant of the solar diagram.	67
Table 50. Instantaneous flow rates of consumer appliances (dm ³ /s).	68
Table 51. Instantaneous flow of type A housing.	69
Table 52. Instantaneous flow type B homes.....	69
Table 53. Internal and external diameters of copper pipes.....	73
Table 54. Dimensioning of the primary circuit pipes.	75
Table 64. Liquid volume inside primary circuit pipes.	83
Table 65. Volume of water within the secondary circuit pipes.	85
Table 66. Volume of water inside the support circuit pipes.....	85
Table 67. Volume of water inside return circuit pipes.....	86
Table 68. Pressure losses of the primary circuit pipes in each section.	88
Table 69. Coefficients for the calculation of the friction factor.	89
Table 70. K-factor of the accessories present in the circuits.	90
Table 71. Accessory pressure losses in each section.	90
Table 72. Monthly fuel savings (m ³).....	94
Table 73. Molar composition of natural gas (%).	95
Table 74. Monthly carbon dioxide savings (m ³).....	95
Table 75. Material costs of the primary circuit.	96
Table 76. Secondary circuit material costs.....	97
Table 77. Material costs of the support circuit.	97
Table 78. Material costs of the recirculation circuit.	98
Table 79. Control system costs and accessories.	98
Table 80. Natural gas tariffs according to consumption rate.....	99
Table 81. Evolution of cash flow during the useful period of the installation.	101

1. Summary

In this project, the design of a solar thermal installation for the production of domestic hot water (DHW) for a building in Barcelona has been carried out. Firstly, the energy consumption of the building was determined from statistical data provided by the CTE and meteorological data. Subsequently, the collector model has been selected according to its performance characteristics, area and price. The necessary capture area has been calculated to cover the minimum fraction of demand stipulated by the current law by different methods, heuristics and energy balances of the elements of the installation. The energy balances have been made taking into account the heat losses of different elements of the installation determined from the thermal resistances of the selected equipment, as well as convection losses due to the action of the wind. This has meant an iterative calculation, as it was necessary to know beforehand the appropriate dimensioning of the pipes, including insulation, together with the meters of pipe and the layout of the collectors. The collectors have been arranged on the terrace facing south with a 40 degree slope, and properly separated from the surrounding obstacles to minimize losses due to shading. The final result of the collector system has been represented in a plan for easy understanding.

Once the catchment area has been determined, the rest of the elements are sized. The support equipment has been sized based on consumption data of the different elements of the houses applying a simultaneity factor, considering a zero solar contribution of the collectors. The design of the heat exchanger was carried out by determining the useful area of exchange and the overall heat transfer coefficient, considering a counter-current exchange. A return network has been designed for the points of consumption furthest away from the DHW storage tank, based on a partial recirculation of the building's consumption. An exhaustive study has been carried out on the load losses of the elements including the necessary accessories (elbows, valves) in order to size the pumping equipment for each circuit. Once the size of all the elements was known, it was possible to determine the amount of fluid that could be found in each circuit, allowing the sizing of the expansion vessels.

With all the elements already designed, an environmental study has been carried out to find out the amount of fuel (natural gas) saved and the CO₂ emissions avoided. With the data of fuel savings and the costs of the materials of the installation, the economic viability study of the project is carried out for a useful period of 25 years, with the help of a subsidy from the Barcelona City Council.

Resumen

En este proyecto se ha realizado el diseño de una instalación solar térmica para la producción de agua caliente sanitaria (DHW) para un edificio de Barcelona. En primer lugar se ha determinado el consumo energético del edificio a partir de datos estadísticos proporcionados por el CTE y datos meteorológicos. Posteriormente se ha seleccionado el modelo del captador en función de sus características de rendimiento, área y precio. Se ha realizado el cálculo del área de captación necesaria para cubrir la fracción mínima de demanda que estipula la ley actual por diferentes métodos, heurísticos y balances de energía de los elementos de la instalación. Los balances de energía se han realizado teniendo en cuenta las pérdidas de calor de distintos elementos de la instalación determinados a partir de las resistencias térmicas de los equipos seleccionados, así como pérdidas de convección por la acción del viento. Esto ha supuesto un cálculo iterativo, pues era necesario conocer con anterioridad el dimensionado adecuado de las tuberías, incluido aislante, junto los metros de tubería y disposición de los captadores. Los captadores se han dispuesto en la terraza orientados al sur con un ángulo de inclinación de 40 grados, y separados apropiadamente de los obstáculos circundantes para minimizar pérdidas por sombras. El resultado final del sistema de captación ha sido representado en un plano para facilitar su comprensión.

Una vez determinada el área de captación, se dimensiona el resto de elementos. El equipo de apoyo se ha dimensionado a partir de datos de consumo de los distintos elementos de las viviendas aplicando un factor de simultaneidad, considerando un aporte solar de los captadores nulo. El diseño del intercambiador de calor se lo realizado determinando el área útil de intercambio y el coeficiente global de transferencia de calor, considerando un intercambio contracorriente. Se ha diseñado una red de retorno para los puntos de consumo más lejanos de 15 del acumulador de DHW, a partir de una recirculación parcial del consumo del edificio. Se ha realizado un estudio exhaustivo de las pérdidas de carga de los elementos incluido accesorios necesarios (codos, válvulas) para dimensionar los equipos de bombeo de cada circuito. Conocido el tamaño de todos los elementos, se ha podido determinar la cantidad de fluido posible que se puede hallar en cada circuito, permitiendo el dimensionado de los vasos de expansión.

Con todos los elementos ya diseñados, se ha realizado un estudio ambiental para saber la cantidad de combustible (gas natural) ahorrado y las emisiones de CO₂ evitadas. Con los datos de ahorro de combustible y los costes de los materiales de la instalación, se realiza el estudio de viabilidad económica del proyecto para un periodo útil de 25 años, con la ayuda de una subvención del ayuntamiento de Barcelona.

2. Objectives

- Design of a solar thermal installation for the production of domestic hot water (DHW). All the decisions and calculations of the project are subject to the restrictions of the regulations in force.
- Carrying out an environmental study to determine the impact of this type of installation.
- Carrying out an economic study to determine the viability of the project.

3. Introduction

The exponential growth of the world's population has led to excessive energy consumption that has so far been covered by the use of fossil fuels, which, at the beginning of their exploitation, were considered inexhaustible. However, nowadays the situation has changed radically, and we find ourselves at a critical moment where we are aware of the worldwide shortage and environmental alterations of these. As a consequence of their scarcity, the price of fossil fuels has been progressively increasing and we have been forced to develop new energy sources to reduce the current energy dependence. These new methods are renewable energies, the energy of the future. Although there are many energy alternatives, some of them have not yet been sufficiently used, either due to technical or economic limitations, and others have hardly been developed or have only been partially developed. In recent years there has been a significant increase in the use of renewable energies, specifically solar energy. Their easy access and commitment to the environment has led to a large number of solar installations. It is estimated that one third of energy consumption in Europe is used for domestic hot water (DHW) and heating of buildings. Solar thermal technology is intended to cover this demand.

3.1. Solar energy

Most of the energy that reaches our planet comes from the Sun, in the form of electromagnetic radiation. It is the largest energy source on Earth and is considered inexhaustible. The solar radiation incident on the Earth can be used by different technologies for functions such as heating water and generating electricity for consumption. The heat is achieved by means of thermal collectors, and the electricity, by means of the so-called photovoltaic modules. Both processes have nothing to do with each other, neither in terms of technology nor in their application. The advantages of solar energy are numerous compared to conventional energy sources. It is the most environmentally friendly form of energy and, as it is inexhaustible, it reduces energy dependency on fossil fuels and pollutants. Solar installations are silent, clean and have a long life span (between 20 and 30 years). (Landa, 2005) However, it has several

restrictions. The power of the radiation varies according to the time of day, the year, atmospheric conditions and latitude of the place. For example, solar radiation is lower in winter, when it is more necessary. So it has to be taken into account that this energy is subject to permanent fluctuations. In addition, it requires large investment facilities and land where many people are not willing to invest. In order to promote this type of technology, subsidies are currently being offered to encourage them. (Energy Factor)

3.2. Solar thermal energy in the world

At the end of 2018, the operating capacity was 480 GWth (686 million m²), and the global solar thermal energy yields of all solar thermal systems installed in 2018 were 396TWh, representing a saving of 42.6 thousand tons of oil and 137.5 thousand tons of CO₂ as shown in Figure 1. This shows the important contribution of this technology to the effort to reduce global greenhouse gas emissions and to reduce dependence on fossil fuels.

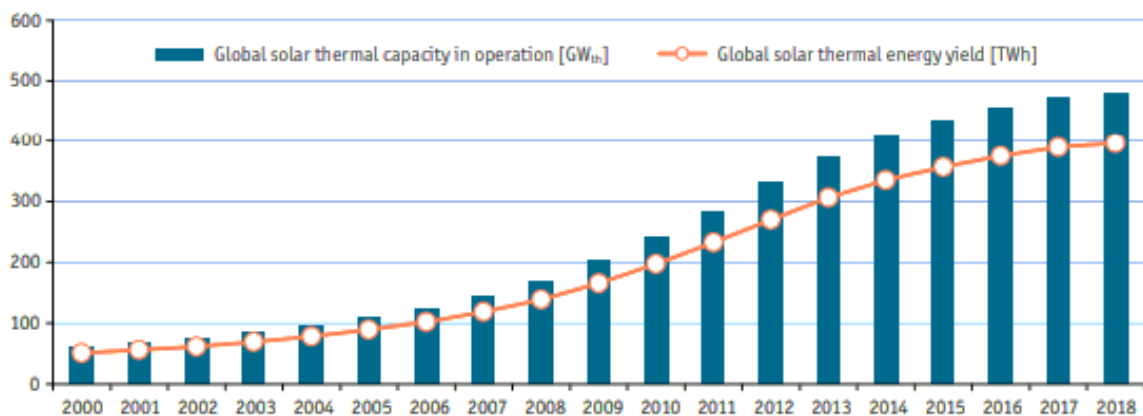


Figure 1. Evolution of the worldwide operating capacity and energy efficiency of thermal installations.

Compared to other forms of renewable energy, the contribution of solar thermal energy to meeting global energy demand is now, in addition to traditional renewable energies such as biomass and hydropower, third behind wind and photovoltaic energy, as shown in Figure 2.

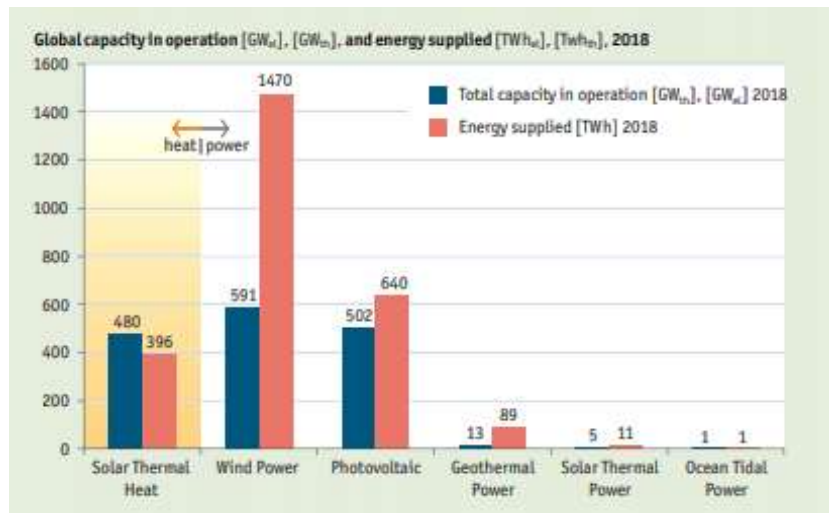


Figure 2 Comparison of the world's operating capacity and energy efficiency of the most used renewable energies.

3.3. Solar thermal applications

A solar thermal system is any installation designed to convert solar radiation into useful heat for use. By the end of 2017, 675 million m² of solar thermal collectors were in operation worldwide. As shown in figure 3, 6% were used for heating swimming pools, 63% were used for domestic hot water preparation in single-family houses and 28% were connected to larger domestic hot water systems for multi-family houses (houses, hotels, hospitals, schools, etc...). About 2% of the world's installed capacity provided heat for domestic hot water and space heating (solar combined systems). The remaining systems accounted for about 1% and supplied heat to other applications such as district heating networks, industrial processes or technically driven solar cooling applications. (Weiss, 2019)

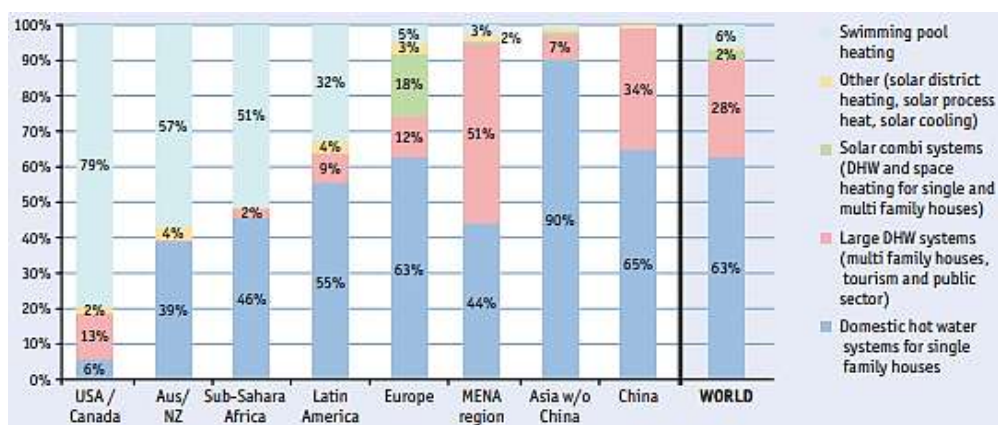


Figure 3 Global solar thermal applications.

3.4. Parts of a solar thermal installation

The components of the system are the same in practically all applications, varying their arrangement and the way they are regulated. The systems that make up a solar thermal hot water installation are the following:

3.4.1. Capturing system

It is the part of the installation in charge of capturing the energy coming from the Sun and transmitting it to the heat-carrying fluid. The most commonly used for the production of low temperature hot water is the flat plate collector with cover, as it has the best performance/price ratio for low temperature systems not exceeding 90°C. For this reason it is the type of collector selected for our project. Figure 4 (Hamzat, 2020) shows the main elements of a typical solar collector.

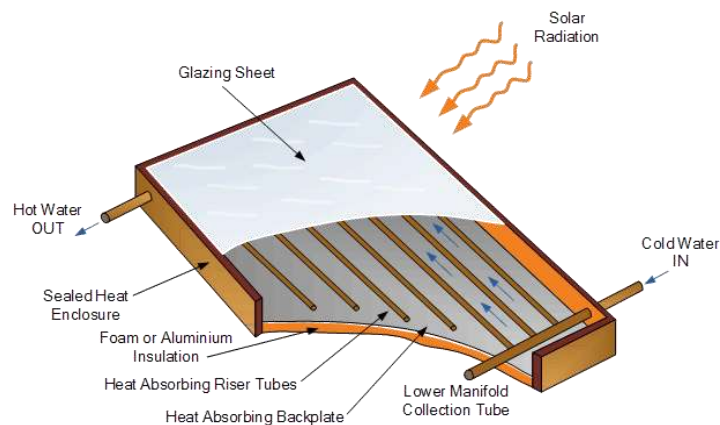


Figure 4 Parts of a conventional flat-plate thermal collector.

- Transparent cover:

Transparent flat element that protects the internal components from external factors. Reduces radiation and convection losses from the collector. Glass covers are often used, as the material resists thermal degradation better than plastics. To absorb the thermal expansion of the components and prevent the entry of water, elastic joints are used between the cover and the housing.

- Absorbent plate:

Its function is to absorb solar radiation, transform it into heat and transmit it to the working fluid circulating in the adjacent pipes. To maximize its function, good thermal contact between the flat part of the absorber and the pipes is essential to facilitate heat transfer by conduction. The material usually used for the absorber is copper. Copper is also the most commonly used material for pipes due to its good thermal conductivity and corrosion resistance.

- Isolation:

Its function is to reduce heat losses by conduction to the outside, for this purpose the insulating material is placed at the back and sides of the collector, since they are the only opaque parts of the collector and through which the solar radiation does not need to enter. The insulating material must have low thermal conductivity as is logical, and must also maintain its properties unaltered and not degrade with heat. The most commonly used material today is usually polystyrene foam, polyurethane or fiberglass.

- Housing:

It is the element that contains the other components that make up the collector, protects them from the weather and gives rigidity to the whole. Normally they include a frame that makes it possible to anchor them to the supporting structure to give the collector the necessary inclination and orientation.

Operation of a typical flat-plate solar collector

Figure 5 (Simon, 2015) shows the operating diagram of a typical flat panel collector. From the solar radiation incident to the collector a part is reflected, another small percentage is absorbed by the roof and a great part crosses it and affects the absorber, which transforms it into heat increasing its temperature. The absorber, when heated, emits radiation at a long wavelength, which cannot go outside because the roof is opaque to this radiation. Incorporated or attached to the absorber is a hydraulic circuit through which the heat-bearing fluid circulates and is heated by the transfer of heat by conduction, a phenomenon that takes place between the absorber and the fluid circuit. The increase in the temperature of the working fluid is the useful effect to be achieved, which in turn lowers the temperature of the absorber, the product of this heat transformation process. Since the absorber, when heated, also loses heat to the surrounding environment, and since the aim of the collector is for the heat to be extracted only by the heat-bearing fluid, protective measures are available to reduce thermal losses due to radiation, convection and conduction. (Development of thermal and fluid installation projects, 2017)

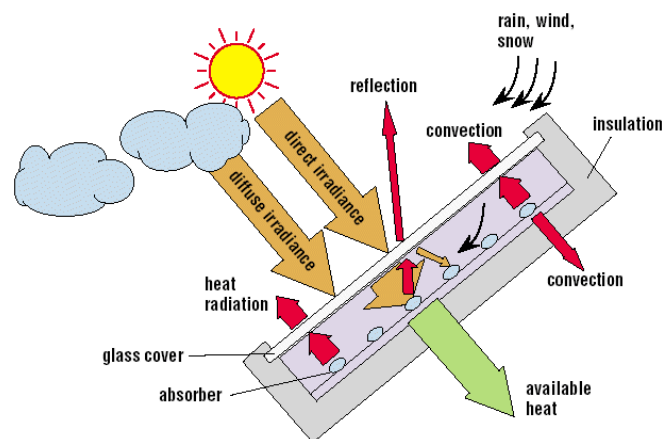


Figure 5 Operation of a solar thermal collector.

Types of collectors

There are many types of collectors on the market today. One way to classify them is by the following criterion:

- Depending on the number of covers: One or several covers, or no cover.
- Depending on the material of the cover: glass or plastic.
- Depending on the material of the absorbing surface: Copper, steel, aluminum or rubber.
- Depending on the type of heat transfer fluid: water or air collectors.
- Depending on the configuration of the absorbing surface: Plates, grill or coil.
- Depending on the working pressure: with vacuum tube, with vacuum tube with heat pipes for phase changes, without vacuum.

Connection of the collection system

Solar thermal systems are usually composed of several collectors. Therefore, when defining and installing a solar thermal system, it must be taken into account that the solar collectors must be distributed in groups. These groups of solar thermal collectors should always be formed by units of the same model and with a distribution as uniform as possible. There are several connection configurations:

- In series: The output of the first solar collector is directly connected to the input of the next one, and so on. The temperature of the input fluid to each collector is higher than that of the previous one, so that at the output of a group of collectors we obtain higher temperatures than when working with the thermal jump of a single collector. This type of connection has the disadvantage that the performance of the collectors decreases proportionally with the increase of the working temperature, and it is not recommended to work with more than three collectors as shown in figure 6.

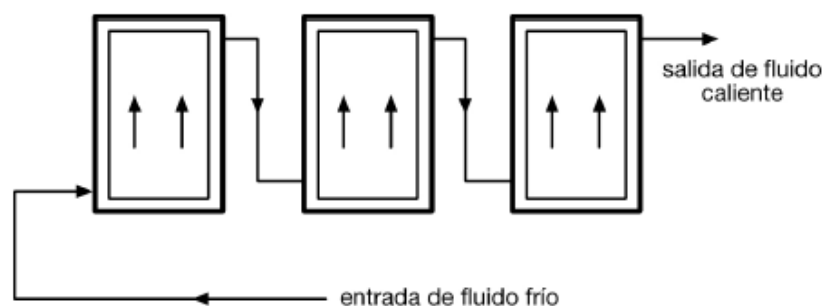


Figure 6 Connection of thermal collectors in series.

The total flow of the group of solar panels will be equivalent to the flow of a single panel, so this type of connection works in lower flows than in parallel, resulting in narrower pipes and shorter paths (lower installation cost and performance). On the other hand, the pressure loss caused by the group will be the equivalent to the sum of the pressure loss of all the solar collectors.

- In parallel: Both the output and the input of the sensors are connected to common input and output points. With this configuration, the temperature of the input fluid is the same in all the collectors and the same happens with the output temperatures, working with the thermal jump of only one collector (this is fulfilled as long as the flow and radiation of each collector is the same). Therefore, all the collectors work in the same point of the performance curve. The total flow of the group of collectors, which is equivalent to the sum of the partial flows of each collector, while the pressure drop of the group is equivalent to that of a single collector. Operating with this type of connection, it is possible to work with high flow rates with a good performance, but requires greater pipe lengths and diameters, and lower temperatures are reached than operating in series due to greater thermal losses. In the parallel connection, the design precaution is that the same flow rate circulates through each coil. Two procedures can be used for this: balancing with valves or with reverse return.

- Balancing with regulation valves:

The different batteries are connected regardless of whether the paths of the different flows are uneven. Naturally, if nothing else is done in the design, certain routes are preferred and others are penalized, and the distribution of flows is totally uncontrolled. In this configuration, it is necessary to use hydraulic balancing valves as shown in Figure 7 (Mechanical engineering), so that they produce an additional pressure drop in the loops that require it to adjust the flow rate in all of them. The advantage of the procedure is that, by reducing the length of the pipes, thermal losses in the circuit are also reduced.

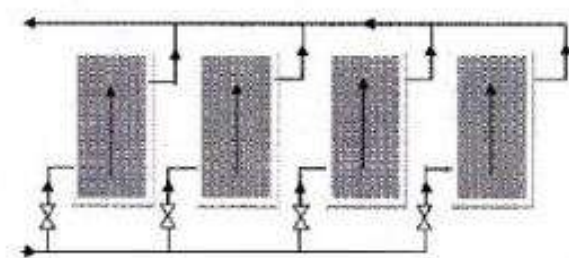


Figure 7 Balancing with flow control valves.

- Inverted and balanced return:

It consists of using an additional pipe in the common supply so that the paths and flows of all the batteries are equalized in the connection, as shown in figure 8 (provided that the same number of accessories is present in each loop). The longer the pipe, the greater the head loss.

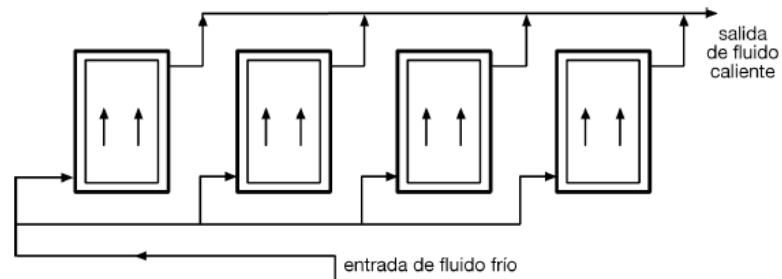


Figure 8 Balancing with inverted return.

- Mixed connection: It is used in installations with a very large catchment area and where the additional temperature requirements are high, as it reduces the diameter of the pipes to be installed, thus reducing their cost (Figure 9).

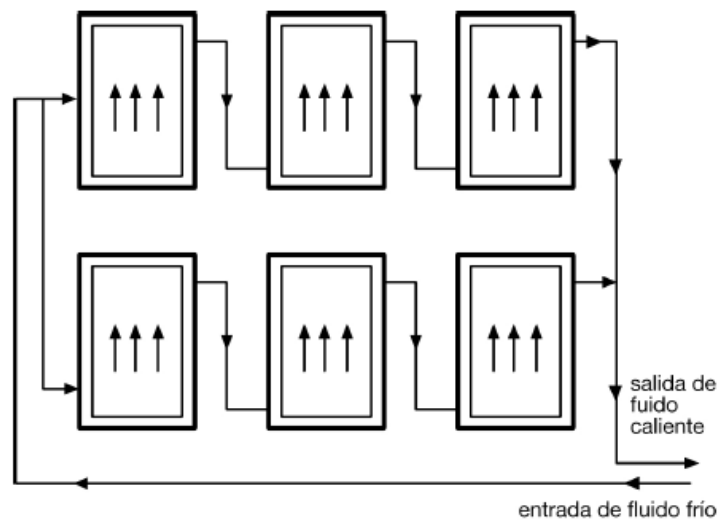


Figure 9 Mixed connection.

In this project, a connection will be made between collector batteries and collectors in total parallel, and the regulation of the hydraulic circuit will be done by means of flow regulating valves. (Ceen, 2018)

3.4.2. Accumulation system

The need for energy does not always coincide in time with the collection obtained from the sun, requiring a system of accumulation of the energy generated to meet the demand at times of little or no solar radiation, as well as solar production at times of little or no consumption.

Its shape is usually cylindrical due to its ease of construction. The height must be greater than the diameter as this favors the phenomenon of stratification; the hot water has a lower density than the cold water, which is stored in the upper part of the tank, where the water for consumption is extracted without the need for the whole tank to be at working temperature. Meanwhile, the water that goes to the collectors is extracted from the lower part where the cold water is, making the collectors work at the lowest possible temperature, which contributes to an improvement in the performance of the collection system. The greater the height of the tank, the greater the temperature difference. For this reason it is advisable to install these tanks vertically, although sometimes, due to space issues, we must place them horizontally, reducing stratification and the performance of the installation. The operating diagram is shown in figure 10.

For this project we will have two vertical accumulation tanks, one located in the secondary circuit where the energy coming from the collection system will be stored (solar accumulator) and a support accumulator where the water will be heated to the desired consumption temperature with the operation of the boiler (DHW accumulator).

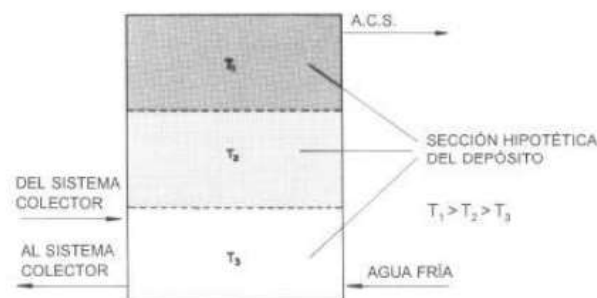


Figure 10 Stratification of an accumulator to obtain DHW.

3.4.3. Exchange system

The use of heat exchangers is intended to transfer the energy from the collectors to the solar storage tank. This exchanger can be located inside the tank, by means of a coil, or it can be external. The heat exchanger is a necessary element when you want to avoid mixing the heating fluid with the DHW consumption fluid. This happens when the heat transfer fluid circulating in

the collectors is a mixture of water and antifreeze, in order to avoid possible frosting of the working fluid. The heat exchangers in a DHW system can be classified as follows:

- For the position:
 - Inside.
 - Outside.
- For its construction.

-Plate: The most used for this type of installation. They have the advantage that once installed the number of plates can be varied, correcting possible dimensioning errors (see figure 12) (Marine Engineering).

-Double-wrapped: The primary circuit envelops the secondary circuit and the exchange takes place through the surface in contact with the accumulated fluid (see figure 11) (Arnabat, 2020).

-Coil: Located in the lower part of the accumulator. It has the advantage that only one pump is required to circulate the heat transfer fluid to the accumulator, while external exchange systems require two pumps (see Figure 11) (Arnabat, 2020).

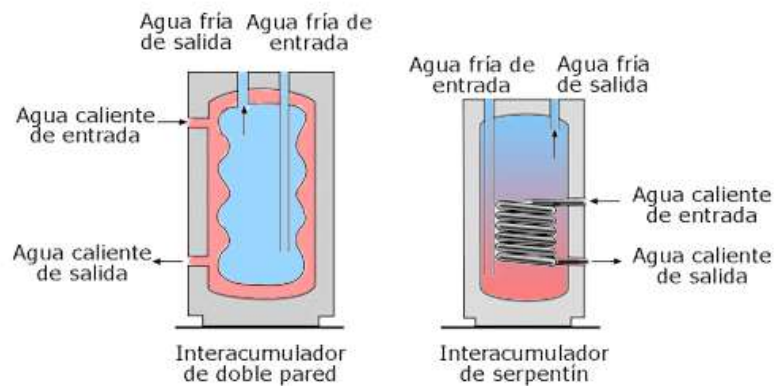


Figure 11 On the right side, exchanger by coil. On the left is the double-shell exchanger.

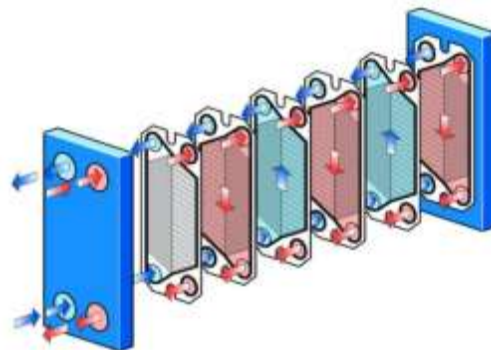


Figure 12 External plate heat exchanger.

The exchanger used for this project will be the external plate exchanger, as it is the most used for this type of installation. It has a higher performance than the coil exchangers, although it has a higher pressure loss in the circuit and a higher cost.

3.4.4. Distribution system

Hydraulic system configured for the correct displacement of the fluid. It consists of the network of pipes and corresponding accessories (valves, fittings, etc...). With respect to the type of circulation the difference is given by the principle that produces the movement of the fluid:

- Installations with thermo siphon circulation: In the collector, the heat-carrying fluid inlet is in the lower part. As it heats up, its temperature increases and its density decreases, so it tends to rise and exit through the upper part of the collector to the coil located in the tank, where it gives up its heat to the water contained in the tank. When the temperature of the fluid decreases, its density increases and tends to go down, closing the circuit. The operating diagram can be seen in figure 13 (GasColdHeat, 2015).

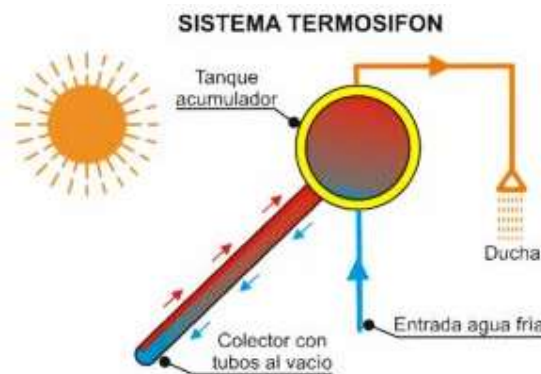


Figure 13. Circulation by thermo siphon effect.

- Forced installations: The action of a pump produces the circulation of the fluid. The movement of the fluid from the collection system to the accumulator in our case will require the use of two pumps, one in our primary circuit (from the collection system to the external exchanger) and the other in the secondary circuit (from the external exchanger to the solar accumulator). Forced circulation systems are more expensive, but produce more hot water than natural circulation systems. The design power of the pump will depend on the flow rate and the pressure losses to be overcome. (Development of thermal and fluid installation projects, 2017)

Distribution system accessories

- Expansion vessel: Safety element designed to absorb volume changes due to thermal expansion of the fluids when heated, thus preventing possible leaks through the safety valve. When the fluid in a circuit is heated, part of it is stored in the expansion vessel and returns to the circuit when it cools down, thus maintaining the pressure within the admissible range and always above atmospheric pressure, thus preventing air from entering the circuit. The expansion vessels will be located, as recommended by the CTE, at the pump suction. There are open and closed expansion vessels. The former must be placed at a height that ensures that the fluid does not overflow and that no air is introduced into the primary circuit. In the installation of this project, closed expansion tanks are used (Figure 14). The closed expansion vessel consists of two zones: one in contact with the circuit and therefore filled with fluid and a second zone filled with air or nitrogen gas. These zones are separated by a waterproof membrane. As the fluid expands, increasing in volume, the membrane gives way, compressing the air and achieving a stable operating pressure. (Robles, 2014)



Figure 14 Components of a closed expansion vessel.

- Air vent: Allows the exit of the air accumulated in the circuit. They are placed at the high points of the collector battery outlet.
- Balancing valves: The balancing valves allow to regulate the flow rate and/or the pressure drop of the circuit allowing the hydraulic balancing of the system.
- Shut-off valves: The installation of shut-off valves, in this case ball valves, makes it possible to manually interrupt the circulation of the heating medium in the various sections of the circuit, for example for repairs or maintenance purposes.
- Non-return valves: They prevent the flow of the fluid in the opposite direction to that desired. They are generally installed after the impulse of the pumps of the circuit.

- Drainage valves: They allow the drainage of water from the installation to facilitate repair or replacement work. They are located in low points of the installation.
- Safety valves: These are devices that limit the maximum pressure of the circuit, set at a pressure that guarantees that at any point of the circuit the maximum working pressure of the components is not exceeded.

3.4.5. Support system

When the available solar energy is not enough to cover the demand for DHW, the support system comes into operation to cover the expected consumption. This must be sized in the most extreme case, where it must completely replace the solar energy system. In our project the support system will be totally centralized and will be formed by a support storage tank that will exchange heat with a gas boiler (natural gas) through a coil. However, there are other options, such as individual boilers per house, individual boiler-support tank assembly or in-line boilers both centralized and individual, which heat the water to the required temperature without requiring support tanks. This last option requires high-powered boilers.

3.4.6. Control system

The fundamental objective of the regulation and control systems is to optimize the performance of the installation and to prevent it from reaching extreme conditions that could lead to breakdowns. The three main elements of this system are:

- The sensors: which are in charge of measuring the variables to be controlled in the installation (temperatures).
- The controller: is the device that generates a control signal from the value of the controlled variable and the set point.
- Actuator: this is the element that, on receiving the control signal, acts on the operating variable, generally regulating the flow of matter or energy.

In solar installations, regulation is carried out by comparing temperatures at different points in the installation, organizing the starting and stopping of pumps, the possible actuation of three-way valves (if any) and any other electromechanical actuation that may be required. (Low Temperature Solar Thermal Energy, 2007)

4. Initial data

4.1. Geographical data

The building on which this project will be based, and for which the dimensioning of a solar thermal installation for the production of domestic hot water will be carried out, is a multi-dwelling building located in the town of Barcelona, specifically in 218 Dos de Maig street.

The main data to be taken into account about the geographical situation are

- Elevation: 42m.
- Latitude: 41°40'68.53"N.
- Length: 2°18'30.18"E.

4.2. Climatic data

In this section we will collect the meteorological data of the city of Barcelona necessary for the realization of the project (see tables 1 to 7). The meteorological data have been previously taken by some meteorological stations in order to obtain some reliable values (data read from the CHEQ4 program and CENSOLAR station).

-Historical minimum temperature:-7°C

Table 1. Monthly average wind speed (m/s).

January	February	March	April	May	June	July	August	September	October	November	December
17,20	13,60	14,30	17,10	13,70	15,10	12,60	13,00	14,30	13,60	15,60	17,10

Table 2. Monthly average temperature of mains water in Barcelona (°C).

January	February	March	April	May	June	July	August	September	October	November	December
9,00	10,00	11,00	12,00	14,00	17,00	19,00	19,00	17,00	15,00	12,00	10,00

Since the solar thermal installation will be carried out at an altitude of 42m, a correction factor will be applied:

$$T_{\text{installation}} = T_{\text{Barcelona}} - B \cdot \Delta z$$

Where:

- Δz the difference in height in metres between the place of installation and the reference height of the provincial capital of that place

- B a constant that takes the following values: 0.0066 for the months from October to March and 0.0033 for the months from April to September.

Table 3. Average monthly temperature of the mains water in the installation (°C).

January	February	March	April	May	June	July	August	September	October	November	December
8,80	9,80	10,80	11,90	13,90	16,90	18,90	18,90	16,90	14,80	11,80	9,80

Table 4. Monthly average temperature of the environment in the hours of sunshine in Barcelona (°C).

January	February	March	April	May	June	July	August	September	October	November	December
11,00	12,00	14,00	17,00	20,00	24,00	26,00	26,00	24,00	20,00	16,00	12,00

Since the solar thermal installation will be carried out at an altitude of 42m, a correction factor will be applied:

$$T_{\text{installation}} = T_{\text{Barcelona}} - B \cdot \Delta z$$

Where:

- Δz the difference in height in metres between the place of installation and the reference height of the provincial capital of that place

- B a constant that takes the following values: 0.01 for the months from October to March and 0.005 for the months from April to September.

Table 5. Monthly average temperature of the environment in the hours of sunshine in the installation (°C).

January	February	March	April	May	June	July	August	September	October	November	December
10,76	11,76	13,76	16,88	19,88	23,88	25,88	25,88	23,88	19,76	15,76	11,76

Table 6. Daily Sun Hours (h)

January	February	March	April	May	June	July	August	September	October	November	December
8,00	9,00	9,00	9,50	9,50	9,50	9,50	9,50	9,00	9,00	8,00	7,50

Table 7. Monthly daily global irradiation on horizontal surface (MJ/m²).

January	February	March	April	May	June	July	August	September	October	November	December
7,80	11,30	15,60	20,50	23,20	25,60	26,40	22,00	17,20	12,00	8,30	6,90

These horizontal radiation values are modified by various correction factors:

- 0.95 if the facility is within an urban area.
- 1.05 if in a clean atmosphere or in a mountain area.
- Lost by tilt, orientation and shadows. These are defined in the section on losses due to inclination, orientation and shadows.
- Total daily useful monthly irradiation on inclined surface:

The incident radiation on the inclined surface of the collector plane is the theoretical total energy that can be expected to be produced on an average day of the month, for each square meter of collector. To know it, the radiation on the horizontal surface H corrected by the coefficient corresponding to the chosen inclination k is multiplied (see table 11):

$$E \left(\frac{\text{MJ}}{\text{m}^2} \right) = H_{\text{horizontal corrected}} \cdot K$$

The k-coefficient represents the ratio of the total energy incident in a day on a surface facing the equator and inclined at a certain angle to a horizontal surface. This value varies for each of the months of the year and depending on the latitude of the place and the angle of inclination (see tables 8 to 10). (Cleanergysolar, 2015):

Table 8.k-values for latitude 41

January	February	March	April	May	June	July	August	September	October	November	December
1,40	1,30	1,18	1,05	0,96	0,93	0,96	1,06	1,22	1,40	1,52	1,50

Table 9.k-values for latitude 42

January	February	March	April	May	June	July	August	September	October	November	December
1,42	1,31	1,19	1,06	0,97	0,94	0,97	1,08	1,24	1,42	1,54	1,52

Table 10.Corrected k-values (latitude 41.4).

January	February	March	April	May	June	July	August	September	October	November	December
1,41	1,30	1,18	1,05	0,96	0,93	0,96	1,07	1,23	1,41	1,53	1,51

Table 11. Overall useful radiation on inclined surface (MJ/m2).

Month	H(MJ/m2)	H corrected (MJ/m2)	K	Hinclined (MJ/m2)
January	7,80	6,52	1,41	9,19
February	11,30	9,45	1,30	12,28
March	15,60	13,04	1,18	15,39
April	20,50	17,14	1,05	17,99
May	23,20	19,40	0,96	18,62
June	25,60	21,40	0,93	19,90
July	26,40	22,07	0,96	21,19
August	22,00	18,39	1,07	19,68
September	17,20	14,38	1,23	17,69
October	12,00	10,03	1,41	14,15
November	8,30	6,94	1,53	10,62
December	6,90	5,77	1,51	8,71

-Daily solar intensity (I) : amount of useful energy collected per unit of time and per surface (see table 12). It is calculated as:

$$I = \frac{E_{\text{useful}}}{\text{Sun hours}}$$

Table 12. Daily solar intensity (W/m2).

Month	Hinclined (MJ/m2)	Hinclined (KWh/m2)	Hours of sunshine(h)	I(W/m2)
January	9,19	2,55	8,00	319,25
February	12,28	3,41	9,00	379,04
March	15,39	4,27	9,00	474,97
April	17,99	5,00	9,50	526,17
May	18,62	5,17	9,50	544,43
June	19,90	5,53	9,50	581,97
July	21,19	5,89	9,50	619,52
August	19,68	5,47	9,50	575,42
September	17,69	4,91	9,00	545,88
October	14,15	3,93	9,00	436,58
November	10,62	2,95	8,00	368,62
December	8,71	2,42	7,50	322,60

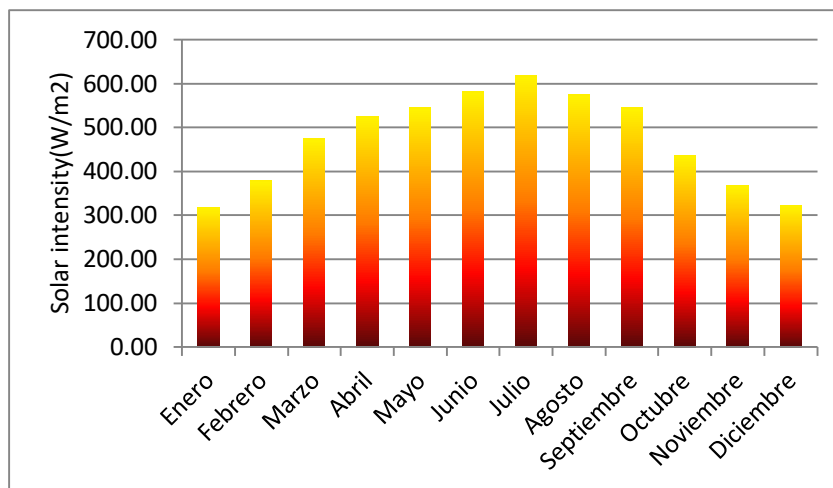


Figure 15 Monthly solar intensity values (MJ/m2).

As we can see in figure 15 there is a general tendency to obtain greater useful intensity in the hottest months, being the month of July when the maximum solar radiation to which our solar collectors are exposed is produced.

4.3. Heat transfer fluid

The heating fluid in our primary circuit will be a mixture of water and antifreeze, since the installation is outdoors and there is a risk of exposure to temperatures below 0°C, so we are obliged to protect the installation against freezing and the formation of ice crystals. The minimum historical temperature in Barcelona is -7 °C. The CTE establishes that the percentage of antifreeze must be capable of preventing frost at this minimum historical temperature with a margin of 5°C, so we must calculate the percentage for -11°C, consulting Figure 16, where we have the freezing curve of mixtures of water with propylene glycol or with ethylene glycol depending on the concentration by weight of antifreeze.

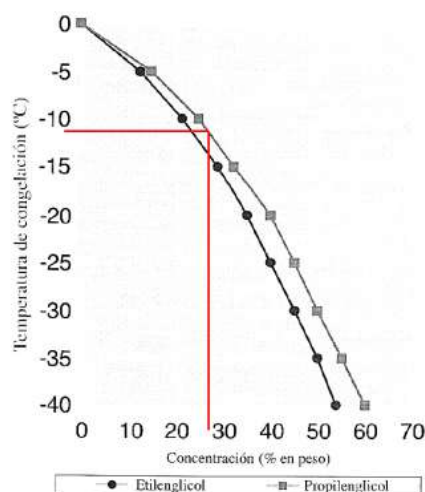


Figure 16 Freezing temperature of water as a function of propylene glycol concentration

Ethylene glycol is more effective in lowering the freezing point of water, but it turns out to be a toxic liquid and propylene glycol is not. We're going with propylene glycol.

We observe from the graph that a minimum concentration of 27% propylene glycol is required. To ensure the margin we will apply a concentration of 30% by weight. In this proportion, the physicochemical properties of the heat transfer fluid can be extracted, depending on the temperature, from the graphs in the appendix. (Besa, 2014)The properties of the heat transfer fluid can be seen in Table 13.

Table 13 Properties of the heat transfer fluid at a reference temperature of 35°C

Propylene Glycol 30%	
Density(Kg/m ³)	1035
Specific heat (J/Kg-K)	3820
Dynamic Viscosity (Pa-s)	0,011
Prandtl(-)	10 ²
Thermal conductivity (W/m-K)	0,44
Coefficient of expansion(K ⁻¹)	0,07

5. Energy demand

In this section we will calculate the energy demand in the city of Barcelona in each month of the year. For this we will need some initial data contemplated in the most recent Technical Building Code (CTE approved on 20 December 2019):

5.1. Initial data

- Average daily consumption per person per day:

In table 14 we can see the data on the daily demand for domestic hot water (DHW) in liters/person for different dwellings at a reference temperature of 60°C as stipulated by the CTE.

Table 14. Daily consumption of DHW per person at a reference temperature of 60°C.

Criterio de demanda	Litros/día-unidad	unidad
Vivienda	28	Por persona
Hospitales y clínicas	55	Por persona
Ambulatorio y centro de salud	41	Por persona
Hotel *****	69	Por persona
Hotel ****	55	Por persona
Hotel ***	41	Por persona
Hotel/hostal **	34	Por persona
Camping	21	Por persona
Hostal/pensión *	28	Por persona
Residencia	41	Por persona
Centro penitenciario	28	Por persona
Albergue	24	Por persona
Vestuarios/Duchas colectivas	21	Por persona
Escuela sin ducha	4	Por persona
Escuela con ducha	21	Por persona
Cuarteles	28	Por persona
Fábricas y talleres	21	Por persona
Oficinas	2	Por persona
Gimnasios	21	Por persona
Restaurantes	8	Por persona
Cafeterías	1	Por persona

- Number of people in the Building

The building consists of a total of 20 dwellings. To determine the total demand of the building we will calculate the total number of people. The same document establishes that the minimum number of people per dwelling will be determined according to the number of bedrooms as we can see in table 15.

Table 14.Number of people according to the number of bedrooms.

Número de dormitorios	1	2	3	4	5	6	≥6
Número de Personas	1,5	3	4	5	6	6	7

There are two types of housing in our building (see table 16).

Table 15.Number of people in the building.

	Type 1 housing	Type 2 housing
N. dwellings	12	8
N.rooms/housing	3	2
N. persons/housing	4	3
N.people in that type of housing	48	24
Total number of homes in the building	20	
Total number of people	72	

- For multi-family dwellings, a centralization factor must be applied to calculate the average total daily consumption, provided by Table 17.

Table 16. Centralisation factor according to the number of dwellings.

Nº viviendas	N≤3	4≤N≤10	11≤N≤20	21≤N≤50	51≤N≤75	76≤N≤100	N≥101
Factor de centralización	1	0,95	0,90	0,85	0,80	0,75	0,70

The average daily consumption at 60°C will be:

$$Q_{DHW} = \frac{28L}{\text{person} \cdot \text{day}} \cdot 72\text{people} \cdot 0,9 = 1814,4 \frac{L}{\text{day}}$$

The consumption of DHW at a temperature different from the reference temperature stipulated by the CTE (60°C) can be obtained with the following expressions:

$$D(T) = \sum_{i=1}^{12} D_i(T)$$

$$D_i(T) = D_i(60^{\circ}\text{C}) \cdot \frac{60 - T_i}{T - T_i}$$

Where:

D(T) = Annual domestic hot water demand at the chosen temperature T.

D_i(T) = Domestic hot water demand for month i, at the chosen temperature T

D_i(60 °C) = Domestic hot water demand for month i, at the temperature of 60 °C.

T = Temperature of the final storage tank.

T_i = Average temperature of cold water in month i.

- Since our reference temperature is going to be 50°C, we must correct our daily consumption:

$$D_i(50) = D_i(60^{\circ}\text{C}) \cdot \frac{60 - 12}{50 - 12} = \frac{28L}{\text{person} \cdot \text{day}} = 72\text{people} \cdot 0,9 \cdot \frac{60 - 12}{50 - 12} = 2291,87 \frac{L}{\text{day}}$$

As the consumption of DHW at 60°C provided by the CTE is given by default at a fixed network water temperature of 12°C, the same value has been used to carry out consumption at 50°C. Once the daily consumption of DHW at 50°C is known, it is necessary to apply corrections to its consumption to obtain a value that is closer to reality, since due to the high temperatures in summer and the low ones in winter it is logical that DHW consumption decreases in the first case and increases in the second. In document DTIE 1.01, the average

deviation of monthly consumption is shown. In table 18 we see the monthly consumption provided by the following expression:

$$\text{Monthly consumption} \left(\frac{\text{L}}{\text{month}} \right) = \text{Daily consumption} \left(\frac{\text{L}}{\text{day}} \right) \cdot \frac{\text{N. days}}{\text{month}} \cdot \text{Desviation factor}$$

Table 17. Corrected monthly consumption (L/month).

Month	Days	Occupation	Consumption (L/day)	Total consumption (L/month)	Deviation factor	Corrected consumption (L/month)
January	31	100%	2291,87	71048,08	1,12	79573,85
February	28	100%	2291,87	64172,46	1,08	69306,26
March	31	100%	2291,87	71048,08	1,03	73179,53
April	30	100%	2291,87	68756,21	1,09	74944,27
May	31	100%	2291,87	71048,08	1,04	73890,01
June	30	100%	2291,87	68756,21	1,01	69443,77
July	31	100%	2291,87	71048,08	0,90	63943,28
August	31	100%	2291,87	71048,08	0,79	56127,99
September	30	100%	2291,87	68756,21	0,92	63255,71
October	31	100%	2291,87	71048,08	0,94	66785,20
November	30	100%	2291,87	68756,21	1,02	70131,33
December	31	100%	2291,87	71048,08	1,08	76731,93

5.2. Calculation of DHW energy demand

Once the monthly water consumption has been determined, we will determine the energy demand for domestic hot water needed in the dwellings throughout the year (see table 19). To calculate the energy demand corresponding to the heating of water from the mains supply up to the consumption temperature of 50°C, we will use the following expression:

$$D_{dhw} = V_{DHW} \cdot \rho \cdot C_p \cdot (T_{use} - T_{net})$$

$$\rho = 1000 \left(\frac{\text{Kg}}{\text{m}^3} \right); C_p = 4180 \left(\frac{\text{J}}{\text{kg} \cdot ^\circ\text{C}} \right)$$

Where:

Ddhw: Energy demand for domestic hot water (MJ)

ρ :Water density(kg/m³).

Cp: Specific heat of the water in (J/kg-°C)

Tuse: Reference temperature of the hot water (°C).

Tnet: Daily monthly cold water temperature in Barcelona (°C).

Table 18.Monthly DHW demand (MJ).

Month	Corrected consumption (L/month)	Tnet(°C)	Tuse(°C)	AT(°c)	Ddhw(MJ)
January	79573,85	8,80	50,00	41,20	13703,89
February	69306,26	9,80	50,00	40,20	11645,95
March	73179,53	10,80	50,00	39,20	11990,90
April	74944,27	11,90	50,00	38,10	11935,47
May	73890,01	13,90	50,00	36,10	11149,85
June	69443,77	16,90	50,00	33,10	9608,10
July	63943,28	18,90	50,00	31,10	8312,50
August	56127,99	18,90	50,00	31,10	7296,53
September	63255,71	16,90	50,00	33,10	8751,93
October	66785,20	14,80	50,00	35,20	9826,51
November	70131,33	11,80	50,00	38,20	11198,29
December	76731,93	9,80	50,00	40,20	12893,73

Therefore, the total annual demand will be 128313,66 MJ.

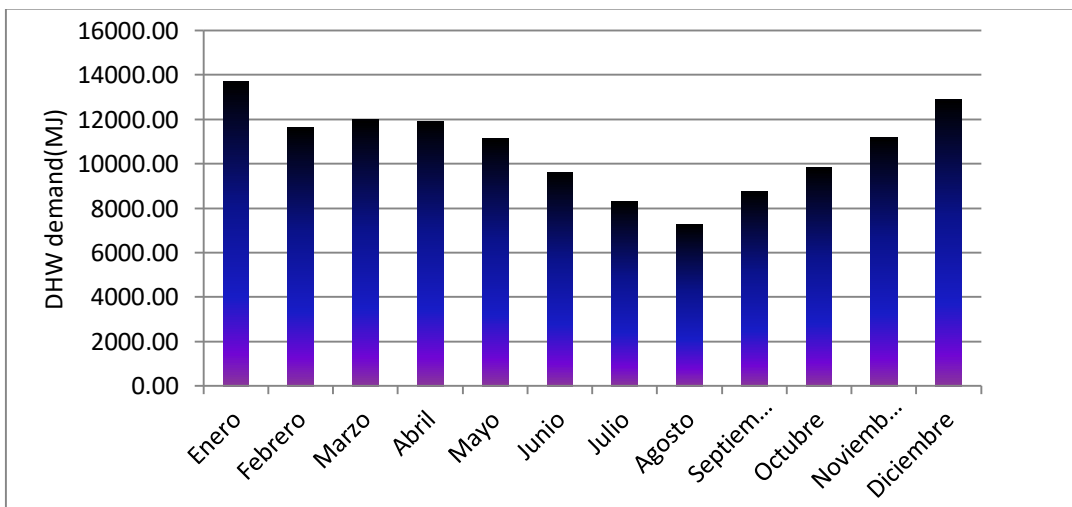


Figure 17. Monthly DHW demand.

For an occupation factor of 100% throughout the year, we can see in Figure 17 how in the coldest months more energy is required to heat the water necessary to cover the demand for DHW, a trend that decreases progressively until the hottest months. (Calculation of the demand for DHW for a building)

6. Consumption mass flow rate.

Once the demand for DHW has been determined, we can determine the monthly mass flow that must circulate through the pipes that supply the hot water to the homes. To make the calculations we need to know the daily hours of sunshine for each month (h), provided by table 6. The monthly mass flows are represented in table 20 from the following equation:

$$\text{Consumption mass flow} \left(\frac{\text{m}^3}{\text{s}} \right) = \left(\frac{\text{Corrected monthly consumption} \left(\frac{\text{L}}{\text{month}} \right)}{\text{days a month} \left(\frac{\text{day}}{\text{month}} \right) \cdot \text{hours of sunshine day} \left(\frac{\text{h}}{\text{day}} \right) \cdot 3600 \left(\frac{\text{s}}{\text{h}} \right) \cdot 1000 \left(\frac{\text{L}}{\text{m}^3} \right)} \right)$$

$$\text{Consumption mass flow} \left(\frac{\text{Kg}}{\text{s}} \right) = \text{Consumption mass flow} \left(\frac{\text{m}^3}{\text{s}} \right) \cdot \rho \left(\frac{\text{Kg}}{\text{m}^3} \right)$$

Table 19. Monthly consumption mass flow rate (Kg/s).

Month	Total corrected consumption (L/month)	Hours of sunshine	Mass flow rate (m ³ /s)	Mass flow rate (kg/s)
January	79573,85	8,00	8,91E-05	8,91E-02
February	69306,26	9,00	7,64E-05	7,64E-02
March	73179,53	9,00	7,29E-05	7,29E-02
April	74944,27	9,50	7,30E-05	7,30E-02
May	73890,01	9,50	6,97E-05	6,97E-02
June	69443,77	9,50	6,77E-05	6,77E-02
July	63943,28	9,50	6,03E-05	6,03E-02
August	56127,99	9,50	5,29E-05	5,29E-02
September	63255,71	9,00	6,51E-05	6,51E-02
October	66785,20	9,00	6,65E-05	6,65E-02
November	70131,33	8,00	8,12E-05	8,12E-02
December	76731,93	7,50	9,17E-05	9,17E-02

Therefore, the annual mass flow will be $7,22 \cdot 10^{(-2)}$ (kg/s).

7. Minimum solar contribution.

In order to be able to size the solar system, we need to know how much energy the system should provide. To do this, and given that we already know the heat needs of the building, the next step is to know what percentage of these needs must be covered by the contribution of solar energy, obtaining the required solar fraction. The current CTE requires a 60% renewable contribution for DHW production when daily consumption is less than 5000L at 60°C (for higher consumption it is 70%). (Quiles, 2019)

So:

$$f = 60\%$$

The size of the installation shall be limited by the fulfillment of the condition that in no month of the year the energy produced by the installation may exceed 110 % of the energy demand and in no more than three months 100 %.

8. Selection of the collector.

Only a part of the solar energy that affects the collector is used. This proportion is determined by the performance of the collector, which is calculated with the following equation:

$$\eta = \eta_0 - \frac{k_1 \cdot (T_e - T_a)}{I} - \frac{k_2 \cdot (T_e - T_a)^2}{I}$$

Where:

T_e =temperature of water entering the collector.

T_a =ambient temperature.

I =overall radiation in W/m².

K_1 =loss factor a₁(W/m² – K). Provided by the supplier. Depends on the collector.

K_2 = loss factor a₂(W/m² – K). Provided by the supplier. Depends on the collector.

η_0 =optical performance. Provided by the supplier. Depends on the sensor. It represents the performance that the collector would have if it did not suffer from thermal losses.

Many suppliers give the performance of the collector without the loss factor of order 2, as it is often negligible and thus we can represent the performance with a straight line.

$$\eta = \eta_0 - \frac{k_1 \cdot (T_m - T_a)}{I}$$

Therefore, the collector's performance is determined by the type of collector and the environmental conditions. Figure 18 shows the optimum yields and loss factors for various types of collectors available on the market: (Rivas, 2016)

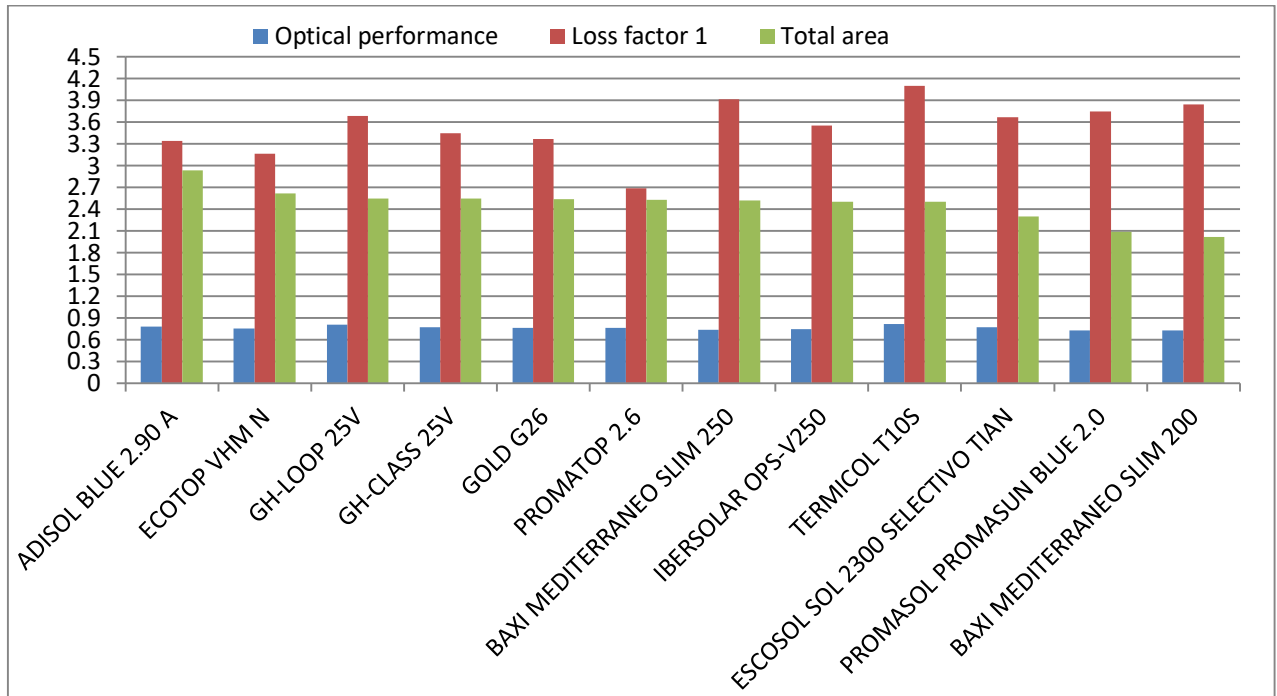


Figure 18 Comparison of properties of commercially available thermal collectors.

When choosing the flat plate collector for our installation, there are several fundamental factors to be taken into account:

- Optical performance.
- Loss factor a_1 (the loss factor a_2 is practically negligible, it will not be taken into account in the selection but in the calculation).
- Total area.
- Price.

The model ESCOSOL SOL 2300 SELECTIVO TITAN is selected among all the study collectors, as its properties are the most balanced: it has a high optical performance, a medium loss factor, a small area and one of the lowest prices.

9. Calculation of the catchment area

We will calculate the necessary catchment area using two methods:

- Heuristics.
- Thermal resistances and energy balances

9.1. Heuristic method

The first step is to find the energy that is capable of producing the selected model. It will depend mainly on the usable energy and the performance of the collector, which vary every month of the year (see table 21). The calculation of the collected energy is the following:

$$\text{Energy produced monthly} \left(\frac{\text{MJ}}{\text{m}^2} \right) = \frac{\text{N. days}}{\text{month}} \cdot I \left(\frac{\text{W}}{\text{m}^2} \right) \cdot \eta_{\text{collector}} \cdot 0,9$$

Two assumptions are made in order to proceed with the calculation:

- A range of losses of 10% of the energy collected is established due to losses in the accumulator, pipes, valves and other accessories.
- The water temperature at the collector inlet is set at 50°C for the summer months and 35°C for the winter months.

Table 20. Energy collected in the collectors (MJ/m²).

Month	Days	Performance	Hinclined (MJ/m ²)	Collected energy (MJ/m ²)
January	31	22,74%	10,03	63,65
February	28	32,76%	13,40	110,60
March	31	43,97%	16,79	205,94
April	30	50,23%	19,63	266,23
May	31	66,47%	20,31	376,68
June	30	70,06%	21,71	410,74
July	31	71,83%	23,11	463,20
August	31	71,39%	21,47	427,63
September	30	69,57%	19,29	362,43
October	31	47,89%	15,43	206,18
November	30	37,05%	11,58	115,86
December	31	24,93%	9,50	66,10

Once the amount of useful energy produced (MJ/m²) has been determined, and knowing the demand for DHW and the solar fraction to be covered (table 22), we can determine the collection area and number of collectors required.

Table 21. Calculation of the necessary collection area and solar fractions obtained.

Month	Energy produced (MJ/m ²)	Ddhw (MJ)	Solar energy produced(MJ) with 12 collectors	f monthly
January	63,65	13703,89	1649,76	12,04%
February	110,60	11645,95	2866,68	24,62%
March	205,94	11990,90	5337,99	44,52%
April	266,23	11935,47	6900,72	57,82%
May	376,68	11149,85	9763,47	87,57%
June	410,74	9608,10	10646,41	110,81%
July	463,20	8312,50	12006,27	144,44%
August	427,63	7296,53	11084,18	151,91%
September	362,43	8751,93	9394,08	107,34%
October	206,18	9826,51	5344,18	54,39%
November	115,86	11198,29	3002,97	26,82%
December	66,10	12893,73	1713,22	13,29%

$$\text{Required catchment area} = \frac{\sum Q_{\text{demanded}} \cdot f}{\sum Q_{\text{produced}}} = 25,03(\text{m}^2)$$

Where:

$\sum Q_{\text{demanded}}$: total energy demand per year (MJ)

$\sum Q_{\text{produced}}$: total energy produced per year (MJ/m²)

f: minimum solar fraction contributed by the installation (%)

$$\text{Number of collectors} = \frac{25,03}{2,16} = 11,59 \rightarrow 12 \text{ pickups} = 25,92(\text{m}^2)$$

$$\text{Annual solar fraction} = \frac{\sum_{i=1}^{12} \text{Solar energy produced, } i}{\sum_{i=1}^{12} \text{E. demand, } i} = \frac{79709,93}{128313,66} * 100 = 62\%$$

The CTE establishes that all solar thermal installations for the production of DHW are subject to the limitation that in no month of the year may the energy produced by the installation exceed 110% of the consumption demand and no more than three months in a row, 100%: If the conditions are not met, one or more of the following corrective measures must be taken:

- Surplus dissipation.
- Partial covering of the collector field.

- Partial emptying of the collector field.
- Diversion of dissipated energy to other existing applications.

The sizing of the installation does not comply with the CTE, since the energy produced by the installation exceeds 110 % of the demand in three months and for more than four 100 %, as we can see in Figure 20. (Catalonia, 2009)

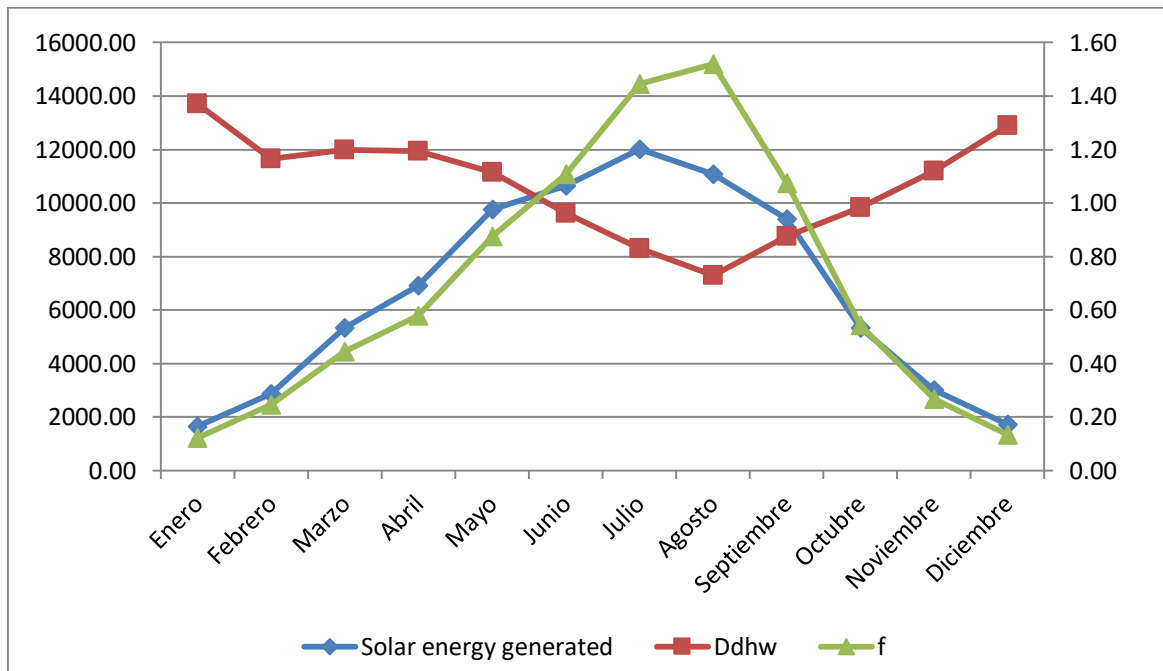


Figure 19. Monthly solar coverage as a function of demand and solar energy produced

9.2. Thermal resistance and energy balance method

In this section, the necessary catchment area will be calculated by means of energy balances in the different elements of the installation (figure 21) (Dominguez, 2009). Initially the calculation will be made considering only the losses given by the normalization curve of the collector. Subsequently, losses will be calculated taking into account external wind and temperature conditions, losses in pipes of the primary and secondary circuits and in the solar storage tank. In this way we will have a very clear idea of the impact of these losses and we will see if the area initially calculated is sufficient to achieve the desired solar coverage.

9.2.1. Loss-free DHW installations

Initially we will estimate the area of collectors needed by solving a system of 7 equations with 7 unknowns obtained from the energy balances made in each of the elements of the installation,

represented in Figure 21, only considering the losses in the collectors given by the normalization curve.

Preliminary calculations

Before starting to solve the system of equations we need to determine the circulating mass flow rate of the circuits.

- Primary circuit circulating flow (m1): we will use the one from the selected collector tests: 70(L/h·m2).

$$70 \frac{\text{L}}{\text{h} \cdot \text{m}^2} \cdot \frac{1\text{h}}{3600\text{s}} \cdot \frac{1,015\text{kg}}{\text{L}} = 0,0197(\text{kg}/(\text{s} \cdot \text{m}^2))$$

- Secondary circuit flow rate (m2): we take the flow rate equally on both sides of the exchanger to facilitate the design of the exchanger, despite a small error due to the difference in density of the circulating fluid.

Starting data:

- Radiation on the inclined plane.
- Collector performance.
- Collector flow.
- Heat exchanger efficiency.
- Temperature of the network.
- Consumption flow.
- Properties of the fluids.
- Supply temperature.

Unknowns:

- Inlet temperature to the collectors (Tci).
- Outlet temperature of the collectors (Tco).
- Heat exchanger inlet temperature (Tici).
- Exchanger outlet temperature (Tico).
- Average tank temperature (Ti).
- Consumption temperature (Tcons).
- Collector area (A).

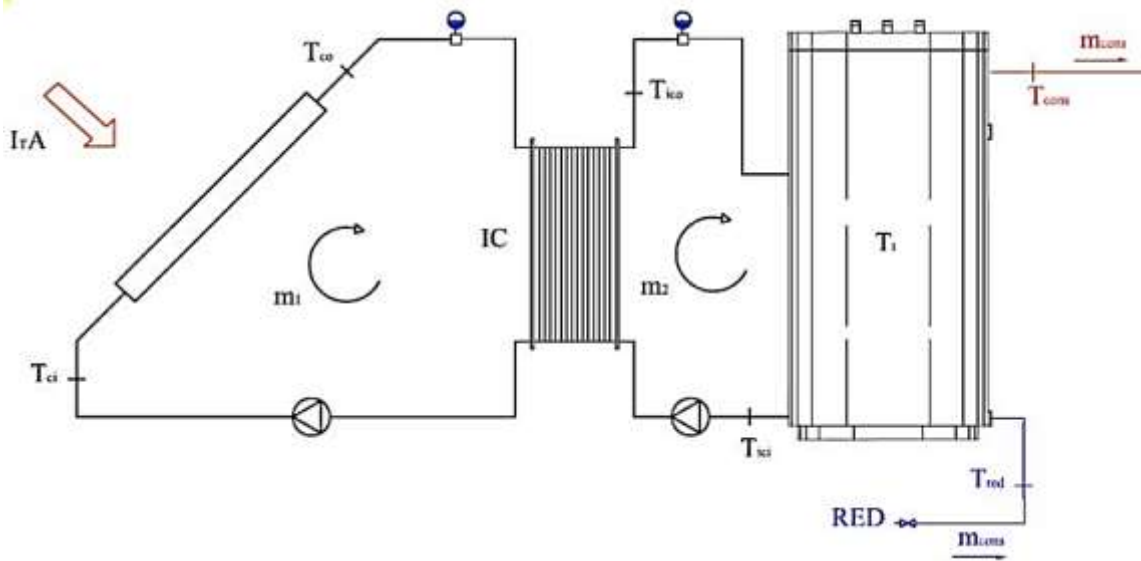


Figure 20. DHW system on which the processes will be performed.

ENERGY BALANCES

- Energy balance in the solar collectors:

$$\frac{dEc}{dt} = I_t \cdot A \cdot \left(a_0 - \frac{T_{ci} - T_o}{I_t} \cdot a_1 - \frac{(T_{ci} - T_o)^2}{I_t} \cdot a_2 \right) - m_1 \cdot Cp_1 \cdot (T_{co} - T_{ci})$$

Taking a stationary balance, the energy that reaches the collectors is equal to the energy evacuated by the fluid, translated into an increase in its temperature.

- Energy balance in the heat exchanger:

$$m_1 \cdot Cp_1 \cdot (T_{co} - T_{ci}) = m_2 \cdot Cp_2 \cdot (T_{ico} - T_{ici})$$

Taking a stationary balance, the energy that reaches the collectors is equal to the energy evacuated by the fluid, translated into an increase in its temperature. The plate heat exchanger to be used in the design of this installation will be symmetrical, i.e. $m_1 = m_2$. A value of efficiency of the exchanger of $\epsilon = 0.8$ will be taken to proceed to the resolution of the system of equations.

- Heat exchanger efficiency:

$$\epsilon_{ic} = \frac{m_2 \cdot Cp_2 \cdot (T_{ico} - T_{ici})}{C_{min} \cdot (T_{co} - T_{ci})}$$

$$C_{min} = \min(m_1 \cdot Cp_1, m_2 \cdot Cp_2)$$

- Energy balance in the storage tank:

$$m_2 \cdot C_{p2} \cdot (T_{ico} - T_{ici}) = m_{cons} \cdot C_{pcons} \cdot (T_{cons} - T_{net})$$

In this equation we relate the energy entering the reservoir and the energy extracted from the reservoir.

- Degree of stratification of the storage tank:

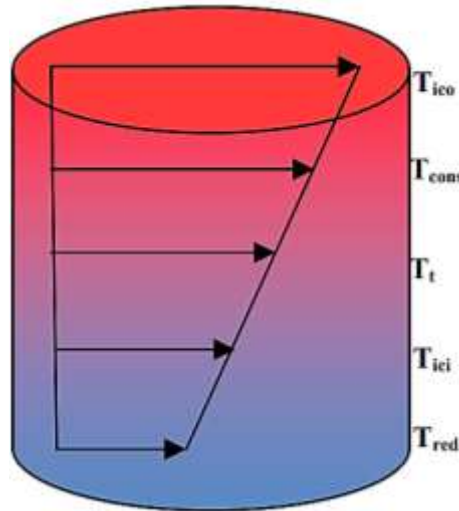


Figure 21 Representation of the stratification temperatures in the solar accumulator.

The degree of stratification is a dimensionless coefficient that represents the profile of the temperature gradient that occurs within the tank (see Figure 22) (Dominguez, 2009). We estimate an initial value of 0.5 to solve the system of equations.

$$\begin{cases} E_t = 0 \rightarrow T_{cons} = T_t \\ E_t = 1 \rightarrow T_{cons} = T_{ico} \end{cases}$$

$$E_t = \frac{T_{cons} - T_t}{T_{ico} - T_t}$$

- Average temperature in the storage tank:

$$m_2 \cdot C_{p2} \cdot T_{ico} + m_{cons} \cdot C_{p2} \cdot T_{net} = (m_{cons} + m_2) \cdot C_{p2} \cdot T_t$$

$$T_t = \frac{T_{ico} \cdot m_2 + T_{net} \cdot m_{cons}}{m_2 + m_{cons}}$$

This is the average value between the temperature at the hottest point, which will be the hot water inlet at the top, and the coldest point, which will be the mains water inlet at the bottom.

- Minimum solar contribution:

$$f = \frac{m_{\text{cons}} \cdot C_{p\text{cons}} \cdot (T_{\text{cons}} - T_{\text{net}})}{m_{\text{cons}} \cdot C_{p\text{cons}} \cdot (T_{\text{sum}} - T_{\text{net}})} = \frac{T_{\text{cons}} - T_{\text{net}}}{T_{\text{sum}} - T_{\text{net}}}$$

The minimum solar contribution (f) represents what temperature can be reached through the exclusive use of our solar system.

The system of equations to be solved is summarized as follows:

$$I_t \cdot A \cdot \left(a_0 - \frac{T_{ci} - T_o}{I_t} \cdot a_1 - \frac{(T_{ci} - T_o)^2}{I_t} \cdot a_2 \right) = m_1 \cdot C_{p1} \cdot (T_{co} - T_{ci})$$

$$m_1 \cdot C_{p1} \cdot (T_{co} - T_{ci}) = m_2 \cdot C_{p2} \cdot (T_{ico} - T_{ici})$$

$$\varepsilon_{ic} = \frac{m_2 \cdot C_{p2} \cdot (T_{ico} - T_{ici})}{C_{min} \cdot (T_{co} - T_{ici})}$$

$$m_2 \cdot C_{p2} \cdot (T_{ico} - T_{ici}) = m_{\text{cons}} \cdot C_{p\text{cons}} \cdot (T_{\text{cons}} - T_{\text{net}})$$

$$T_t = \frac{T_{ico} \cdot m_2 + T_{\text{net}} \cdot m_{\text{cons}}}{m_2 + m_{\text{cons}}}$$

$$E_t = \frac{T_{\text{cons}} - T_t}{T_{ico} - T_t}$$

$$f = \frac{m_{\text{cons}} \cdot C_{p\text{cons}} \cdot (T_{\text{cons}} - T_{\text{net}})}{m_{\text{cons}} \cdot C_{p\text{cons}} \cdot (T_{\text{sum}} - T_{\text{net}})} = \frac{T_{\text{cons}} - T_{\text{net}}}{T_{\text{sum}} - T_{\text{net}}}$$

In a first simulation we calculated the area of panels needed to obtain the 60% solar fraction with annual averages (table 23). Later, with the obtained area, we will calculate with monthly averages the solar fractions and the rest of unknowns (table 24). The system of equations has been solved with the Mathematica program.

Table 22. Calculation of the necessary catchment area in the system without losses.

Annual	A(m ²)	T _{ci} (K)	T _{co} (K)	T _{ici} (K)	T _{ico} (K)	T _t (K)	T _{cons} (K)	f
	21,73	307,61	311,60	306,61	310,29	306,89	308,59	60,00%

The total necessary area of capture without suffering losses from the system is 21.73m², which corresponds to:

$$N. \text{ collectors} = \frac{A}{\text{Useful area collector}} = \frac{21,73\text{m}^2}{2,16\text{m}^2} = 10,06 \rightarrow 11 \text{ collectors}$$

As we know that this resolution does not include the losses caused by the system, 10 collectors will not be enough, so we initially consider that we will need 11 collectors in total. Once we find the catchment area, we solve the system of equations on a monthly basis.

Table 23. Results of simulation of the system of equations without losses in the system.

Month	Tci(K)	Tco(K)	Tici(K)	Tico(K)	Tt(K)	Tcons(K)	f
January	21,29	24,02	20,61	23,12	20,83	21,98	31,98%
February	26,54	29,64	25,76	28,62	25,98	27,30	43,52%
March	32,61	36,46	31,65	35,20	31,91	33,55	58,04%
April	36,42	40,75	35,34	39,32	35,62	37,47	67,12%
May	40,40	44,86	39,29	43,39	39,57	41,48	76,40%
June	45,99	50,74	44,80	49,18	45,10	47,14	91,35%
July	52,47	57,33	51,26	55,73	51,53	53,63	111,67%
August	53,34	57,70	52,26	56,26	52,47	54,37	114,07%
September	45,16	49,59	44,06	48,14	44,32	46,23	88,60%
October	36,96	40,51	36,08	39,35	36,29	37,82	65,39%
November	27,74	30,89	26,96	29,86	27,19	28,52	43,77%
December	22,11	24,88	21,42	23,97	21,65	22,81	32,36%

We observe that in the months of July and August the minimum solar contribution exceeds 110%, not complying with the CTE. As these calculations are not definitive, since the losses caused by the system have not been included, no protection measures will be taken for the time being.

9.2.2. Installation of DHW with losses

Once calculations have been made for an ideal installation in which only the losses in the collectors given by their normalization curve have been taken into account, in this section we will proceed to calculate them, to check if, once taken into account, the area calculated previously is enough.

Among the most remarkable are:

- Losses in the collectors.
- Losses in the pipes of the primary circuit.
- Losses in the solar accumulator.

Losses in the collectors

When we select a collector from the market, the supplier provides us with a normalization curve that predicts the thermal losses of the collector. However, these normalization curves do not take into account the effect of the wind, which produces a difference between the real conditions and those predicted by the normalization curve. For this reason, a non-stationary heat transfer model was developed to calculate heat losses in the collectors, taking into account local wind speed values in the city of Barcelona.

The heat transfer processes contemplated in the model are:

- Forced convection at the back of the manifolds.
- Driving in the box.
- Conduction in the insulation.
- Convection in the heat transfer fluid.
- Conduction in the tubes.
- Conduction in the absorber plate.
- Radiation between the absorber plate and the cover glass due to the temperature difference between the two.
- Natural convection in the internal air layer between the cover glass and the absorber plate.
- Driving on the glass.
- External forced convection on the glass of the collectors.
- Radiation between the glass cover and the sky.

Losses in the back of the collector:

Insulating conduction resistance:

The thermal conduction resistance in the insulator depends on the type of insulator and its thickness. We calculate the resistance of each insulator according to the following expression:

$$R. \text{ insulating} \left(\frac{K}{W} \right) = \frac{e \text{ insulating}}{k \text{ insulating} \cdot A \text{ insulating}}$$

Where:

- e: Insulator thickness (m).
- K: Thermal conductivity of the insulating material (W/m-K)
- A: Opening area of a collector (m²)

As we have two different insulators we must calculate the insulation of each one of them to obtain the total insulation.

$$R. \text{ polyurethane } \left(\frac{K}{W} \right) = \frac{e \text{ polyurethane}}{K \text{ polyurethane} \cdot A \text{ polyurethane}} = \frac{0,025}{0,03 \cdot 2,3} = 0,36$$

$$R. \text{ glass wool } \left(\frac{K}{W} \right) = \frac{e \text{ glass wool}}{K \text{ glass wool} \cdot A \text{ glass wool}} = \frac{0,025}{0,035 \cdot 2,3} = 0,31$$

$$R. \text{ insulating } \left(\frac{K}{W} \right) = R. \text{ polyurethane } \left(\frac{K}{W} \right) + R. \text{ glass wool } \left(\frac{K}{W} \right) = 0,67$$

Box driving resistance:

$$R. \text{ box } \left(\frac{K}{W} \right) = \frac{e \text{ box}}{k \text{ box} \cdot A \text{ box}} = \frac{e \text{ aluminum}}{K \text{ aluminum} \cdot A \text{ aluminum}} = \frac{0,002}{205 \cdot 2,3} = 4,24 \cdot 10^{-6}$$

Where:

- e: Thickness of the box (m)
- K: Thermal conductivity of the box material (W/m-K)
- A: Opening area of a collector (m²)

Convection resistance of the rear side

This is a forced convection thermal resistance that is calculated using the following expression:

$$R_{\text{conv. rear side}} \left(\frac{K}{W} \right) = \frac{1}{A_{\text{box}} \cdot h_{\text{conv. rear side}}}$$

Where:

- h_{conv. rear side}: Air convection coefficient (W/m²-K)
- A: Opening area of a collector (m²)

With the properties of the air already known (see appendix), and knowing that it is a forced convection process, we will determine the Reynolds number:

$$\text{Reynolds forced conv.} = \frac{\rho_{\text{air}} \cdot v_{\text{air}} \cdot L_c}{\mu_{\text{air}}}$$

Where:

- L_c corresponds, for vertical collectors facing south, to the width of the collector (m).
- ρ_{air} : air density ($\frac{\text{Kg}}{\text{m}^3}$).
- v_{air} : average air speed ($\frac{\text{m}}{\text{s}}$).
- μ_{air} : dynamic air viscosity ($\text{N} - \frac{\text{s}}{\text{m}^2}$).

Once the Reynolds number is calculated, we can calculate the Nusselt number using the following expression as long as we assume that the airflow is parallel to the plate:

$$\text{Nu rear side} = 8,948 \cdot \text{Re}^{0,395} \cdot \text{Pr}^{1/3}$$

Then the subsequent convection coefficient:

$$h_{\text{conv. rear side}} \left(\frac{\text{W}}{\text{m}^2 \cdot \text{K}} \right) = \frac{\text{Nu rear side} \cdot k_{\text{air}}}{L_c}$$

In table 25 we can see the monthly post-convection values.

Table 24. Monthly convection resistances at the back of the manifold (K/W).

Month	wind speed (m/s)	Reynolds	Nusselt	He conv. rear side (W/m ² -K)	Rconv.rear side (K/W)
January	4,78	404313,65	1162,22	23,44	0,02
February	3,78	316828,67	1058,99	21,42	0,02
March	3,97	329036,73	1074,36	21,86	0,02
April	4,75	387278,73	1142,57	23,47	0,02
May	3,81	304538,70	1041,29	21,58	0,02
June	4,19	328498,86	1073,97	22,32	0,02
July	3,50	270794,05	997,82	20,80	0,02
August	3,61	279390,69	1009,90	21,05	0,02
September	3,97	311094,95	1051,70	21,86	0,02
October	3,78	302315,79	1038,35	21,52	0,02
November	4,33	354526,62	1105,48	22,63	0,02
December	4,75	398365,46	1156,60	23,40	0,02

Losses in the upper part of the collector

Resistance of the glass:

$$R_{\text{glass}} \left(\frac{\text{K}}{\text{W}} \right) = \frac{e_{\text{glass}}}{k_{\text{glass}} \cdot A_{\text{glass}}} = \frac{0,004}{0,8 \cdot 2,16} = 2,13 \cdot 10^{-3}$$

Where:

- e: Thickness of the glass cover (m)
- k: Thermal conductivity of glass (W/m-K)
- A: Collector useful area (m²)

Upper outer convection resistance (R_{conv.upper}):

$$R_{\text{conv. upper part}} \left(\frac{\text{K}}{\text{W}} \right) = \frac{1}{h_{\text{upper part}} \cdot A_{\text{box}}}$$

The same calculation procedure is followed as for the subsequent convection resistance, only another correlation is used to find the Nusselt number.

$$\text{Reynolds forced conv.} = \frac{\rho_{\text{air}} \cdot v_{\text{air}} \cdot L_c}{\mu_{\text{air}}}$$

Once the Reynolds number is calculated, we can calculate the Nusselt number using the following expression as long as we assume that the airflow is parallel to the plate:

$$\text{Nu upper part} = 0,105 \cdot \text{Re}^{0,646} \cdot \text{Pr}^{1/3}$$

Then the higher convection coefficient:

$$h_{\text{conv. upper part}} \left(\frac{\text{W}}{\text{m}^2 \cdot \text{K}} \right) = \frac{\text{Nu upper part} \cdot k_{\text{air}}}{L_c}$$

The upper monthly convection heaters can be seen in table 26:

Table 25. Monthly convection resistances at the top of the manifold (K/W).

Month	wind speed(m/s)	Reynolds	Nusselt	He conv. upper part (W/m ² -K)	Rconv. upper part (K/W)
January	4,78	404313,65	396,37	7,99	0,06
February	3,78	316828,67	338,90	6,86	0,07
March	3,97	329036,73	347,23	7,07	0,07
April	4,75	387278,73	385,32	7,91	0,06
May	3,81	304538,70	329,81	6,84	0,07
June	4,19	328498,86	346,95	7,21	0,06
July	3,50	270794,05	306,50	6,39	0,07
August	3,61	279390,69	312,76	6,52	0,07
September	3,97	311094,95	334,97	6,96	0,07
October	3,78	302315,79	328,25	6,80	0,07
November	4,33	354526,62	364,31	7,46	0,06
December	4,75	398365,46	392,93	7,95	0,06

Higher radiation resistance (R.higher radiation)

To calculate this resistance we need to calculate the temperature of the sky and the temperature of the glass on the outside of the collector.

- Temperature of the sky:

The temperature of the sky is a value that is obtained by correlations. The correlation used is valid for 3 °C < Tamb < 45° C and its monthly value is represented in table 27.

$$T_{sky} = 0,0552 \cdot (T_{amb})^{1,5}$$

Table 26. Monthly sky temperatures (°K).

Month	Average room temperature during sunshine hours(K)	T Sky(K)
January	283,91	264,06
February	284,91	265,46
March	286,91	268,26
April	290,03	272,65
May	293,03	276,89
June	297,03	282,58
July	299,03	285,44
August	299,03	285,44
September	297,03	282,58
October	292,91	276,72
November	288,91	271,07
December	284,91	265,46

The temperature of the glass will be explained later on as it depends on the heat flow of different branches.

Upper outer radiation resistance:

$$\text{Rad. upper part} \left(\frac{\text{K}}{\text{W}} \right) = \frac{1}{\epsilon_{\text{glass}} \cdot A \cdot \sigma \cdot ((T_{\text{upper part glass}})^2 + (T_{\text{sky}})^2) \cdot (T_{\text{upper part glass}} + T_{\text{sky}})}$$

Where:

- ε is the emissivity of the crystal with a value of 0.1.
- T upper part glass: temperature of the glass of the upper cover (K).
- Tsky : temperature of the sky(K).
- σ Stefan-Boltzmann's constant ($5.67 \cdot 10^{-8} \frac{\text{W}}{\text{m}^2} \cdot \text{K}^4$).
- A: Useful area of the collector (m²).

The monthly values of the upper radiation between the roof and the sky are represented in table 28.

Table 27. Radiation resistance between the deck and the sky (K/W).

Month	Average room temperature during sunshine hours(K)	T Sky(K)	T upper glass(K)	R.rad. upper range (K/W)
January	283,91	264,06	286,36	0,98
February	284,91	265,46	289,05	0,96
March	286,91	268,26	292,85	0,92
April	290,03	272,65	296,15	0,89
May	293,03	276,89	300,19	0,85
June	297,03	282,58	304,64	0,81
July	299,03	285,44	308,80	0,78
August	299,03	285,44	308,27	0,78
September	297,03	282,58	304,21	0,81
October	292,91	276,72	298,11	0,86
November	288,91	271,07	292,20	0,91
December	284,91	265,46	287,37	0,96

Radiation resistance between the glass and the plate

$$R_{rad. inside} \left(\frac{K}{W} \right) = \frac{(\epsilon_{glass} + \epsilon_{plate} - \epsilon_{glass} \cdot \epsilon_{plate})}{\epsilon_{glass} \cdot \epsilon_{plate} \cdot A \cdot \sigma \cdot ((T_{lower part glass})^2 + (T_{plate})^2) \cdot (T_{lower part glass} + T_{plate})}$$

Where:

- ε is the emissivity of the crystal with a value of 0.1.
- ε is the emissivity of the plate with a value of 0.06.
- T lower part glass: temperature of the lower cover glass (K).
- T Plate: collector absorption plate temperature (K).
- σ Stefan-Boltzmann's constant ($5.67 \cdot 10^{-8} \frac{W}{m^2} \cdot K^4$).
- A: Absorbing useful area (m²).

In order to solve the above equation I must know the temperature of the interior of the crystal, which we calculate in the following way:

$$T_{lower part glass} = (q_1 + q_2) \cdot R_{glass} + T_{upper part glass}$$

$$q1(W) = \frac{T_{\text{glass}} - T_{\text{sky}}}{R_{\text{rad. upper outer}}}$$

$$q2(W) = \frac{T_{\text{glass}} - T_{\text{ambient}}}{R_{\text{conv. upper outer}}}$$

The temperature of the plate will be detailed later as it is calculated.

The monthly values of radiation between plate and glass are shown in table 29.

Table 28. Radiation resistance between inner cover and plate (K/W).

Month	Temp. amb. sunshine hours(K)	Tsky (K)	q1 (W)	q2 (W)	Tupper part glass (K)	T lower part glass(K)	T,plate (K)	Rad. inside between plate and glass (K/W)
January	283,91	264,06	22,81	42,33	286,36	286,51	308,75	2,07
February	284,91	265,46	24,68	61,38	289,05	289,25	316,21	1,97
March	286,91	268,26	26,65	90,65	292,85	293,12	326,15	1,84
April	290,03	272,65	26,53	104,64	296,15	296,46	332,23	1,75
May	293,03	276,89	27,46	105,70	300,19	300,50	337,05	1,68
June	297,03	282,58	27,40	118,57	304,64	304,98	344,13	1,59
July	299,03	285,44	30,07	134,90	308,80	309,19	351,65	1,51
August	299,03	285,44	29,30	130,13	308,27	308,64	350,24	1,52
September	297,03	282,58	26,79	107,91	304,21	304,52	341,77	1,61
October	292,91	276,72	24,92	76,46	298,11	298,35	329,05	1,77
November	288,91	271,07	23,15	52,94	292,20	292,37	317,40	1,93
December	284,91	265,46	22,71	42,32	287,37	287,53	309,77	2,05

Convection resistance between the glass and the plate

$$R_{\text{natural indoor conv.}} \left(\frac{K}{W} \right) = \frac{1}{h_{\text{natural indoor}} \cdot A_{\text{absorber}}}$$

The convection resistance between the plate and the glass is a natural convection phenomenon, and is calculated as follows:

Calculation of the number of Grashof (Gr):

$$Gr = \frac{g \cdot B \cos(\alpha) \cdot (T_{plate} - T_{inner\ glass}) \cdot Lc^3}{\nu \cdot \alpha_{air}}$$

Where:

Lc:Length of glass plate.

g:9,8(m/s²) .

Thermal passivity coefficient (β) = 2/(Plate+Inside glass).

α Thermal air diffusivity (m²/s).

ν :Kinematic viscosity of air(m²/s).

Note that we have multiplied by cos(β) for the effect of the collector tilt.

$$\text{Reynolds natural convection} = Gr \cdot Pr$$

Once we have calculated Reynolds' number, we can calculate Nusselt's number using the following expression:

$$Nu_{indoor} = 4,328 \cdot 10^{-10} \cdot Ra^2 - 1,478 \cdot 100^{-6} \cdot Ra + 1,001$$

Next is the natural convection coefficient:

$$h_{natural\ indoor\ conv} \left(\frac{W}{m^2 \cdot K} \right) = \frac{Nu_{natural\ indoor} \cdot k_{air}}{Lc}$$

The monthly values of natural convection inside the collector are shown in table 30.

Table 29.Natural convection resistance inside the collector (K/W).

Month	Gr	Rayleigh	Nusselt	He natural indoor conv.(W/m ² -K)	R.natural indoor conv.(K/W)
January	37977,26	27825,67	1,29	1,18	0,41
February	44566,69	32738,12	1,42	1,30	0,37
March	52066,94	38230,80	1,58	1,45	0,33
April	53627,92	39236,51	1,61	1,50	0,32
May	52003,93	38015,72	1,57	1,47	0,33
June	52676,58	38709,99	1,59	1,50	0,32
July	54915,58	40455,94	1,65	1,56	0,31
August	53951,84	39745,96	1,63	1,53	0,31
September	50346,08	36997,40	1,54	1,45	0,33
October	44394,58	32453,16	1,41	1,32	0,37
November	39065,02	28669,13	1,31	1,22	0,40
December	37280,50	27385,78	1,29	1,18	0,41

Loss of useful heat

Absorber driving resistance

The resistance of the absorber plate, being a non-linear heat transfer, is usually calculated experimentally by performing an energy balance on the plate between the absorber temperature and the average temperature of the fluid passing through the tubes.

$$R. \text{ cond. absorber } \left(\frac{K}{W} \right) = 0,012$$

Conduction resistance in the inner tubes

The collector is made up of 10 tubes with a diameter of 12 (mm) and 2 collectors with a diameter of 22 (mm). As we have two different types of tubes we must calculate the conduction resistance of each one.

$$R. \text{ cond. tubes } \left(\frac{K}{W} \right) = \frac{\ln\left(\frac{D_{\text{ext}}}{D_{\text{int}}}\right)}{2 \cdot \pi \cdot k_{\text{tube}} \cdot L_{\text{tube}}} = \frac{\ln\left(\frac{0,012}{0,01}\right)}{2 \cdot \pi \cdot 385,2 \cdot 1,9} = 3,97 \cdot 10^{-5}$$

$$R. \text{ cond. collector tubes } \left(\frac{K}{W} \right) = \frac{\ln\left(\frac{D_{\text{ext}}}{D_{\text{int}}}\right)}{2 \cdot \pi \cdot k_{\text{tube}} \cdot L_{\text{tube}}} = \frac{\ln\left(\frac{0,022}{0,02}\right)}{2 \cdot \pi \cdot 385,2 \cdot 1,213} = 3,25 \cdot 10^{-5}$$

Where:

- D_{ext} : External diameter of tubes (m).
- D_{int} : Internal diameter of tubes (m) .
- L_{tube} : Length of tube(m) .
- k_{tube} : k Thermal conductivity of pipe material (W/m-K) .
- N_{tubes} : Number of tubes per manifold (-).

$$R. \text{ total cond. tubes } \left(\frac{K}{W} \right) = \left(\left(\frac{1}{R_{\text{cond. tubes}} \cdot N_{\text{tubes}}} \right) + \left(\frac{1}{R_{\text{cond. collector}} \cdot N_{\text{collector tubes}}} \right) \right)^{-1} = 5,58 \cdot 10^{-5}$$

Convection resistance inside the tubes:

$$R_{\text{conv. inside tubes}} \left(\frac{K}{W} \right) = \frac{1}{h_{\text{inside tubes}} \cdot \pi \cdot D_{\text{int}} \cdot L_{\text{tubes}} \cdot N_{\text{tubes}}}$$

The resistance of the heat transfer fluid is forced internal convection. The heat transfer fluid chosen for the frost protection of the installation is propylene glycol at 30% concentration. Its properties can be seen in the heat transfer fluid section.

Calculating Reynolds' number:

$$\text{Reynold tubes} = \frac{\rho_{\text{fluid}} \cdot v_{\text{fluid}} \cdot D_{\text{int}}}{\mu_{\text{fluid}}} = \frac{4 \cdot \frac{q_{\text{collector}}}{n_{\text{tubes}}} \cdot \rho_{\text{fluid}}}{\pi \cdot D_{\text{int}} \cdot \mu_{\text{fluid}}} = \frac{1015 \cdot 0,53 \cdot 0,02}{0,002} = 271,34$$

Where:

- ρ : fluid Density of the water/propylene glycol mixture (Kg/m³).
- v fluid: Speed inside the tubes (m/s).
- D_{int} : Internal diameter of tubes(m).
- μ fluid: Dynamic viscosity of the water/propylene glycol mixture (N-s/m²).

The internal convection in the tubes is calculated with the Dittus-Boelter equation:

$$\text{Nusselt} = 0,023 \cdot \text{Re}^{0,8} \cdot \text{Pr}^{0,4} = 1,8$$

Next is the convection coefficient:

$$h_{\text{inside tubes}}(\text{W/m}^2 \cdot \text{K}) = \frac{k_{\text{fluid}} \cdot \text{Nu}}{D_{\text{int}}} = \frac{0,48 \cdot 1,8}{0,02} = 86,25$$

The convection thermal resistance will be:

$$R_{\text{inside tubes conv.}} \left(\frac{\text{K}}{\text{W}} \right) = \frac{1}{h_{\text{inside tubes}} \cdot \pi \cdot D_{\text{int}} \cdot L_{\text{tubes}} \cdot N_{\text{tubes}}} = \frac{1}{86,25 \cdot \pi \cdot 0,02 \cdot 1,9 \cdot 10} = 1,94 \cdot 10^{-2}$$

Where:

- $h_{\text{inside tubes}}$: Fluid convection coefficient (W/m²-K).
- D_{int} : Internal pipe diameter (m).
- L_{tubes} : Length of a tube (m).
- N_{tubes} : Number of tubes per collector (-).

Lateral heat loss

Insulating conduction resistance:

On the side the only insulation is polyurethane, with a thickness of 25mm.

$$\text{Side(m}^2\text{)} = (2 - \text{high collector} + 2 - \text{width collector}) - \text{catcher thickness} = (2 \cdot 1,9 + 2 \cdot 1,213) \cdot 0,106 = 0,66\text{m}^2$$

$$\text{R. side insulating conduction } \left(\frac{\text{K}}{\text{W}}\right) = \frac{e \text{ insulating}}{k \text{ insulating} \cdot A_{\text{side}}} = \frac{0,025}{0,03 \cdot 0,66} = 1,26$$

Resistance to the driving of the box:

$$\text{R. side box conduction } \left(\frac{\text{K}}{\text{W}}\right) = \frac{e \text{ box}}{k \text{ box} \cdot A. \text{ side}} = \frac{0,002}{205 \cdot 0,66} = 1,48 \cdot 10^{-5}$$

Loss of collector

Once all the thermal resistances have been calculated, we can calculate the losses caused in the collector (tables 31,32,33, and 35).

Losses produced in the lower part of the collector:

$$Q. \text{ lower part(W)} = \frac{T_{\text{plate}} - T_{\text{ambient}}}{\text{Req. lower part}} = \frac{T_{\text{plate}} - T_{\text{ambient}}}{R_{\text{insulating}} + R_{\text{box}} + R_{\text{conv. lower part}}}$$

Table 30.Heat loss from the bottom of the collector (W).

Month	Q lower part loss(W)
January	35,92
February	45,15
March	56,64
April	61,03
May	63,51
June	68,03
July	75,85
August	73,84
September	64,58
October	52,15
November	41,16
December	35,95

Losses produced on the upper part of the sensor:

It takes into account, through the equation with which the thermal losses at the top are defined (qupper), that the flow that circulates through the convection and radiation resistances between the absorber plate and the cover glass, coincides with the flow that circulates through the glass and in turn with the sum of the flow that circulates through the Rrad.glass-sky and the flow that circulates through Rconv.outside , as we see in figure 23.

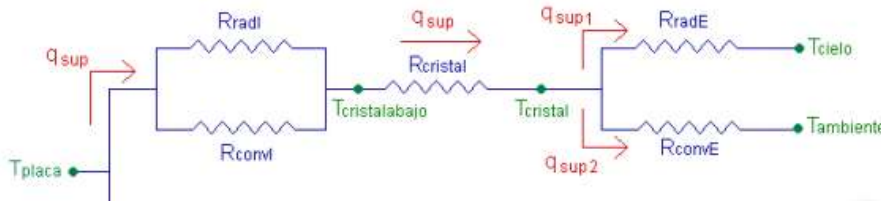


Figure 22 Diagram of thermal resistances in the upper part of the collector.

$$Q_{upper\ part}(W) = q_{upper} = q_{upper1} + q_{upper2}$$

$$\frac{T_{plate} - T_{lower\ part\ glass}}{\frac{R_{radI} \cdot R_{conv.I}}{R_{radI} + R_{conv.I}}} = \frac{T_{lower\ part\ glass} - T_{glass}}{R_{glas}} = \frac{T_{glass} - T_{sky}}{R_{rad.glass} - T_{sky}} + \frac{T_{glass} - T_{ambiente}}{R_{conv.outside}}$$

Table 31 Heat loss from the top of the collector (W).

Month	Q upper part loss(W) (W)
January	65,14
February	86,06
March	117,30
April	131,17
May	133,17
June	145,97
July	164,97
August	159,43
September	134,71
October	101,38
November	76,09
December	65,02

Losses produced on the side

$$Q_{side}(W) = \frac{T_{plate} - T_{ambiente}}{R_{eq.\ side}} = \frac{T_{plate} - T_{ambiente}}{R_{insulating} + R_{box}}$$

Table 32. Heat loss from the side of the collector (W).

Month	Q side loss(W)
January	19,67
February	24,78
March	31,07
April	33,42
May	34,86
June	37,30
July	41,67
August	40,55
September	35,43
October	28,62
November	22,56
December	19,68

Useful heat

To determine the useful heat transferred to the heat transfer fluid, it is necessary to determine the monthly temperature of the water inside the collector (Table 34). The temperature of the water in the collector is defined as:

$$T_{\text{water}} = \frac{T_{\text{ci}} + T_{\text{co}}}{2} = \frac{T_{\text{collector water inlet}} + T_{\text{collector water outlet}}}{2}$$

Table 33. Average monthly water temperature inside the collector (°C)

Month	Tci(K)	Tco(K)	Twater(K)
January	294,44	297,17	295,81
February	299,69	302,79	301,24
March	305,76	309,61	307,69
April	309,57	313,90	311,73
May	313,55	318,01	315,78
June	319,14	323,89	321,51
July	325,62	330,48	328,05
August	326,49	330,85	328,67
September	318,31	322,74	320,53
October	310,11	313,66	311,89
November	300,89	304,04	302,47
December	295,26	298,03	296,65

$$Q_{\text{useful}}(W) = \frac{T_{\text{plate}} - T_{\text{water}}}{R_{\text{plate}} + R_{\text{tube}} + R_{\text{fluid}}}$$

Table 34. Heat losses yielded to heat transfer fluid (W).

Month	Q _{useful} (W)
January	413,69
February	478,52
March	590,09
April	655,18
May	679,83
June	722,92
July	754,58
August	689,45
September	679,07
October	548,68
November	477,26
December	419,39

The calculation of thermal resistances and heat loss is an iterative process, since initially the values of the glass and plate temperatures are not known. Below is a summary of the useful heat and thermal losses obtained by the manufacturer's curve (table 36) and by thermal resistances (table 37).

Table 35. Summary of useful heat and losses of the collector according to the manufacturer's curve

Month	Incident radiation (W)	Useful curve (W)	Q _{loss} (W)	Optical losses(W)	Thermal losses(W)	Q _{available} (W)
January	689,58	445,58	243,99	155,15	88,84	534,42
February	818,72	506,62	312,10	184,21	127,89	634,51
March	1025,94	628,41	397,53	230,84	166,69	795,10
April	1136,52	707,94	428,58	255,72	172,86	880,80
May	1175,96	728,77	447,20	264,59	182,60	911,37
June	1257,06	775,82	481,25	282,84	198,41	974,22
July	1338,16	792,23	545,94	301,09	244,85	1037,08
August	1242,91	708,32	534,60	279,66	254,94	963,26

September	1179,10	723,39	455,70	265,30	190,40	913,80
October	943,01	579,78	363,23	212,18	151,05	730,83
November	796,23	515,21	281,02	179,15	101,87	617,08
December	696,82	452,88	243,94	156,79	87,16	540,04

Table 36. Summary of useful heat and losses of the collector by thermal resistances.

Month	Qavailable (W)	Quseful (W)	Qlower part (W)	Qside (W)	Qupper part(W)	Thermal losses(W)
January	534,42	413,69	35,92	19,67	65,14	120,73
February	634,51	478,52	45,15	24,78	86,06	155,99
March	795,10	590,09	56,64	31,07	117,30	205,01
April	880,80	655,18	61,03	33,42	131,17	225,62
May	911,37	679,83	63,51	34,86	133,17	231,54
June	974,22	722,92	68,03	37,30	145,97	251,29
July	1037,08	754,58	75,85	41,67	164,97	282,49
August	963,26	689,45	73,84	40,55	159,43	273,82
September	913,80	679,07	64,58	35,43	134,71	234,72
October	730,83	548,68	52,15	28,62	101,38	182,15
November	617,08	477,26	41,16	22,56	76,09	139,81
December	540,04	419,39	35,95	19,68	65,02	120,65

Annual results

Table 37 Comparison of results obtained with thermal resistance and curvature of the manufacturer.

Method	Useful heat(W)	Total losses (W)
Thermal resistors	592,39	201,99
Manufacturer's curve	630,41	163,96

The calculation of the losses produced in the collector by means of the thermal resistances results in a value quite similar to that obtained from the yield curves provided by the manufacturer, and is equivalent to the losses produced by wind (Table 38).

$$Q_{\text{thermal resistors}} - Q_{\text{manufacturer}} = 38,02W$$

Losses in the solar accumulator

The solar storage tank will be at a higher temperature than the ambient temperature most of the time, so it is also necessary to calculate the losses of this element (see figure 24) (Dominguez, 2009). The tank will be installed in the engine room and therefore out of the action of the wind, which will cause the losses suffered to be less than those of the elements calculated above. The accumulator selected is the "AISI 316L DV stainless steel accumulator", of the SUICALSA brand. The characteristics of the model can be seen in the appendix. For the calculation of the losses we will assume that inside there are no movements of the fluid. Finally, the external convection will be of the natural type.

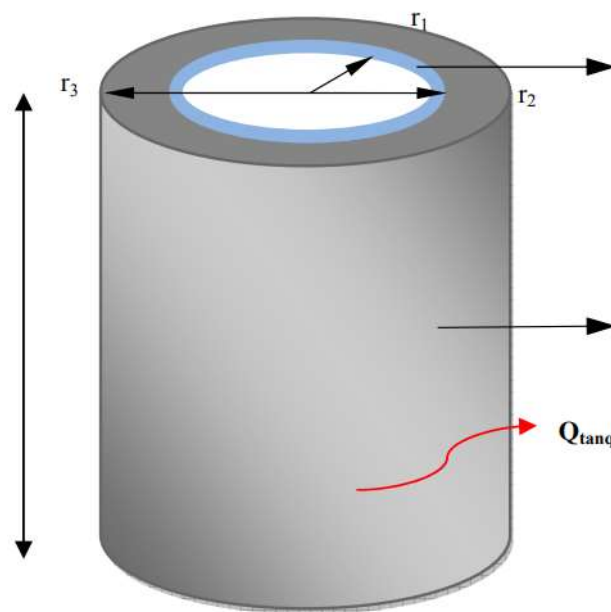


Figure 23. Diagram of the solar storage and heat losses.

Tank driving resistance:

$$R_{\text{cond. tank}} \left(\frac{K}{W} \right) = \frac{\ln \left(\frac{D_{\text{ext. steel}}}{D_{\text{int. steel}}} \right)}{2 \cdot \pi \cdot H_{\text{tank}} \cdot K_{\text{steel}}} = \frac{\ln \left(\frac{1,25}{1,245} \right)}{2 \cdot \pi \cdot 2,878 \cdot 16,3} = 1,36 \cdot 10^{-5}$$

Where:

- Dext :External diameter of tank steel (m).
- Dint:Steel inner diameter of tank (m) .
- H tank: Tank height (m).
- k steel :k Thermal conductivity of steel(W/m-K) .

Insulating conduction resistance:

$$R_{\text{tank insulating}} \left(\frac{\text{K}}{\text{W}} \right) = \frac{\ln \left(\frac{\text{Dext. insulating}}{\text{Dint. insulating}} \right)}{2 \cdot \pi \cdot H_{\text{tank}} \cdot k_{\text{insulating}}} = \frac{\ln \left(\frac{1,35}{1,25} \right)}{2 \cdot \pi \cdot 2,878 \cdot 0,038} = 1,12 \cdot 10^{-1}$$

Where:

- Dext :External diameter of the tank's insulation (m).
- Dint:Inner diameter of the tank's insulator (m).
- H tank: Tank height (m).
- k insulating: Thermal conductivity of the insulation (W/m-K).

Convection resistance of the outside air:

$$R_{\text{conv. outside air}} \left(\frac{\text{K}}{\text{W}} \right) = \frac{1}{h_{\text{outside air}} \cdot A_{\text{ext}}} = \frac{1}{h_{\text{outside air}} \cdot \pi \cdot \text{Dext. insulating} \cdot H_{\text{tank}}}$$

To calculate the convection thermal resistance, the following calculation sequence is followed:

- Determination of air properties:

To determine these properties, we must know the temperature of the room. We have considered a temperature of 24°C for the summer months and a temperature of 14°C for the winter months. The properties are shown in table 39.

Table 38. Air properties inside the engine room.

		Density (Kg/m ³)	Dynamic Viscosity (N- s/m ²)	Thermal conductivity (W/m-K)	Specific heat (J/Kg- K)	Cinematic viscosity	Pr	Thermal diffusivity
Boiler room temperature (during summer)	24	1,19	1,84E-05	0,03	1007	1,60E-05	0,73	2,11E-05
Boiler room temperature (during winter)	14	1,23	1,80E-05	0,02	1007	1,46E-05	0,73	1,99E-05

- Calculation of the number of Grashof (Gr)

$$Gr = \frac{g \cdot B \cdot (T_{\text{surface tank}} - T_{\text{engine room}}) \cdot H_{\text{tank}}^3}{\nu \cdot \alpha_{\text{air}}}$$

We will assume that at all times the surface temperature of the tank (Tt) will be 5°C higher than the temperature of the room.

- Calculation of the Nusselt number using the Churchill and Chu correlation for natural convection in vertical walls:

$$Nu = \left\{ 0,825 + \frac{0,387 \cdot Ra^{1/6}}{[1 + (0,492/Pr)^{9/16}]^{8/27}} \right\}$$

- Next, the calculation of the natural convection coefficient:

$$he \left(\frac{W}{m^2 \cdot K} \right) = \frac{Nu \cdot K}{D_{\text{ext. insulating}}}$$

The monthly values of convection resistance are shown in Table 40.

Table 39. Monthly convection resistance in the engine room (K/W)

Month	Gr	Rayleigh	Nusselt	he(W/m ² -K)	Rconvection (K/W)
January	1,39E+10	1,02E+10	250,67	4,58	0,02
February	1,39E+10	1,02E+10	250,67	4,58	0,02
March	1,39E+10	1,02E+10	250,67	4,58	0,02
April	1,39E+10	1,02E+10	250,67	4,58	0,02
May	1,16E+10	8,51E+09	236,83	4,42	0,02
June	1,16E+10	8,51E+09	236,83	4,42	0,02
July	1,16E+10	8,51E+09	236,83	4,42	0,02
August	1,16E+10	8,51E+09	236,83	4,42	0,02
September	1,16E+10	8,51E+09	236,83	4,42	0,02
October	1,39E+10	1,02E+10	250,67	4,58	0,02
November	1,39E+10	1,02E+10	250,67	4,58	0,02
December	1,39E+10	1,02E+10	250,67	4,58	0,02

Solar tank losses

The losses in the solar tank are shown in Table 41, and are calculated as:

$$Q \text{ tank losses (W)} = \frac{T_t - T_{\text{engine room}}}{R_{\text{eq.}}} = \frac{T_t - T_{\text{engine room}}}{R_{\text{cond. tank}} + R_{\text{cond. insulating}} + R_{\text{conv. air}}}$$

Table 40. Monthly heat loss from solar storage tank(W).

Month	Q tank loss(W)
January	52,53
February	92,09
March	137,71
April	166,28
May	119,13
June	161,42
July	210,62
August	217,84
September	155,49
October	171,42
November	101,40
December	58,82

Pipeline losses

The thermal losses suffered by the fluid until it reaches the solar accumulator must be evaluated

Thermal losses in the primary circuit:

- Flow pipe from solar collectors to external exchanger on the outside of the building
- Flow pipe from solar collectors to external exchanger inside the building
- Return line from external plate exchanger to solar collectors inside the building.
- Return line from external plate exchanger to solar collectors outside the building.

The thermal losses caused from the external heat exchanger to the solar accumulator (secondary circuit) have not been taken into account due to the short length of the pipe, as we will see later.

Thermal resistances of the pipes

In order to proceed with the calculation of the thermal resistances in the pipes, we must first define the nominal diameter of the pipes, thickness of the pipes, material of the pipe, insulating material and thickness of the insulator (see figure 25) (Dominguez, 2009). These elements have been sized in the section on sizing pipes and insulation. The dimensioning of the pipes and the insulation depends on the number of collectors, as well as the calculation of the thermal resistances. This section, as well as the sizing of the pipes, insulators and the resolution of the new system of equations detailed in the following section, has been carried out with 11 and 12 collectors respectively, since, as we will see below, 11 collectors have not been sufficient to cover 60% of the demand and the sections have had to be recalculated. Due to the fact that we have different sections of work, each one of them subjected to different conditions (different length of pipe, flow rate, pipe diameter, ambient temperature, thickness of insulation, etc..) we will have to take into account many global thermal resistances for the modeling of the ducts, having to solve each case separately.

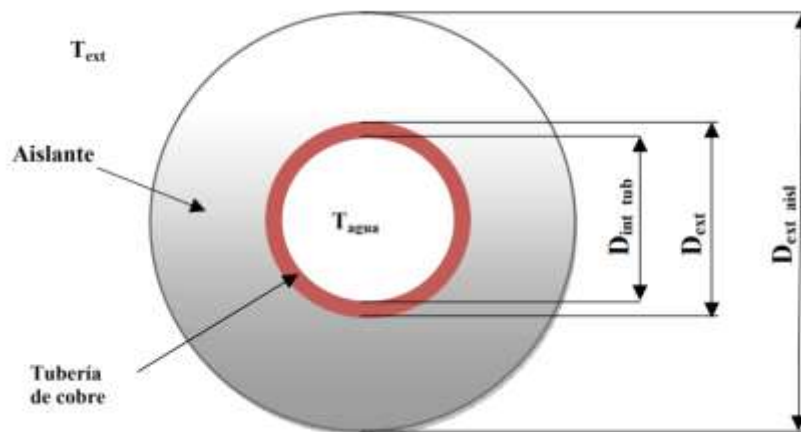


Figure 24 Piping diagram.

Convection resistance in the heat transfer fluid

$$R_{\text{conv. fluid}} \left(\frac{\text{K}}{\text{W}} \right) = \frac{1}{h_{\text{inside tube}} \cdot A_{\text{inside tube}}} = \frac{1}{h_{\text{inside tube}} \cdot \pi \cdot D_{\text{inside tube}} \cdot L_{\text{tube}}}$$

In this case the flow inside the pipes is turbulent. The correlation used is that of Dittus-Boelter.

$$\text{Nusselt} = 0,023 \cdot \text{Re}^{4/5} \cdot \text{Pr}^{1/3}$$

Pipeline conduction resistance:

$$R_{\text{conduction tubes}} \left(\frac{\text{K}}{\text{W}} \right) = \frac{\ln\left(\frac{D_{\text{ext}}}{D_{\text{int}}}\right)}{2 \cdot \pi \cdot k_{\text{tube}} \cdot L_{\text{tube}}}$$

Insulator conduction resistance:

$$\text{Rinsulating conduction} \left(\frac{K}{W} \right) = \frac{\ln\left(\frac{D_{ext}}{D_{int}}\right)}{2 \cdot \pi \cdot k_{insulating} \cdot L_{tube}}$$

Convection resistance in the outside air

$$\text{Routside air conv.} \left(\frac{K}{W} \right) = \frac{1}{h_{outside air} \cdot A_{ext}} = \frac{1}{h_{outside air} \cdot \pi \cdot D_{ext} \cdot L_{tube}}$$

To obtain the convection coefficient of the outside air we must distinguish between the two types of existing flows. The pipes circulating outside are subject to external cross-flow due to wind, while those running indoors will have a natural convection mechanism due to the stability of the air.

For forced convection we take the following correlation:

$$\text{Nusselt} = 0,193 \cdot \text{Re}^{0,618} \cdot \text{Pr}^{1/3}$$

Evaluating the Re and Pr for outdoor conditions.

As for natural convection, the correlation found is that of Churchill and Chu for horizontal cylinders:

$$\text{Nu} = \left\{ 0,6 + \frac{0,387 \cdot \text{Ra}^{1/6}}{[1 + (0,559/\text{Pr})^{9/16}]^{8/27}} \right\}^2$$

Being Rayleigh's number:

$$\text{Ra} = \text{Pr} \cdot \frac{g \cdot B \cdot (\text{Texternal surface} - T_{amb}) \cdot D_{ext}^2}{\nu_{air} \cdot \alpha_{air}}$$

The temperature of the external surface of the ducts has been estimated at 10°C above the temperature of the engine room. From the thermal resistances found for each section, the product UA of each section is calculated, which represents the inverse of the sum of the resistances of each section:

$$UA = \frac{1}{\sum R_t}$$

The heat lost on each stretch will be:

$$Q \text{ in condition x(W)} = UA_x \cdot A_{Tml} = UA_x \cdot \frac{(T_i - T_{amb}) - (T_o - T_{amb})}{\ln\left(\frac{T_i - T_{amb}}{T_o - T_{amb}}\right)}$$

9.2.3. Calculation of the catchment area with losses

Once the system losses have been determined, the system of 7 equations 7 unknowns proposed above is modified (see figures 26, 27 and 28) (Dominguez, 2009). The set of equations to be solved is the following:

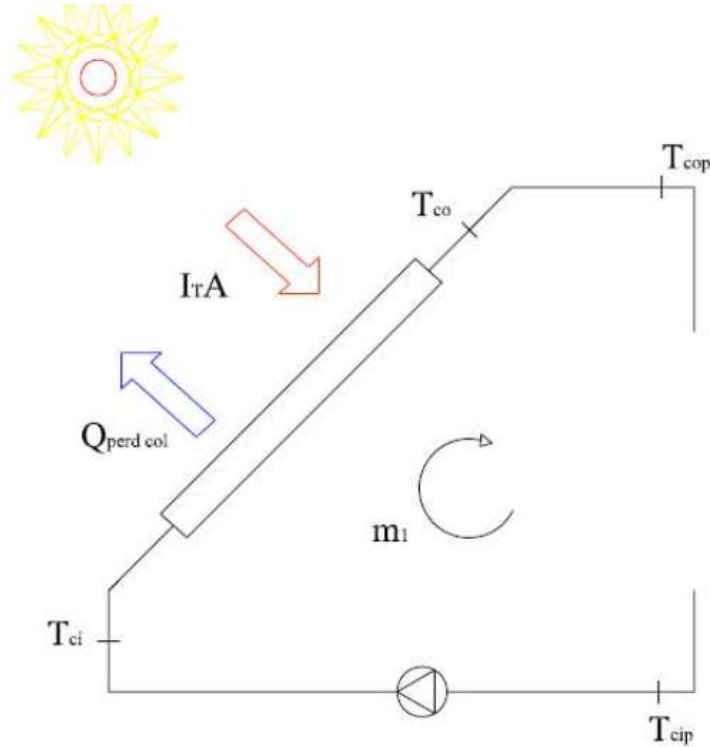


Figure 25. Energy balance in collectors with wind losses.

$$I_t \cdot A \cdot a_o - Q_{\text{lost in one collector}} \cdot N_{\text{collectors}} = m_1 \cdot C_{p1} \cdot (T_{co} - T_{ci})$$

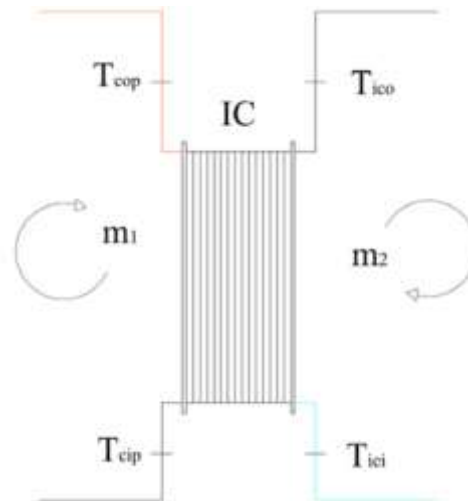


Figure 26 Energy balance in the exchanger with system losses.

$$m_1 \cdot C_{p1} \cdot (T_{cop} - T_{cip}) = m_2 \cdot C_{p2} \cdot (T_{ico} - T_{ici})$$

$$\epsilon_{ic} = \frac{m_2 \cdot Cp_2 \cdot (T_{ico} - T_{ici})}{C_{min} \cdot (T_{cop} - T_{ici})}$$

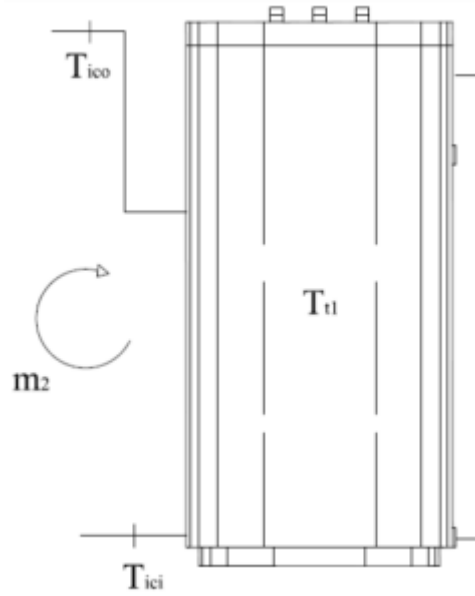


Figure 27. Energy balance in the solar accumulator with losses in the system.

$$m_2 \cdot Cp_2 \cdot (T_{ico} - T_{ici}) = m_{cons} \cdot Cp_{cons} \cdot (T_{cons} - T_{net}) + Q \text{ tank loss}$$

$$T_t = \frac{T_{ico} \cdot m_2 + T_{net} \cdot m_{cons}}{m_2 + m_{cons}}$$

$$E_t = \frac{T_{cons} - T_t}{T_{ico} - T_t}$$

$$f = \frac{m_{cons} \cdot Cp_{cons} \cdot (T_{cons} - T_{net})}{m_{cons} \cdot Cp_{cons} \cdot (T_{sum} - T_{net})} = \frac{T_{cons} - T_{net}}{T_{sum} - T_{net}}$$

$$Q_{lost \text{ leg outbound}}(W) = UA_x \cdot \frac{(T_{co} - T_{amb}) - (T_{cop} - T_{amb})}{\ln\left(\frac{T_{co} - T_{amb}}{T_{cop} - T_{amb}}\right)} = m \cdot Cp_1 \cdot (T_{co} - T_{cop})$$

$$Q_{lost \text{ leg inland}}(W) = UA_x \cdot \frac{(T_{co} - T_{room}) - (T_{cop} - T_{room})}{\ln\left(\frac{T_{co} - T_{room}}{T_{cop} - T_{room}}\right)} = m \cdot Cp_1 \cdot (T_{co} - T_{cop})$$

$$Q_{lost \text{ leg of return outside}}(W) = UA_x \cdot \frac{(T_{cip} - T_{amb}) - (T_{ci} - T_{amb})}{\ln\left(\frac{T_{cip} - T_{amb}}{T_{ci} - T_{amb}}\right)} = m \cdot Cp_1 \cdot (T_{cip} - T_{ci})$$

$$Q_{lost \text{ part of return inside}}(W) = UA_x \cdot \frac{(T_{cip} - T_{room}) - (T_{ci} - T_{room})}{\ln\left(\frac{T_{cip} - T_{room}}{T_{ci} - T_{room}}\right)} = m \cdot Cp_1 \cdot (T_{cip} - T_{ci})$$

The results obtained by solving the system of equations again have been obtained using the Mathematica program.

The annual results obtained for the 11-collector system are shown in table 42.

Table 41. Annual system simulation results with losses for 11 collectors.

Annual	A(m ²)	Tci	Tco	Tici	Tico	Tt	Tcons	Tcop	Tcip	f
	21,73	306,8	310,42	305,92	309,22	306,22	307,72	310,4	306,82	57,62%

As we can see, the losses suffered are sufficient for eleven collectors not to be enough, so we repeat the calculations for twelve collectors. By adding one more collector, the total flow of the primary circuit is different and the pipe sections can be affected, so we will recalculate the overall resistance of the six different pipe sections in the new conditions. Once recalculated, the system of equations for twelve collectors will be solved again.

The annual results obtained for the 12-collector system are shown in table 43.

Table 42. Annual system simulation results with losses for 12 collectors.

Annual	A(m ²)	Tci	Tco	Tici	Tico	Tt	Tcons	Tcop	Tcip	f
	25,92	308,76	312,37	307,87	311,18	308,15	309,66	312,36	308,77	62,95%

The monthly results of the system of equations for 12 collectors are shown in table 44.

A profile of the evolution of temperatures has been made in figure 29.

Table 43. Monthly system simulation results with losses for 12 collectors.

Month	Tci(°C)	Tco(°C)	Tcip(°C)	Tcop(°C)	Tici(°C)	Tico(°C)	Tt(°C)	Tcons(°C)	f
January	21,25	23,78	21,26	23,77	20,63	22,94	20,84	21,89	31,78%
February	26,61	29,53	26,63	29,52	25,90	28,57	26,13	27,35	43,65%
March	32,51	36,09	32,50	36,07	31,63	34,90	31,89	33,39	57,63%
April	35,89	39,89	35,91	39,88	34,92	38,57	35,24	36,90	65,63%
May	40,27	44,42	40,28	44,40	39,25	43,05	39,55	41,30	75,90%
June	45,64	50,05	45,65	50,03	44,56	48,59	44,88	46,74	90,14%
July	52,53	57,13	52,55	57,11	51,41	55,61	51,73	53,67	111,80%
August	53,91	58,11	53,93	58,09	52,89	56,72	53,17	54,95	115,91%
September	45,00	49,14	45,02	49,13	43,99	47,78	44,28	46,03	88,00%
October	36,83	40,18	36,84	40,16	36,01	39,07	36,27	37,67	64,98%
November	27,52	30,43	27,53	30,42	26,80	29,47	27,04	28,26	43,08%
December	22,03	24,59	22,04	24,58	21,40	23,75	21,62	22,68	32,05%

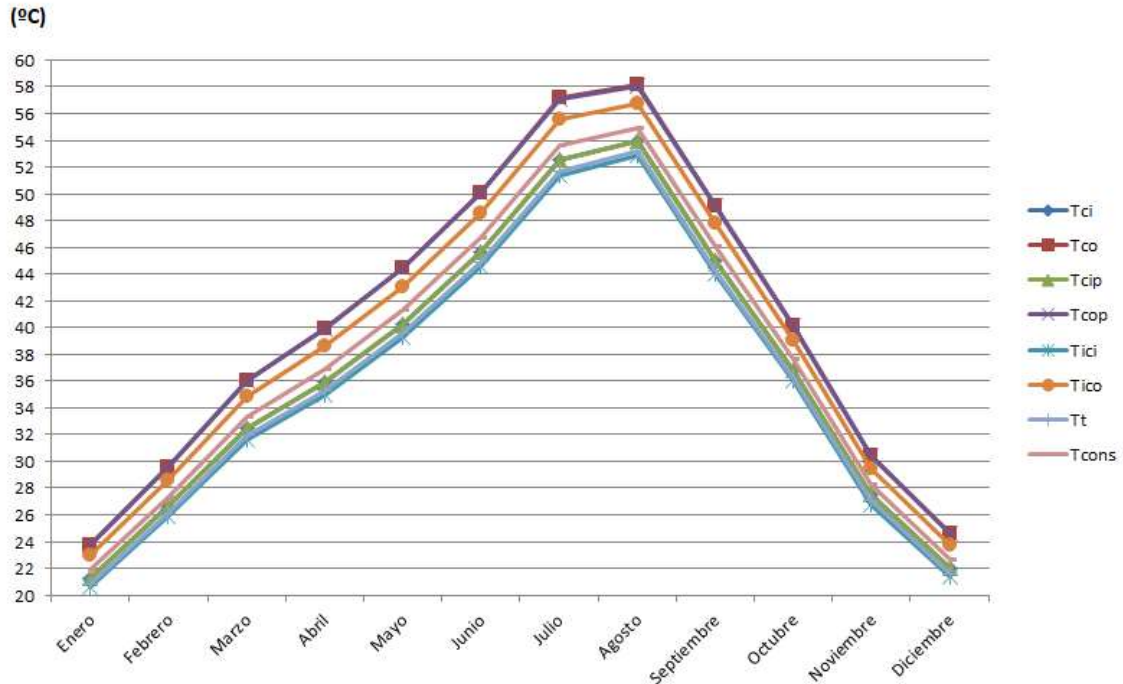


Figure 28 Evolution of monthly system temperatures (°C).

10. Comparison of methods

Once the dimensioning of the DHW collection area occupied by this project has been carried out using the heuristic method and the calculation of thermal resistances, we will draw some brief conclusions:

Both methods have shown the same catchment area value, so both methods are valid for calculating the number of panels required. For future installations the heuristic method will be used to get a fairly accurate idea of the catchment area, as it requires much less calculation. However, it has a number of limitations. Incorrect collector water temperature values are introduced, resulting in winter solar coverage far below reality, while in summer it presents values far above the permitted limits, suggesting that a powerful heat dissipation system such as an air heater will be required.

The thermal resistance method has shown much more consistent solar coverage values, exceeding the limit allowed by the CTE only in July and August. It has been determined through the Mathematica program that covering one of the collectors during those months with a blanket results in a solar coverage of less than 110% and more than 100%. Being an extremely cheap and effective correction measure, and fully validated by the CTE, this measure will be used. It has also been observed that, although the methods have shown very different monthly coverage (see figure 30), the annual solar coverage of both are very similar (see table 45).

Table 44. Comparison of results of the methods of calculation of the catchment area and annual solar fraction.

Calculation methods	Catchment area(m2)	Number of collectors	Annual solar fraction
Heuristic	25,92	12	62%
Thermal resistors	25,92	12	63%

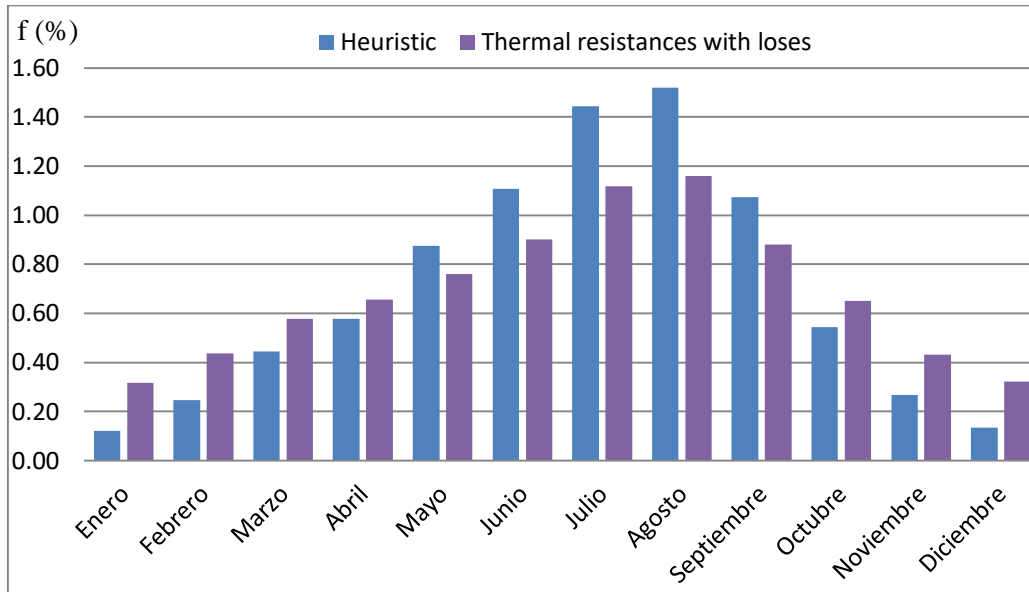


Figure 29 Monthly differences of the solar fraction of the methods used.

11. Lost due to shadows, orientation and inclination

The CTE specifies that losses due to orientation, inclination and possible shadows must be lower than the limits in Table 46.

Table 45 Maximum allowable losses.

Case	Orientation and inclination	Shadows	Total
General	10%	10%	15%
Overlay	20%	15%	30%
Architectural Integration	40%	20%	50%

- Architectural integration: the collectors fulfil an energy function and replace conventional building elements
- Overlapping: the placement of the collectors is parallel to the building envelope

- General case: all other situations.

Our project deals with a general case, as can be seen in Figure 31.

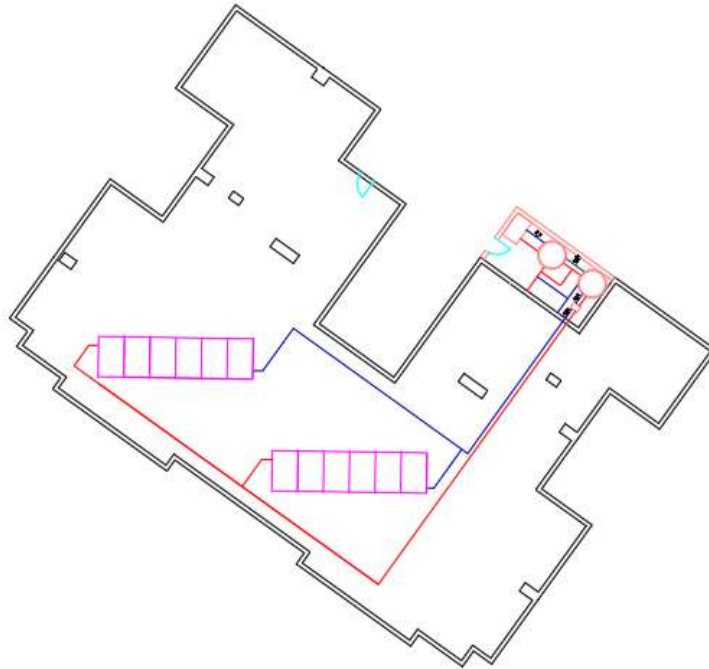


Figure 30 Plan of the terrace. Representation of the elements of the primary circuit and engine room. Own elaboration.

The orientation (α) of the solar collectors is always towards the Earth's equator, so in our case it means south orientation (figure 32).

The tilt angle (β) is that which forms the surface of the module with the horizontal plane (Figure 32). The optimal inclination of the collectors depends on the period of use:

- Constant annual consumption: the geographical latitude.
- Preferential consumption in winter: geographical latitude + 10°.
- Preferential consumption in summer: geographical latitude - 10°.

In our case it is an annual consumption of DHW, and the inclination of the collectors will be 40°, very close to the latitude of the place.

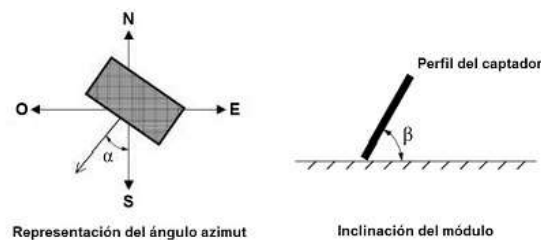


Figure 31 Azimuth angle and inclination of sensors.

Losses due to orientation and tilt can easily be obtained from Figure 33.

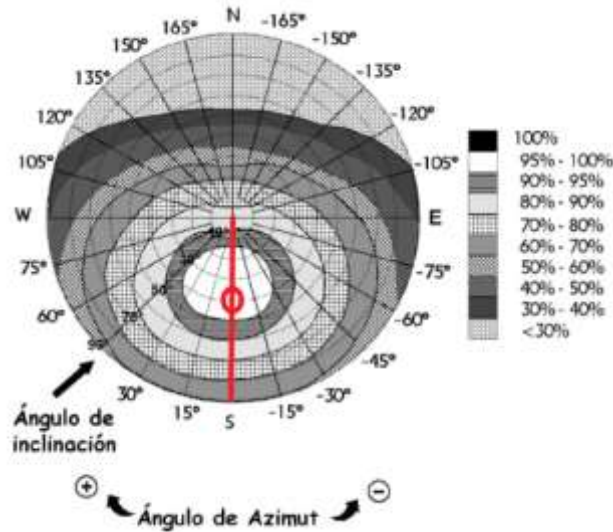


Figure 32 Percentage representation of slope and orientation losses of the collectors.

This figure is valid for a latitude (Φ) of 41° , very close to that of our case (41.4°).

The calculation of the losses by inclination and orientation is made with the following formula:

$$\begin{aligned} \text{Loses}(\%) &= 100 \cdot [1,2 \cdot 10^{-4} \cdot (\beta - \beta_{\text{optimum}})^2 + 3,5 \cdot 10^{-5} \cdot \alpha^2] \\ &= 100 \cdot [1,2 \cdot 10^{-4} \cdot (40 - 41,4)^2 + 3,5 \cdot 10^{-5} \cdot 0^2] = 2,35 \end{aligned}$$

Tilt and orientation losses are within the 10% limit.

To calculate the loss of shadows, the distance between the elements of the installation must be taken into account, as well as the distance from other external objects that could cast shadows on our sensors, as shown in figure 34.

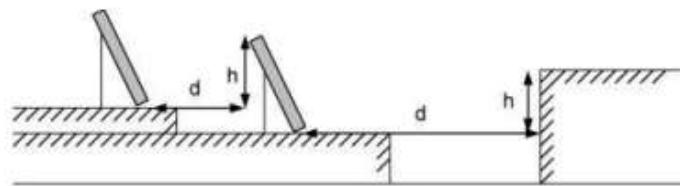


Figure 33 Distance between rows of sensors and nearby obstacles.

The distance d , measured on the horizontal, between a row of collectors and an obstacle of height h , which can produce shadows on the installation, must be

$$d = h / \tan(61^\circ - \text{latitude})$$

Due to space problems, and to prevent losses due to shadows exceeding the established limits, the collectors must be located on an 80 cm concrete floor. The height of the inclined collectors is 122.63 cm. From this value, and for a wall height of 140 cm, the distance between the wall

and the rows of collectors must be a minimum of 135.56 cm. The distance between rows of collectors must be a minimum of 3.35 cm. All distances are shown in Figure 35.

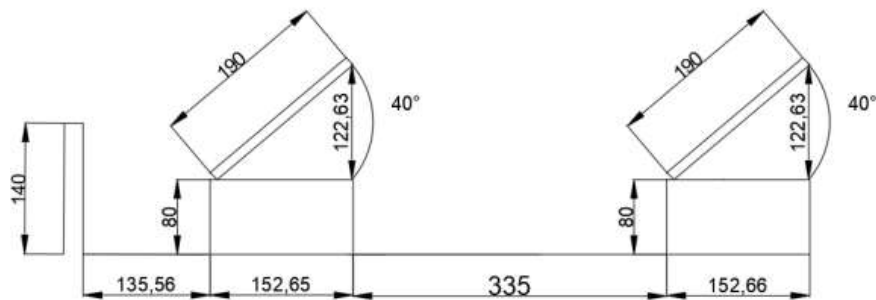


Figure 34 Distance between rows of collectors and nearby obstacles taken at our facility. Own elaboration.

Shadows cast by buildings or large surrounding obstacles must also be taken into account. To do this we must compare the "profile" of the obstacles that will cast a shadow on our panels, with the diagram of apparent trajectories of the sun. To make this profile it is necessary to know the angles of azimuth and inclination of the obstacles with respect to a reference point in the plane, which will be located in the centre of each of the battery sets (tables 47 and 48).

Table 47. Azimuth and elevation angle of the left building from the nearest collector array.

6 PANEL SET					
POINT	X	Y	Z	ANGLE(°)	ANGLE OF ELEVATION(°)
P1	-3,70	8,40	3,00	24,00	17,00
P2	2,10	16,70	3,00	-7,00	17,00
P3	2,10	16,70	0,00	-7,00	0,00
P4	-3,70	8,40	0,00	24,00	0,00

Table 46. Azimuth and elevation angle of the right building to the nearest collector array

6 PANEL SET					
POINT	X	Y	Z	ANGLE (°)	ANGLE OF ELEVATION(°)
P1	6,00	17,20	4,00	-109,00	25,00
P2	6,80	-9,00	4,00	-37,00	25,00
P3	6,80	-9,00	0,00	-37,00	0,00
P4	6,00	17,20	0,00	-109,00	0,00

Once we have obtained the coordinates of azimuth and elevation, we can represent the shadow profile on the diagram of the trajectory of the sun (figure 36).

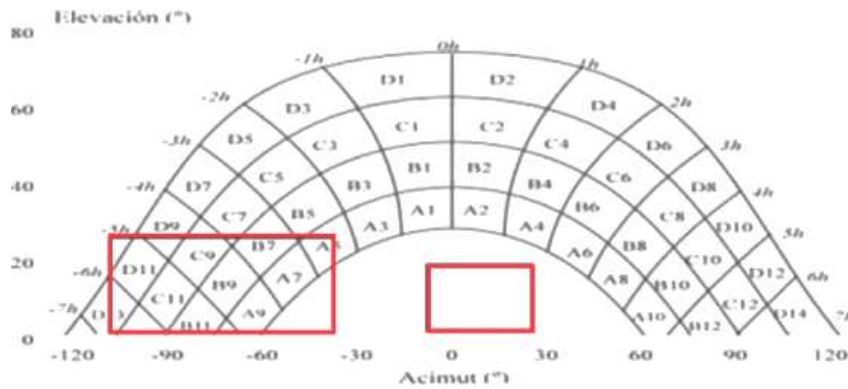


Figure 35. Solar trajectory diagram.

Then, to calculate the % of losses due to shadows, we must consult the reference tables. Select the table whose azimuth and elevation coordinates most closely resemble your own. In our case this corresponds to table 5-J, represented as table 49.

Table 47. Percentage of losses for each quadrant of the solar diagram.

Tabla 5-J

$\beta = 35^\circ$ $\alpha = -60^\circ$	A	B	C	D
13	0,00	0,00	0,00	0,56
11	0,00	0,04	0,60	2,09
9	0,27	0,91	1,42	3,49
7	1,51	1,51	2,10	4,76
5	2,25	1,95	2,48	5,48
3	2,80	2,08	2,56	5,68
1	2,78	2,01	2,43	5,34
2	2,32	1,70	2,00	4,59
4	1,52	1,22	1,42	3,46
6	0,62	0,67	0,85	2,20
8	0,02	0,14	0,26	0,92
10	0,02	0,04	0,03	0,02
12	0,00	0,01	0,07	0,14
14	0,00	0,00	0,00	0,12

The total shade loss will be equal to the sum of the quadrants within the red area, considering the losses of some quadrants as partial (75%, 50% and 25% respectively)

$$S. \text{ losses}(\%) = 1 \cdot (0,27 + 1,51 + 0,91 + 0,6 + 2,09) + 0,75 \cdot 1,42 + 0,5 \cdot (2,25 + 1,51 + 0,04 + 0,56) + 0,25 \cdot 3,49 = 9,5$$

Shadow losses are within the 10% limit. The total sum of losses amounts to 12%, which is an acceptable value for the general case. (Miralles, 2013)

12. Sizing of the installation

12.1. Dimensioning the support system

The dimensioning of the support system must be done for the most unfavorable case, assuming a zero solar contribution.

12.1.1. Dimensioning of the DHW storage tank

According to the ETC, section HS4, the volume of the tank shall be calculated according to the expected time of use, applying the following expression:

$$V = Q \cdot t \cdot 60$$

Where:

V is the volume of the tank [L]

Q is the maximum simultaneous flow rate of the building [dm³ /s]

t is the estimated time (from 15 to 20) [min].

Process of calculating the simultaneous maximum flow of the building

- Determination of the instantaneous flow of each device. The CTE establishes the following flow rates per device (Table 50):

Table 48. Instantaneous flow rates of consumer appliances (dm³/s).

CAUDALES INSTANTANEOS MINIMOS DE SUMINISTRO PARA CADA TIPO DE APARATO:	Tipo de aparato	Caudal instantáneo mínimo de agua fría [dm ³ /s]	Caudal instantáneo mínimo de ACS [dm ³ /s]
		Lavamanos	0,05
	Lavabo	0,10	0,07
	Ducha	0,20	0,10
	Bañera de 1,40 m o más	0,30	0,20
	Bañera de menos de 1,40 m	0,20	0,15
	Bidé	0,10	0,07
	Inodoro con cisterna	0,10	-
	Fregadero doméstico	0,20	0,10
	Lavavajillas doméstico	0,15	0,10
	Lavadero	0,20	0,10
	Lavadora doméstica	0,20	0,15
	Grifo aislado	0,15	0,10
	Grifo garaje	0,20	-

- Determination of the flow rate installed in each house (tables 51 and 52):

It is equivalent to the sum of the minimum installed flow rates of each device, taken from the table in the previous section.

Table 49. Instantaneous flow of type A housing.

Type A housing			
Devices	Individual instantaneous flow (dm ³ /s)	Number	Instantaneous flow (dm ³ /s)
Hand washers	0,03	2	0,06
Basin	0,065	2	0,13
Shower	0,10	1	0,10
Bathtub of 1,4 or more	0,20	1	0,20
Bide	0,065	1	0,065
Household sink	0,10	1	0,10
Domestic dishwasher	0,10	1	0,10
Domestic washing machine	0,15	1	0,15
Isolated tap	0,10	1	0,10
Total		11	1,005

Instantaneous flow for type A homes: $1,005 \left(\frac{\text{dm}^3}{\text{s}} \right)$.

Table 50. Instantaneous flow type B homes.

Type B housing			
Devices	Individual instantaneous flow (dm ³ /s)	Number	Instantaneous flow (dm ³ /s)
Hand washers	0,03	1	0,03
Basin	0,065	1	0,065
Shower	0,10	1	0,10
Bathtub of 1,4 or more	0,20	1	0,20
Bide	0,065	1	0,065
Household sink	0,10	1	0,10
Domestic dishwasher	0,10	1	0,10
Domestic washing machine	0,15	1	0,15
Isolated tap	0,10	1	0,10
Total		9	0,91

Instantaneous flow for type B homes: $0,91 \left(\frac{\text{dm}^3}{\text{s}} \right)$.

- Determination of the simultaneity coefficient for each type of housing:

$$Kv \text{ home} = \frac{1}{\sqrt{n-1}}$$

Where:

KV: Simultaneity coefficient for a dwelling (non-dimensional)

n: Number of appliances inside the dwelling.

$$Kv \text{ home A} = \frac{1}{\sqrt{n-1}} = \frac{1}{\sqrt{11-1}} = 0,316$$

$$Kv \text{ home B} = \frac{1}{\sqrt{n-1}} = \frac{1}{\sqrt{9-1}} = 0,353$$

- Determination of the simultaneous flow rate for each type of dwelling:

Knowing the simultaneity coefficients, we can already calculate the simultaneous or maximum flow for each type of dwelling as

$$Q_{\max} = Kv \cdot Qi$$

Where:

Q_{\max} : Maximum or simultaneous flow for a house $\left(\frac{\text{dm}^3}{\text{s}}\right)$

KV: Simultaneity coefficient for a house (non-dimensional)

Qi : Installed flow in each house $\left(\frac{\text{dm}^3}{\text{s}}\right)$

$$Q_{\max} \text{ home A} = 1,005 \cdot 0,316 = 0,318 \left(\frac{\text{dm}^3}{\text{s}}\right)$$

$$Q_{\max} \text{ home B} = 0,91 \cdot 0,353 = 0,322 \left(\frac{\text{dm}^3}{\text{s}}\right)$$

- Normalization of the maximum or simultaneous flow of the houses:

In this case there are two different types of housing, with two different maximum flows. As to apply the simultaneity to a set of the dwellings, all of them must be equal, we must obtain an equivalent type of supply. We will carry out the weighted average of the maximum flows:

$$Q_{\max. \text{ homes}} = \frac{Q_{\max. \text{ type A}} \cdot N_{\text{dwellings A}} + Q_{\max. \text{ type B}} \cdot N_{\text{dwellings B}}}{N_{\text{dwellings A}} + N_{\text{dwellings B}}} = \frac{0,318 \cdot 12 + 0,322 \cdot 8}{20} = 0,319 \left(\frac{\text{dm}^3}{\text{s}}\right)$$

- Determination of the building's simultaneity coefficient:

As a previous step to the calculation of the maximum flow of the building, we calculate the simultaneity coefficient of the building (or the set of houses), using the following equation:

$$K_e = \frac{19 + N}{10 \cdot (N + 1)}$$

Where:

KE: Simultaneity coefficient of the building (non-dimensional)

N: Number of dwellings in the building.

For our building of 20 houses we get the following value:

$$K_{e \text{ building}} = \frac{19 + N}{10 \cdot (N + 1)} = \frac{19 + 20}{10 \cdot (20 + 1)} = 0,186$$

It is advisable not to consider simultaneity coefficients of a building lower than 0.2. We take a value of 0.2.

- Maximum or simultaneous flow of the building:

$$Q_{\text{max building}} = K_e \text{ building} \cdot N \cdot \text{homes} \cdot Q_{\text{max. homes}} = 0,186 \cdot 20 \cdot 0,319 = 1,278 \left(\frac{\text{dm}^3}{\text{s}} \right)$$

With this flow rate we will size the DHW tank. (Miranda, Simultaneous flow calculation in a residential building, 2004)

Determination of the volume of the DHW storage tank:

$$V. \text{ accumulator DHW(L)} = Q \text{ simultaneous of the building} \cdot t - 60 = 1,278 \cdot 17,5 \cdot 60 = 1341,39$$

We will select an accumulator of the brand Suicasa model IV of stainless steel AISI 316, with a total volume of accumulation of 1500L. The characteristics of the equipment can be seen in the appendix.

12.1.2. Dimensioning of the auxiliary boiler

For the sizing of the auxiliary boiler and due to the fact that we are looking for a single device for the purposes it must serve, in this case DHW, we will have to take into account the maximum thermal demand necessary, which occurs in the month of January. The boiler will be designed so that it is capable of covering the entire DHW demand, in the most extreme case where the installation cannot provide energy from the sun in the month of maximum demand. The first step to be able to select the boiler is to know its useful power, which is detailed through the following expression:

$$P.\text{useful(KW)} = \frac{V.\text{acumulator DHW} \cdot C_e \cdot (TDHW - T_{\text{net}})}{t} = \frac{1500 \cdot 4,18 \cdot (50 - 8,8)}{3600} = 64,17$$

Where:

- Puseful: Useful power of the boiler in Kw.
- Cp: Specific water heat kJ/(kg·°C).
- Vacuumator DHW: Conventional accumulation volume in liters.
- TDHW: DHW preparation temperature in °C.
- Tnet: Cold water temperature of the network in °C.
- t: Preparation time (1 hour approximately).

The boiler output will be greater than the useful power obtained, due to heat losses in the boiler, storage and circuit which are estimated at approximately 25%, as well as deviations in consumption during some peak periods with respect to the foreseen averages, which make it advisable to increase the output by an additional 15%. Therefore the power to be installed will be:

$$P.\text{installed} = 1,4 \cdot P.\text{useful} = 89,84(\text{KW})$$

This is the power required to select the boiler. A boiler of the manufacturer Baxiroca model CPA-100BTH of 100 KW has been selected. The characteristics of the equipment can be seen in the appendix.

12.2. Dimensioning of pipes

12.2.1. Method of sizing the pipes

For DHW circuits, the fluid flow rate must be between the following values:

- metal pipes: between 0.50 and 2.00 m/s
- thermoplastic and multilayer pipes: between 0.50 and 3.50 m/s

We calculate the inside diameter of the tube from an initial velocity within the range:

$$D = \sqrt{(4 \cdot Q) / (v_0 \cdot \pi)}$$

Where:

Q: The flow rate of the pipe section (m³/s).

v₀: initial velocity taken to determine the internal diameter (m/s).

D: internal diameter of the pipe(m).

It must be taken into account that there may be bifurcations and branches in the circuit, so the flow rate through each of them must be determined, as there will be sections of different diameters and speeds. To know the internal and external diameter of the pipes, we observe in table 53 (Energy Efficiency) the values available for copper pipes, material that we selected for our installation:

Table 51. Internal and external diameters of copper pipes.

Diámetro exterior nominal	Espesores					
	0.75	1	1.2	1.5	2	2.5
	Diámetro interior					
6	4,5	4				
8	6,5	6				
10	8,5	8				
12	10,5	10				
15	13,5	13				
18	16,5	16				
22		20	19,6	19		
28		26	25,6	25		
35		33	32,6	32		
42		40	39,6	39		
54			51,6	51		
63				60	59	
80				77	76	
100					96	95

Once the internal diameter of our pipe has been selected, we calculate a new velocity:

With the selected diameter, we determine the new working speed:

$$v = \frac{(4 \cdot Q)}{(\pi \cdot D^2)}$$

If it is within the permitted range, with the value of the internal diameter obtained and the working flow rate we determine the friction losses in copper pipe from figure 37.

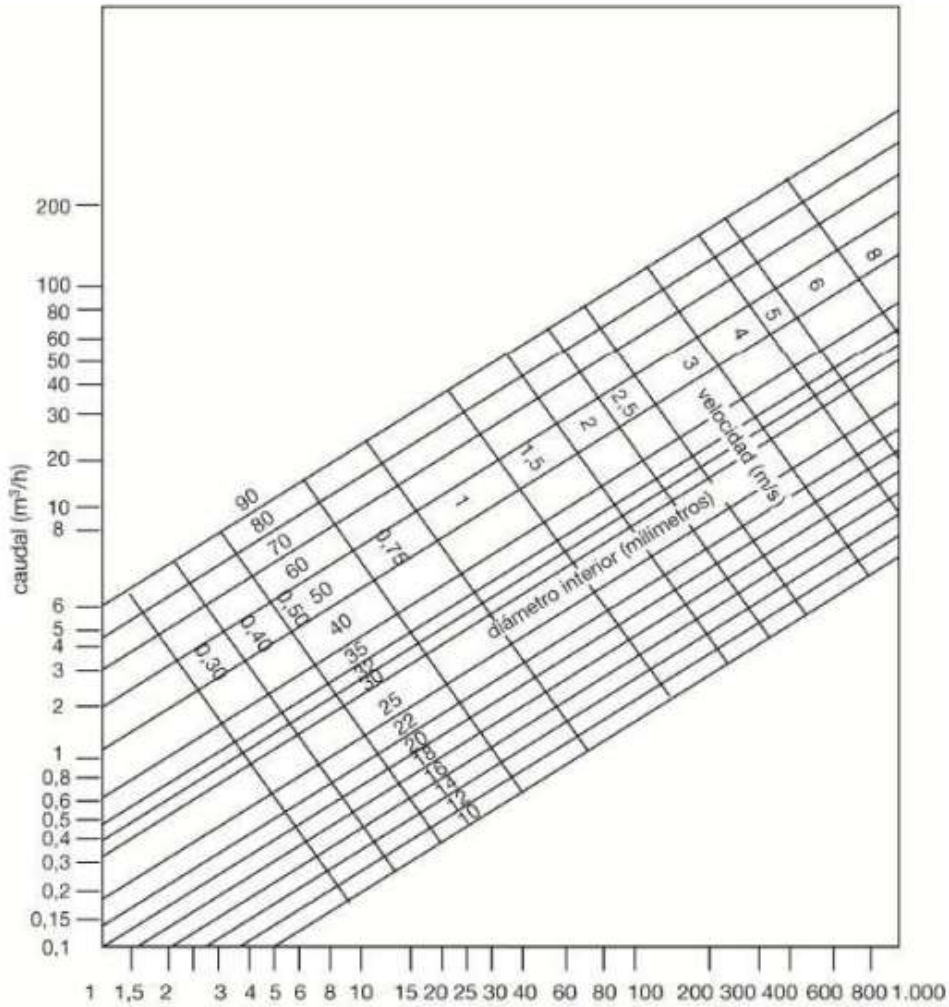


Figure 36 Diagram of friction losses in copper pipe.

According to the CTE section HS4, the losses per meter of pipe should not exceed 40mm.c.a. If it is higher, the pipe should be resized with a new speed. (Ponce, 2013) We then proceed to size the pipes of each of our working circuits.

12.2.2. Sizing of pipes per circuit

Primary circuit

The sizing of the pipes in our primary circuit is summarized in figure 38.

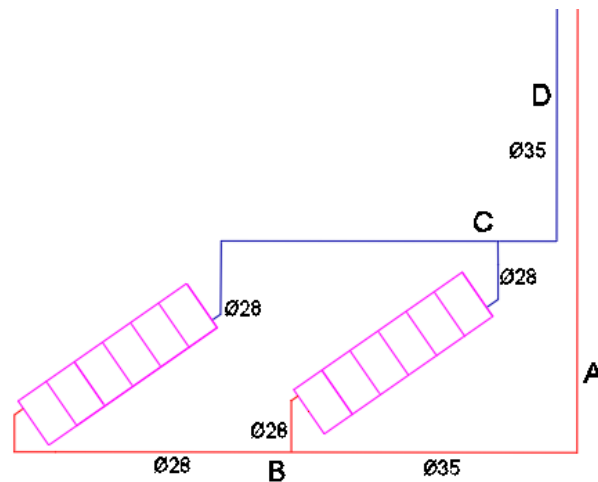


Figure 37 Primary circuit diagram. Own elaboration.

Table 52. Dimensioning of the primary circuit pipes.

PRIMARY LOOP	L. pipe	Flow (m ³ /h)	v leg(m /s)	d.int (mm)	mm.c.a per meter	mm.c.a/m mixture 30% propylene glycol
Hot stretch outside hot a-b	24,00	1,81	0,63	32,00	11,00	14,30
Outdoor hot section first battery	2,00	0,91	0,51	25,00	15,00	19,50
Outdoor hot section second battery	11,00	0,91	0,51	22,00	17,00	22,10
Cold outer section c-d	9,00	1,81	0,63	32,00	11,00	14,30
Cold outer section first battery	2,50	0,91	0,51	25,00	15,00	19,50
Cold outer section second battery	13,00	0,91	0,43	22,00	17,00	22,10
Interior hot section	1,00	1,81	0,63	32,00	11,00	14,30
Interior cold section	1,00	1,81	0,63	32,00	11,00	14,30

The total flow rate of the circuit has been defined by the recommended flow rate per collector (70L/m²-h):

$$Q = Q_{\text{collector}} \cdot A \cdot N$$

Where:

- Q: the flow rate of the primary circuit (l/h).
- Q collector: the unit flow rate of the collector (L/h-m²).
- A: the area of the collector (m²).
- N: number of collectors.

The total circuit flow for the 12-collector system is 1814.4 L/h, which is equivalent to 1.81(m³/h). These are divided equally for the two groups of collectors (batteries), so the pipe diameter is altered. We can see that the velocities obtained are within the limit and the load losses per meter of pipe are also within the limit. Since the copper pipe load loss diagram is intended for water, a correction factor of 1.3 is applied to determine the losses per meter of heat transfer fluid. All sizing conditions are met (see Table 54).

Secondary circuit

As the total flow rate through the primary circuit is equivalent to that of the secondary circuit, the diameters of the secondary circuit are 32mm, the velocity is 0.63 m/s and the pressure losses per meter are 11mm.c.a., as the fluid circulating in the secondary circuit is water. All the dimensioning conditions are met.

Support circuit

The flow rate that circulates through the support system in the most unfavorable month, for which the system has been sized, is 1.88m³/h, as will be seen in the section on sizing the support system. An internal pipe diameter of 22mm has been selected, so the speed is 1.37m/s and the pressure losses per meter are 23mm.c.a. All the dimensioning conditions are met.

Return circuit

In compliance with the provisions of Section HS 4 of the CTE, the DHW distribution network must be equipped with a return network when the length of the pipe to the furthest point of consumption is equal to or greater than 15 m, a situation that occurs in this project. In any case, the recirculation flow must be at least 10% of the feed water, the minimum return diameter must be at least 16 mm and the thermal losses from the furthest point must not exceed 3°C. In our case we have determined a return of 15% of the feed water, thus obtaining a return flow of 0.69 m³/h. An internal diameter of 20mm has been selected, so that the recirculation speed is

0.61m/s and the pressure loss per meter is 23. All the dimensioning conditions are met. (Díaz, 2018)

12.3. Dimensioning the pipe insulation

The thickness of the insulation is defined by RITE in Figure 39 (José) as a function of where the pipe runs (inside or outside the building), for a reference material with a thermal conductivity of 0.04(W/m·°C) at 10°C.

ESPESOR (mm) AISLAMIENTO TERMICO		
DIAMETRO EXTERIOR TUBERIA (mm)	ACS	
	INTERIOR	EXTERIOR
D ≤ 35	30	40
35 < D ≤ 60	35	45
60 < D ≤ 90	35	45
90 < D ≤ 140	35	45
140 < D	40	50
$\lambda_{ref} = 0,040 \text{ (W/m} \cdot \text{K) a } 10^{\circ}\text{C}$		

Figure 38 Minimum insulation thicknesses for DHW pipes.

For insulation materials with a conductivity λ different from 0.040 (W/m-K) at 10 °C, the RITE indicates the following expression for the calculation of the minimum thickness e:

$$e = \frac{D_i}{2} \cdot \left[\exp \left(\frac{\lambda}{0,04} \cdot \ln \frac{D_i + 2 \cdot e_{ref}}{D_i} \right) - 1 \right]$$

Where:

e: minimum insulation thickness in mm.

e_{ref}: minimum thickness of insulation, in mm (according to the table above).

D_i: inner diameter of the insulation, in mm.

λ : Thermal conductivity of the insulation material, in (W/m-K).

As we have different outer pipe diameters, the thickness required is different for each of them:

- 35mm outside diameter pipes-Minimum thickness of 35.1mm. 40mm will be used.
- 28mm outside diameter pipes - minimum thickness 25.7mm. One of 32mm will be used.
- Internal pipes of 35mm external diameter - minimum thickness of 26.58mm. One of 32mm will be used.

- Inner pipes of 25mm outer diameter - minimum thickness of 26.28mm. One of 32mm will be used.
- 22mm outside diameter inner pipes - minimum thickness 26.14mm. One of 32mm will be used.

For our installation we will use an insulation of 0.037 (W/m-K) at 10°C mm, which is the flexible tubular insulation M1 of Salvador Escoda. The characteristics of the same can be consulted in the appendix.

12.4. Dimensioning of the solar storage tank

The ETC specifies that the volume of the solar storage tank must be between the following values:

$$50 \leq \frac{V}{A} \leq 180$$

Where A is the catchment area and V is the accumulation volume.

Since we have a total of 12 collectors, the collection area is 25.92 m². It is recommended that the accumulation volume be enough to store the total daily consumption. January is the month with the highest daily consumption, with a total of 2566.9L/day. We therefore select an accumulation volume of 3000L. (HE 4)

$$50 < \frac{3000}{25,92} < 180 \rightarrow 50 < 115,74 < 180 \rightarrow \text{Cumple el CTE}$$

We chose the Suicasa DV/AISI 316 stainless steel solar accumulator. The properties of the accumulator can be seen in the appendix.

12.5. Dimensioning of the plate heat exchanger

The CTE in section 3.3.4 of the "HE Basic Document on Energy Saving" establishes that the minimum heat exchanger power must comply with the following ratio:

$$Q_{min} \geq 500 \cdot A$$

Where:

Q_{min} = Minimum heat exchanger power (W).

A = Area of collectors (m²).

Therefore the minimum power required for our installation will be:

$$Q_{min}(W) = 500 \cdot 25,92 = 12960$$

The selected model is the Suicasa IP3705. The characteristics of the equipment can be seen in the appendix. The following method is available to determine the minimum number of plates required:

Effective temperature difference method:

The aim of this method is to calculate the value of the overall heat transfer coefficient of the exchanger (U). This method states that the total heat flow transferred between the hot and cold fluids when passing through a plate heat exchanger can be expressed as:

$$Q = U \cdot A \cdot F \cdot \Delta T_m$$

Where

-U is the overall heat transfer coefficient (W/m²·°C).

-A is the total transfer area (m²).

-F is the factor that takes into account that the ends of the exchanger have half the surface area and transfer less heat (F countercurrent = 1).

- ΔT_m is the logarithmic mean temperature because the temperature difference between the two fluids is not constant throughout the exchanger (K).

Calculation process

- Determination of mass expense in each channel:

$$m_{\text{primary channel}} = \frac{m_{\text{primary}}}{\left(\frac{N_{\text{plates}} - 1}{2}\right)} = \frac{5,11 \cdot 10^{-1}}{\left(\frac{12 - 1}{2}\right)} = 9,28 \cdot 10^{-2} \left(\frac{\text{Kg}}{\text{s}}\right)$$

$$m_{\text{secondary channel}} = \frac{m_{\text{secondary}}}{\left(\frac{N_{\text{plates}} - 1}{2}\right)} = \frac{5,11 \cdot 10^{-1}}{\left(\frac{12 - 1}{2}\right)} = 9,28 \cdot 10^{-2} \left(\frac{\text{Kg}}{\text{s}}\right)$$

-With 12 plates on the hot side of the exchanger (primary circuit) and 12 plates on the cold side (secondary circuit).

-The number of plates required is an iterative process. A minimum of 24 plates (22 usable plates) are required in our exchanger.

- Determination of the area of the channels (A.channel)

$$A. \text{ channel} = b \cdot w = 0,0025 \cdot 0,314 = 7,85 \cdot 10^{-4} (\text{m}^2)$$

To know the section of the channel, we will need the width of the exchanger (w) and the distance between plates or width of the channel (b). These data are obtained from the technical characteristics of the exchanger, according to the manufacturer's sheet (see annex)

- Determination of the fluid flow speed inside the channels:

$$v \text{ primary channel} = \frac{m_{\text{primary channel}}}{\rho_{\text{glicol}} \cdot A_{\text{channel}}} = \frac{9,28 \cdot 10^{-2}}{1015 \cdot 7,85 \cdot 10^{-4}} = 0,117 \left(\frac{\text{m}}{\text{s}}\right)$$

$$v \text{ secondary channel} = \frac{m_{\text{secondary channel}}}{\rho_{\text{agua}} \cdot A_{\text{channel}}} = \frac{9,28 \cdot 10^{-2}}{1000 \cdot 7,85 \cdot 10^{-4}} = 0,118 \left(\frac{\text{m}}{\text{s}}\right)$$

- Determination of the characteristic length:

$$l_c = \frac{4 \cdot A. \text{ channel}}{P_c} \cong \frac{4 \cdot b \cdot w}{2 \cdot (b + w)} = \frac{4 \cdot 0,0025 \cdot 0,314}{2 \cdot (0,0025 + 0,314)} = 4,96 \cdot 10^{-3} (\text{m})$$

Where:

A_c is the area of the channel (m²).

P_c is the perimeter of the channel (m).

- Determination of Reynolds' number:

$$\text{Reynolds primary channel} = \frac{v. \text{ primary channel} \cdot l_c \cdot \rho_{\text{glicol}}}{\mu_{\text{glicol}}} = \frac{0,117 \cdot 4,96 \cdot 10^{-3} \cdot 1015}{0,002} = 293,34$$

$$\text{Reynolds secondary channel} = \frac{v. \text{ secondary channel} \cdot l_c \cdot \rho_{\text{water}}}{\mu_{\text{water}}} = \frac{0,118 \cdot 4,96 \cdot 10^{-3} \cdot 1000}{8,95 \cdot 10^{-4}} = 655,5$$

- Determination of the Prandtl number:

$$\text{Pr hot side} = \frac{\mu_{\text{glycol}} \cdot C_{p\text{glycol}}}{k_{\text{glycol}}} = \frac{0,002 \cdot 3850}{0,48} = 16,04$$

$$\text{Pr cold side} = \frac{\mu_{\text{water}} \cdot C_{p\text{water}}}{k_{\text{water}}} = \frac{8,95 \cdot 10^{-4} \cdot 4180}{0,58} = 6,45$$

- Determination of the Nusselt number:

For the calculation of convection coefficients we will use the following correlation for turbulent flow, since plate corrugations generate turbulence:

$$\text{Naked hot side} = 0,4 - \text{Pr}^{0,4} \cdot \text{Re}^{0,64} = 0,4 \cdot 16,04^{0,4} \cdot 293,34^{0,64} = 46,05$$

$$\text{Nu cold side} = 0,4 - \text{Pr}^{0,4} \cdot \text{Re}^{0,64} = 0,4 \cdot 6,45^{0,4} \cdot 655,5^{0,64} = 53,52$$

- Determination of the convection coefficient:

$$h \text{ hot side} \left(\frac{\text{W}}{\text{m}^2 \cdot \text{K}} \right) = \frac{\text{Nu} \cdot k_{\text{glycol}}}{l_c} = \frac{46,05 \cdot 0,48}{4,96 \cdot 10^{-3}} = 4456,44$$

$$h \text{ cold side} \left(\frac{\text{W}}{\text{m}^2 \cdot \text{K}} \right) = \frac{\text{Nu} \cdot k_{\text{agua}}}{l_c} = \frac{53,52 \cdot 0,58}{4,96 \cdot 10^{-3}} = 6257,43$$

- Determination of the logarithmic temperature increase

$$\Delta T_{\text{ml}} = \frac{(T_{\text{co}} - T_{\text{ico}}) - (T_{\text{ci}} - T_{\text{ici}})}{\ln \left(\frac{(T_{\text{co}} - T_{\text{ico}})}{(T_{\text{ci}} - T_{\text{ici}})} \right)}$$

We will choose the most unfavorable month in terms of the higher power required in the exchanger to ensure its correct operation. Given that the month with the greatest solar coverage and highest temperatures is July, we will make the calculations using the temperature data for that month.

- Determination of the heat transmission coefficient:

$$U \left(\frac{\text{W}}{\text{m}^2 \cdot \text{K}} \right) = \frac{1}{\frac{1}{h_c} + \frac{e_{\text{plate}}}{k_{\text{plate}}} + \frac{1}{h_f} + R_{\text{dirt}}} = \frac{1}{\frac{1}{4456,44} + \frac{0,001}{15} + \frac{1}{6257,43} + 3 \cdot 10^{-5}} = 2079,56$$

Where:

- h_c :Heat transfer coefficient by convection of the hot fluid (W/m²-K)
- h_f :Heat transfer coefficient by convection of the cold fluid (W/m²-K).
- e :exchanger plate thickness (m).
- k :thermal conductivity of the plate material (W/m-K).
- R_{dirt} :heat resistance caused by contaminants in the fluids that are deposited on the plate surfaces (K /W).

- Determination of the exchange surface:

$$A_{\text{exchange}}(\text{m}^2) = (N_{\text{plates}} - 2) \cdot \text{useful area per plate} = (24 - 2) \cdot 0,25 = 5,5$$

The end plates are not involved in the heat exchange of the fluids.

- Determination of the power of the exchanger:

$$Q(\text{W}) = U \cdot A_{\text{exchange}} \cdot \Delta T_{\text{ml}} = 2079,56 \cdot 5,5 \cdot 1,2 = 13707,22$$

The power obtained in the exchange is higher than that requested by the CTE, so the number of plates selected (24) is enough for the design. (Quarry)

12.6. Sizing of expansion vessels

For the dimensioning of this element we will rely on the UNE 100155:2004 standard, as recommended by the RITE. In this standard, the minimum volume of an expansion vessel is calculated according to the expression

$$V = V_t \cdot C_e \cdot C_p$$

Where:

- V : Minimum volume of an expansion vessel.
- V_t : Total volume enclosed in the circuit elements.
- C_e : Coefficient of expansion of the fluid.
- C_p : Coefficient of fluid expansion.

Primary circuit

The total volume to be determined is inside the pipes, collectors and external plate heat exchanger:

$$V_t = V_{\text{pipes}} + V_{\text{collectors}} + V_{\text{plate exchanger}}$$

$$V_{\text{pipelines}} = \sum L_{\text{pipes},i} \cdot \pi \cdot R_{\text{pipes}^2,i}$$

$$V_{\text{collectors}} = V_{\text{inside a collector}} \cdot N_{\text{collectors}}$$

The volume of liquid inside the sensors is a data given by the manufacturer. The volume of liquid inside the exchanger is based on the size given by the manufacturer. The volume of water in each section is detailed in table 64.

Table 53.Liquid volume inside primary circuit pipes.

	L pipes(m)	D.int(m)	Vpipes(L)
Hot stretch outside hot a-b	24,00	0,032	19,58
Outdoor hot section first battery	2,00	0,025	1,00
Outdoor hot section second battery	11,00	0,022	4,24
Cold outer section c-d	9,00	0,032	7,34
Cold outer section first battery	2,50	0,025	1,24
Cold outer section second battery	12,00	0,022	4,63
Interior hot section	1,00	0,032	0,82
Cold section inside	1,00	0,025	0,50

$$V_{\text{. pipes}} = 38,04L$$

$$V_{\text{. collectors}} = \frac{2,5L}{\text{collector}} \cdot 12\text{collectors} = 30L$$

$$V_{\text{. hot side exchanger}} = 32L$$

$$V_{\text{. total circuit}} = 100,14 L$$

The C_e represents the coefficient of expansion of the fluid. The UNE 100155 standard provides an empirical formula for obtaining it, to which a correction factor must be applied because it is a mixture with a coolant. For temperatures between 30°C and 120°C the equation applies. For our case I consider the maximum temperature of 70°C.

$$C_e = (3,24 \cdot t^2 + 102,13 \cdot t - 2708,3) \cdot 10^{-6}$$

The correction factor for a water-glycol mixture is calculated by following the steps below:

$$f_{\text{corrector}} = a \cdot (1,8 \cdot t + 32)^b$$

$$a = -0,013 \cdot (G^2 - 143,8 \cdot G + 1918,2)$$

$$b = 3,5 \cdot 10^{-4} \cdot (G^2 - 94,57 \cdot G + 500)$$

G being the percentage of glycol in the working fluid, 30% for our case.

$$C_e \text{ corrected} = C_e \cdot f = 0,02 \cdot 1,37 = 0,028$$

The C_p represents the pressure coefficient. In the case of a closed expansion vessel with diaphragm, as will be the case with our installation, it applies to the following expression:

$$C_p = \frac{P_{\text{max}}}{P_{\text{max}} - P_{\text{min}}}$$

P_{max} : maximum operating pressure. This will be slightly lower than the set pressure of the safety valve, which is between 6 and 10 bar. Taking 6 bar:

$$P_{\text{max}} = 0,9 \cdot P_{\text{vs}} + 1 = 6,4 \text{ bar}$$

P_{min} : corresponds to the static pressure resulting from the difference between the highest point of the installation and the location of the expansion vessel (in this case the difference is zero, as the boiler room is located in an isolated room at the same height as the roof), plus the filling pressure which varies between 1.5-2.5 bar (we take 2). In any case, a minimum pressure with a safety margin of 0.2 bar should be taken for maximum temperatures of 90°C. Therefore:

$$P_{\text{min}} = 1 + 0,2 + 2 = 3,2 \text{ bar}$$

$$C_p = \frac{P_{\text{max}}}{P_{\text{max}} - P_{\text{min}}} = \frac{6,4}{6,4 - 3,2} = 2$$

$$V. \text{ expansion vessel of the primary circuit} = V_t \cdot C_e(\text{corrected}) \cdot C_p = 5,59L$$

The UNE 100155 standard establishes that this volume must be at least 6% of the total volume of the circuit, which is equivalent to 6 liters, so this condition is not met. Therefore, we will select an 8L expansion vessel from the manufacturer Grundfos. The characteristics of the

equipment can be seen in the appendix. We determine the volume of the expansion vessel for the rest of the circuits, taking into account that the fluid for the rest is water.

Secondary circuit:

$$V_t = V_{\text{pipes}} + V_{\text{solar tank}} + V_{\text{plate exchanger}}$$

Table 54. Volume of water within the secondary circuit pipes.

	L pipe	D.int(m)	Vpipes(L)
One-way section exchanger-accumulator	1,00	0,032	0,80
One-way stretch accumulator-exchanger	1,00	0,032	0,80

$$V_{\text{pipes}} = 1,61\text{L}$$

$$V_{\text{solar tank}} = 3000\text{L}$$

$$V_{\text{hot side plate exchanger}} = 23,24\text{L}$$

$$V_{\text{total circuit}} = 3024,85\text{ L}$$

$$V_{\text{expansion vessel of the secondary circuit}} = V_t \cdot C_e \cdot C_p = 3024,85 \cdot 0,02 \cdot 2 = 122,91\text{L}$$

The UNE 100155 standard establishes that this volume must be at least 6% of the total volume of water in the installation, which is equivalent to 181.49 liters, so this condition is not met. Therefore, we will select a 200L expansion vessel from the manufacturer Grundfos. . The characteristics of the equipment can be seen in the appendix.

Support circuit:

$$V_t = V_{\text{pipes}} + V_{\text{accumulator coil}} + V_{\text{boiler}}$$

Table 55. Volume of water inside the support circuit pipes.

	L pipe	D.int(m)	Vpipes(L)
Auxiliary boiler-accumulation outgoing section	1,00	0,022	0,38
Accumulated auxiliary boiler section	1,00	0,022	0,38

$$V_{\text{pipes}} = 0,76\text{L}$$

$$V_{\text{accumulator coil}} = 8,6\text{L}$$

$$V_{\text{boiler}} = 170\text{L}$$

$$V_{\text{total circuit}} = 179,36\text{ L}$$

The volume of water that can be accumulated in the coil and in the boiler is provided for the manufacturer.

$$V_{\text{expansion vessel of the support circuit}} = V_t \cdot C_e \cdot C_p = 179,36 \cdot 0,02 \cdot 2 = 7,28\text{L}$$

The UNE 100155 standard establishes that this volume must be at least 6% of the total volume of water in the installation, which is equivalent to 10.76 liters, so this condition is not met. Therefore, we will select an 11L expansion vessel from the manufacturer Grundfos. . The characteristics of the equipment can be seen in the appendix.

Return circuit:

$$V_t = V_{\text{pipes}} + V_{\text{solar tank}}$$

$$V_{\text{solar tank}} = 1500\text{L}$$

The return network is on the first floor of the building, as it is more than 15 meters away from the DHW tank. The total length of this semi-closed circuit (it is no longer closed when a consumer appliance is opened) has been estimated at 70 m in total, both ways. The return network has a fixed diameter of 20mm, but the distribution pipes and their branches have different dimensions. In order to simplify the calculation, the entire length of the flow of the largest diameter has been assumed, putting us in the case of more volume and therefore more restrictive. Table 67 provides the fluid contained in the pipes.

Table 56. Volume of water inside return circuit pipes.

	L pipe	D.int(m)	Vpipes(L)
One-way circuit	35,00	0,03	24,73
Lap circuit	35,00	0,02	10,99

$$V_{\text{pipes}} = 35,72\text{L}$$

$$V_{\text{solar tank}} = 1500\text{L}$$

$$V_{\text{total circuit}} = 1535,72\text{ L}$$

$$V. \text{ expansion vessel of the return circuit} = V_t \cdot C_e \cdot C_p = 1535,72 \cdot 0,02 \cdot 2 = 62,4L$$

The UNE 100155 standard establishes that this volume must be at least 6% of the total volume of water in the installation, which is equivalent to 92.14 liters, so this condition is not met. Therefore, we will select a 100L expansion vessel from the manufacturer Grundfos. . The characteristics of the equipment can be seen in the appendix. (Miranda, Calculation of closed expansion tanks, 2019)

12.7. Dimensioning of the pumping system

The pumping system consists of all the pumps that keep the fluids in the rest of the systems circulating. In order to know which pumps are suitable for each purpose, it is necessary to know the working temperatures of the fluids, the flows transported and the pressure losses they experience along the circuits.

Primary circuit

The total head loss is obtained by determining the sum of the head losses in each of the following elements:

- Piping
- Panels
- Heat exchanger hot side
- Piping elements (elbows, valves, filters, etc..)

Pipeline losses.

In the section on sizing of pipes, we have explained the method for determining the pressure losses per linear meter, based on the data of the circulating flow and the selected pipe diameter. As the pipes that circulate outside have different diameters, it will be necessary to calculate the pressure losses of each one. The pressure losses of each section are shown in Table 68.

Table 57 losses of the primary circuit pipes in each section.

	L pipe	Flow (m ³ /h)	d.int (mm)	mm.c.a per meter	mm.c.a/m mixture 30% propylene glycol	mm.c.a
Hot stretch outside hot a-b	24,00	1,81	32,00	11,00	14,30	343,20
Outdoor hot section first battery	2,00	0,91	25,00	15,00	19,50	39,00
Outdoor hot section second battery	11,00	0,91	22,00	17,00	22,10	243,10
Cold outer section c-d	9,00	1,81	32,00	11,00	14,30	128,70
Cold outer section first battery	2,50	0,91	25,00	15,00	19,50	48,75
Cold outer section second battery	13,00	0,91	22,00	17,00	22,10	287,30
Interior hot section	1,00	1,81	32,00	11,00	14,30	14,30
Interior cold section	1,00	1,81	32,00	11,00	14,30	14,30

As the fluid circulating in this circuit is not pure water, a correction factor is applied to the losses per meter

$$\text{Pressure losses corrected} = \text{Pressure losses} \cdot 1,3 = 1104,35 \text{ mm. c. a.}$$

Pressure losses in the panels

The selected collectors are formed by a bundle of 10 parallel copper pipes connected to the upper and lower collector pipes. Therefore, as the tubes, the collectors and the coils of these are all in parallel, the total loss of charge of the collectors will be that produced in one of the parallel tubes and in the collector pipes. In the calculations, it has been seen that the losses caused in the two collector pipes are negligible compared to those caused to the pipes.

Previously, in the calculation of thermal resistances in the collector, we already determined the turbulence regime inside the collectors, being this in laminar flow. For the calculation of pressure losses we proceed with the following equation:

$$h = \frac{f \cdot L_{\text{tube}} \cdot v^2}{D_{\text{int.tube}} \cdot 2g} = \frac{0,24 \cdot 1,9 \cdot 0,53^2}{0,01 \cdot 2 \cdot 9,8} 0,653 (\text{m. c. a.}) = 653 (\text{mm. c. a.})$$

Where:

f: friction coefficient. In the case of laminar regime it is equivalent to $64/Re$.

L: length of collector tube

Dint: internal diameter of the collector tube.

g: gravity(m/s²).

v: fluid flow speed.

Pressure losses in the heat exchanger

In a plate heat exchanger, the pressure drop is defined by the expression

$$AP = 4 \cdot f \frac{L \cdot \rho \cdot v^2}{lc \cdot 2}$$

Where f is the friction factor determined by the following correlation of Shah and Focke provided by table 69.

$$f = C \cdot Re^m$$

Table 58. Coefficients for the calculation of the friction factor.

Re	C	M
Re<10	17	-1
10<Re<101	6,29	-0,57
101<Re<855	1,141	-0,2
Re>855	0,581	-0,1

The side of the sensor that is in contact with the primary circuit has a Reynolds of 269, thus defining the value of the constants.

$$AP = 901,87 \text{ Pa} = 297,784 \text{ mm. c. a.}$$

Pressure losses of accessories

To calculate the individual pressure losses of the connection pieces, we will use the K-factor method, by which it is determined that for each connection piece, we have a characteristic and determined K-factor, as can be seen in table 70.

Table 59.K-factor of the accessories present in the circuits.

Accessories	k
Short radius 90° elbows	0,90
45° short radius elbows	0,45
Sharp contractions	0,35
Abrupt widening	0,20
T-branch	1,80
Check Valve(flap)	12,00
Safety valve	2,00
Flow regulation valve (seat)	3,00
Ball valve	0,50

$$h = K \cdot \left(\frac{v^2}{2 \cdot g} \right)$$

Where:

h: pressure or energy loss (m).

K: empirical (dimensionless) coefficient.

v: average flow velocity (m/s) .

g: acceleration of gravity (m/s²)

The arrangement of these accessories in each of the sections can be seen in the general diagram of the process. In figure 71 we see the summary of pressure losses by accessories in the affected sections:

Table 60.Accessory pressure losses in each section.

Sections	L pipe	mm.c.a.k method
Hot section a-b	23,00	38,02
Outside hot section with outside diameter 28	2,00	18,13
Outside hot section with outside diameter 28	11,00	50,38
Cold section c-d	8,00	456,19
Outside cold section of outside diameter 28	2,50	89,29
Outside cold section of outside diameter 28	13,00	169,05

Therefore, the total load losses of the primary circuit are:

$$AP_{\text{primary circuit}} = AP_{\text{pipes}} + AP_{\text{hot side exchanger}} + AP_{\text{collector}} + AP_{\text{accessories}} = 2517,31 \text{ mm. c. a.}$$

Most pump manufacturers give the properties of their products in the form of graphs relating the pump head in meters and the flow rate in m³/h. For this reason it is advisable to pass the calculated head loss and the mass flow rate through the pipes to these units.

$$H_{\text{pump}}(\text{m}) = \frac{AP}{\rho_{\text{heat carrier}} \cdot g} = 2,48$$

$$Q_{\text{circuit}} \left(\frac{\text{m}^3}{\text{h}} \right) = \frac{m1}{\rho_{\text{heat carrier}}} = 1,81$$

With this data we selected the commercial pump MAGNA1 32-40 F. All pumps have been supplied by the manufacturer Grundfos. (Grundfos) The pump's operating curve and power consumption can be seen in the appendix.

Secondary circuit

The pressure losses in the secondary circuit are determined in the same way. As the heat exchanger is very close to the solar accumulator, the pipe losses are much lower. The number of fittings is also lower. The internal diameter of these pipes is 32mm.

$$AP_{\text{pipes}} = 22 \text{ mm. c. a.}$$

$$AP_{\text{cold side exchanger}} = 249,71 \text{ mm. c. a.}$$

$$AP_{\text{accessories}} = 454,19 \text{ mm. c. a.}$$

$$AP_{\text{solar tank}} = (0,1 \cdot AP_{\text{secondary circuit}}) \text{ mm. c. a.}$$

$$AP_{\text{secondary circuit}} = AP_{\text{pipes}} + AP_{\text{cold side exchanger}} + AP_{\text{accessories}} + AP_{\text{solar tank}} = 806,56 \text{ mm. c. a.}$$

$$H_{\text{pump}}(\text{m}) = \frac{AP}{\rho_{\text{heat carrier}} \cdot g} = 0,81$$

$$Q_{\text{circuit}} \left(\frac{\text{m}^3}{\text{h}} \right) = \frac{m1}{\rho_{\text{heat carrier}}} = 1,81$$

With this data we selected the commercial pump UPS 20-60 N 150. In the appendix you can see the working curve of the pump and the power consumption.

Support circuit

Similarly, the load losses of the support circuit are determined. As the boiler is very close to the DHW storage tank, the pipe losses are much lower. The number of fittings is also lower. The internal diameter of these pipes is 22mm.

$$\text{AP pipes} = 46 \text{ mm. c. a.}$$

$$\text{AP accessories} = 454,19 \text{ mm. c. a.}$$

$$\text{AP support tank and boiler} = (0,2 \cdot \text{AP support circuit}) \text{ mm. c. a.}$$

$$\text{AP support circuit} = \text{AP pipes} + \text{AP boiler} + \text{AP accessories} + \text{AP support tank} = 625,23 \text{ mm. c. a.}$$

$$H_{\text{pump}}(\text{m}) = \frac{\text{AP}}{\rho_{\text{heat carrier}} \cdot g} = 0,63$$

$$Q_{\text{circuit}} \left(\frac{\text{m}^3}{\text{h}} \right) = \frac{m_1}{\rho_{\text{heat carrier}}} = 1,88$$

With this data we selected the commercial pump MAGNA3 25-40. In the appendix you can see the working curve of the pump and power consumption.

Recirculation circuit

As we do not have detailed plans of the building's pipe distribution network, we do not know exactly the length of the return network, nor the number of fittings required. We do know the diameter of the pipes, so we will assume a return network length of 35 m from the most unfavorable point to determine the pressure losses to be overcome. We will also have to take into account the pressure losses in the accessories, which can be estimated as 20% or 30% of the losses in the pipes. The recirculation flow shall be 15% of the maximum consumption flow of the building.

$$Q_{\text{return circuit}} \left(\frac{\text{m}^3}{\text{h}} \right) = Q_{\text{max. building}} \cdot 0,15 = 1,27 \cdot 0,15 \cdot 3600 = 0,69$$

With this flow rate and an internal return diameter of 20 mm, the pressure losses obtained from the pressure drop graph from the most unfavorable point amount to:

$$\text{AP} = 1046,5 \text{ mm. c. a.}$$

$$H_{\text{pump}}(\text{m}) = \frac{AP}{\rho_{\text{heat carrier}} \cdot g} = 1,05$$

With this data we selected the commercial pump MAGNA3 25-40. In the appendix you can see the working curve of the pump and the power consumed.

13. Environmental study

Every project dedicated to the implementation of solar energy contributes to minimizing the emission of greenhouse gases, especially CO₂, the main cause of the effect. Using the sun as an energy source not only achieves this, but also avoids the emission of other harmful gases such as carbon monoxide (CO), nitrogen oxides (NO_x) or sulphur oxides (SO_x).

The back-up boiler will use natural gas as its fuel, a non-renewable energy source made up of a mixture of gases frequently found in fossil fuels, dissolved or associated with oil or coal deposits. Although its composition varies depending on the reservoir from which it is extracted, it is primarily composed of methane in amounts that can commonly exceed 90 or 95% and usually contains other gases such as nitrogen, ethane, CO₂, H₂S, butane, propane, mercaptans and traces of heavier hydrocarbons. The solar thermal installation will contribute to reducing the consumption of this non-renewable energy for the consumption of DHW. A series of calculations will then be made to determine the extent of the environmental impact of this installation:

Fuel saving:

The fuel saving generated is represented in table 72. To calculate the fuel saving of the installation we will take into account the following expression:

$$V = \frac{Q}{LCV \cdot \eta_{\text{boiler}}}$$

Where:

Q: energy provided by the solar collectors (in MJ)

V: volume of fuel (to produce all that energy)(in m³).

LCV: is the lower calorific value of the fuel used in the installation. In the case of natural gas it is 39.6 (MJ/N-m³).

η_{boiler} : boiler efficiency (which in this case is 95.5%)

Table 61. Monthly fuel savings (m3).

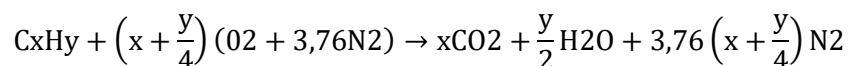
Month	DDHW(MJ)	Solar energy(MJ)	Fuel saving(m3)
January	13703,89	4354,75	115,51
February	11645,95	5083,77	134,85
March	11990,90	6909,97	183,29
April	11935,47	7833,00	207,78
May	11149,85	8462,27	224,47
June	9608,10	8660,60	229,73
July	8312,50	8312,50	220,50
August	7296,53	7296,53	193,55
September	8751,93	7701,97	204,30
October	9826,51	6384,83	169,36
November	11198,29	4824,16	127,96
December	12893,73	4132,40	109,62
Annual	128313,66	79956,76	2120,91

So we have an annual saving of 2120.91 m3 of natural gas.

According to the natural gas catalogue, the composition of the gas is as follows

- 91.4% methane (CH₄);
- 7.2% ethane (C₂H₆);
- 0.8% of higher hydrocarbons (we assume it is all propane);
- 0.6% Nitrogen (N₂);

Considering that the combustion of Natural Gas with air is a stoichiometric reaction, that is to say, in which the amount of air is the necessary one to burn the fuel completely and the only products that are formed are CO₂, H₂O and N₂, we have the following relation (terms x w y expressed in moles):



As the composition of Natural Gas is expressed in % of volume, we need to pass it to moles, applying the formula of the equation of state of the ideal gases, PV=nRT.

Taking for a pressure of 1 atm and 25°C, and if we take V=1m³ we have that n = 40,89 (mol /m³). Once we know the number of total moles of 1 m³ of gas, we will have to multiply this value by the corresponding number of percent of the components of Natural Gas, since the production in volume is the same as in moles. In Table 73 we see the molar composition of natural gas.

Table 62. Molar composition of natural gas (%)

Natural gas components	Composition	Moles
Methane	0,91	37,38
Ethane	0,07	2,94
N2	0,01	0,33
Superior hydrocarbons (we assume all propane)	0,01	0,25

By performing carbon, hydrogen, oxygen and nitrogen balance according to the previous stoichiometry ratio, we obtain 44.23 moles of CO₂ per m³ of Natural Gas.

We will then calculate the mass corresponding to these 44.23 moles of CO₂ by applying the following expression:

$$n = \frac{m}{Pm}$$

Where:

- m: is the amount of mass in grams [gr].
- Pm: is the molecular weight of CO₂ in grams [gr]. 44g value.

The amount of CO₂ in 1 m³ of natural gas is 1,946Kg. With this data we can calculate the consumption of CO₂ savings, which is shown in table 74.

Table 63 Monthly carbon dioxide savings (m3).

Month	Fuel saving (m3)	CO2 emissions savings(kg)
January	115,51	224,80
February	134,85	262,44
March	183,29	356,71
April	207,78	404,36
May	224,47	436,84
June	229,73	447,08
July	220,50	429,11
August	193,55	376,66
September	204,30	397,59
October	169,36	329,60
November	127,96	249,03
December	109,62	213,32
Annual	2120,91	4127,55

Considering that the useful life of this type of installation is usually about 25 years, the total CO2 savings amount to 103.18 tons, contributing greatly to the welfare of the planet. (Díaz, 2018)

14. Economic study

As we saw before, this type of installation means a considerable energy saving, but now we are going to study if there is also a saving at an economic level. To do this, we first calculate the initial costs that involve all the elements necessary for the operation of the installation, provided by tables 75,76,77,78 and 79.

Table 64. Material costs of the primary circuit.

PRIMARY LOOP			
Team	Euros/Unit	Units	Total
Solar Panels ESCOSOL SOL 2300 Selective Titan Manufacturer Salvador Escoda	505,00	12	6060,00
Panel connection accessories	43,85	10	438,50
Collector supports	44,50	12	534,00
Concrete floor	30,00	22	660,00
Expansion vessel	51,00	1	51,00
Circulation pump	955,00	2	1910,00
DN 32 copper pipes	8,89	47	417,83
DN 25 copper pipes	6,26	30	187,80
Insulation DN 35 external	17,27	47	811,69
Insulation DN 28 external	15,73	30	471,90
Propylene Glycol	9,15	50	457,50
Manometer	9,40	2	18,80
Automatic purge	2,00	2	130,00
DN32 fill and drain valve	50,00	1	50,00
DN32 flap check valve	28,23	2	56,46
DN32 ball valve	41,83	2	116,02
Safety valve DN25	58,01	2	378,80
Balancing Valve DN25	189,40	4	113,48
DN25 ball valve	28,37	12	6060,00

Table 65 Secondary circuit material costs.

SECONDARY CIRCUIT			
Team	Euros/Unit	Units	Total
Expansion vessel	519,00	1	519,00
Circulation pump	728,00	2	1456,00
Copper pipes DN 32	8,89	2	17,78
SECONDARY CIRCUIT	17,27	2	34,54
Manometer	9,40	2	18,80
DN32 flap valve	28,23	2	56,46
DN32 ball valve	41,83	12	501,96
Solar accumulator	7613,00	1	7613,00
Plate heat exchanger	2582,00	1	2582,00

Table 66 Material costs of the support circuit.

SUPPORT CIRCUIT			
Team	Euros/Unit	Units	Total
Expansion vessel	51,00	1	51,00
Circulation pump	857,00	2	1714,00
DN 22 copper pipes	5,09	2	10,18
Insulation DN 22 inside	8,09	2	16,18
Manometer	9,40	2	18,80
Non return valve valve DN22	12,48	2	24,96
DN22 ball valve	18,58	12	222,96
Solar accumulator support	7040,00	1	7040,00
Support boiler	2856,00	1	2856,00

Table 67. Material costs of the recirculation circuit.

RECIRCULATION CIRCUIT	Euros/Unit	Units	Total
Expansion vessel	319,00	1	319,00
Circulation pump	857,00	2	1714,00
Manometer	9,40	2	18,80
DN20 copper pipes	3,42	50	119,70
Insulation DN 22 inside	7,30	50	255,50

Table 68. Control system costs and accessories.

Others	Euros/Unit	Units	Total
BW-H Komfort control system	577,17	1	577,17
Accessories (elbows, extensions,...)			2000

We do not know the exact number of accessories, as we do not know for sure the number of them in the recirculation circuit. We assume a total expenditure on them of EUR 2 000. The expansion vessels, collectors, support collectors, accessories and insulators are obtained from the manufacturer Salvador Escoda (Salvador Escoda)The accumulators and heat exchangers are obtained from the brand SUICALSA (Suicalsa)The boiler is obtained from the manufacturer Baxi (Baxi). The Grundfos bombs. AntiFrost brand antifreeze. The prices of the pipes as well as the other elements have been obtained from price generator software (CYPE ingenieros).

$$\text{Material costs(€)} = 43081,7$$

Additional expenses:

$$\text{Engineering and assembly (10\% material costs)(€)} = 4308,17$$

$$\text{IVA(€)} = 4856,39$$

A IVA of 21% has been applied on the total cost of materials that did not include VAT.

$$\text{Total cost of the project(€)} = 52246,26$$

Grants

The Barcelona City Council has been developing different programs and initiatives for several years with the fundamental objective of promoting the development of renewable energies and currently offers subsidies over the total budget for this type of installation. The subsidy is 50% of the total budget, with a maximum of 3,500(€) per house and a maximum of 60,000(€) per building. (Barcelona, 2019)

$$\text{Project grant(€)} = \text{Total cost of the project} \cdot 0,5 = 26123,13$$

Amortization period

Once the final investment is known, it is necessary to carry out a study on the economic viability of the installation. The aim is to analyse whether it is possible to recover the investment made thanks to the fuel savings achieved, before the end of the project's useful life. To do this, an annual economic savings study is carried out. We must take into account the amount of primary energy that we are going to save, and the price of this energy.

$$\text{Annual solar energy produced(KW} \cdot \text{h)} = 22210,23$$

The natural gas tariff set by the Ministry of Industry is determined in Table 80(BOE-A-2019-4677, 2019).

Table 69. Natural gas tariffs according to consumption rate.

		Tarifa	
		Fijo (€/cliente)/mes	Variable cent/kWh
T.1	Consumo inferior o igual a 5.000 kWh/año.	4,27	5,188812
T.2	Consumo superior a 5.000 kWh/año e inferior o igual a 50.000 kWh/año.	8,38	4,501412
T.3	Consumo superior a 50.000 kWh/año e inferior o igual a 100.000 kWh/año.	60,38	3,879513
T.4	Consumo superior a 100.000 kWh/año.	181,72	3,569013

For our case, with an annual consumption of 35642.97 KW-h/year, we are in tariff 2.

Taking into account the efficiency of the boiler, we can already determine the annual economic savings that we will obtain thanks to our solar installation:

$$\left(\frac{\text{Annual saving(KW} \cdot \text{h)}}{\eta_{\text{boiler}}} \cdot \text{T2 rate} = \frac{22210,23}{0,952} \cdot \frac{4,501412}{100} \right) = 1050,18 \left(\frac{\text{€}}{\text{year}} \right)$$

To determine when the initial investment is recovered and the solar plant begins to yield a profit, the net present value (VAN) is calculated.

$$VAN = A \cdot \sum \left(\frac{1+c}{1+i} \right)^t - C_{mto} \cdot \sum \left(\frac{1+f}{1+i} \right)^t - I_0$$

Where:

- A is fuel economy.
- I_0 is the initial investment.
- C_{mto} is the cost of maintenance.
- c is the increase in the price of fuel.
- i is the interest rate.
- f is the value of inflation.

-Maintenance costs have been considered to be 0.5% of the initial cost, this being equal to the value of the subsidy. These costs increase over time as the materials are more likely to deteriorate.

-The price of natural gas has increased from 2016 to 2019 by 7.6%. From the end of 2021, the price of natural gas is expected to increase by about 4% per year. We estimate an annual increase of 4%.

-The interest rate can be estimated from Euribor, the average interest rate at which financial institutions lend money to each other on the interbank euro market, and whose value is widely used as a reference for bank loans. It is currently at -0.366%. The interest rate is estimated as Euribor plus approximately 0.5%. We will estimate an interest rate value of 0.5%.

-Inflation is measured by the consumer price index (CPI). At the end of 2019 it ended at 0.8% due to the rise in fuel price.

Table 81 shows the progression for each one-year period:

Table 70. Evolution of cash flow during the useful period of the installation.

Year	Income	Costs	Grant	Net profit	Cash flow	Accumulated cash flow
0					-52246,26	-52246,26
1	1092,19	131,66	26123,13	27083,66	26948,92	-25297,35
2	1135,88	132,71		1003,16	993,21	-24304,14
3	1181,31	133,78		1047,54	1031,98	-23272,16
4	1228,57	134,85		1093,72	1072,12	-22200,04
5	1277,71	135,92		1141,78	1113,66	-21086,38
6	1328,82	137,01		1191,80	1156,67	-19929,71
7	1381,97	138,11		1243,86	1201,18	-18728,53
8	1437,25	139,21		1298,03	1247,26	-17481,27
9	1494,74	140,33		1354,41	1294,96	-16186,31
10	1554,53	141,45		1413,08	1344,33	-14841,98
11	1616,71	142,58		1474,13	1395,43	-13446,55
12	1681,38	143,72		1537,65	1448,33	-11998,23
13	1748,63	144,87		1603,76	1503,07	-10495,15
14	1818,58	146,03		1672,55	1559,74	-8935,41
15	1891,32	147,20		1744,12	1618,40	-7317,01
16	1966,97	148,38		1818,60	1679,11	-5637,90
17	2045,65	149,56		1896,09	1741,95	-3895,95
18	2127,48	150,76		1976,72	1806,99	-2088,96
19	2212,58	151,97		2060,61	1874,31	-214,65
20	2301,08	153,18		2147,90	1943,98	1729,33
21	2393,12	154,41		2238,72	2016,10	3745,43
22	2488,85	155,64		2333,21	2090,74	5836,17
23	2588,40	156,89		2431,51	2167,99	8004,16
24	2691,94	158,14		2533,80	2247,95	10252,11
25	2799,61	159,41		2640,21	2330,70	12582,81

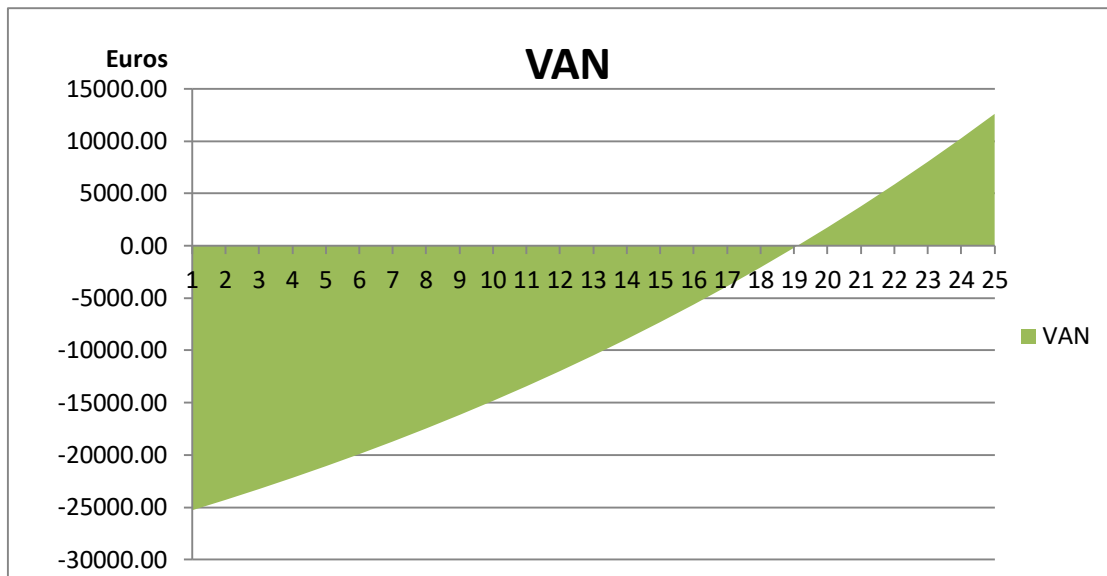


Figure 39. Graphical representation of the evolution of the accumulated cash flow.

As can be seen in Figure 41, the return period of the installation is 19 years, providing a total of 12596.62 euros of profit at the end of its useful life. Without the subsidy provided, the cost of the project is depreciated over 30 years.

15. Conclusions

- With a total catchment area of 25.92 m², the energy objective of covering 60% of DHW's annual demand is achieved, reaching 63%.
- The covered demand has meant an annual saving of 22210.23 KW-h in natural gas, avoiding the emission of a total of 4127.55 kg of CO₂ annually, demonstrating the environmental benefit that these facilities have.
- The cost of the installation has been very high, but due to the subsidies offered the project has been profitable, amortizing its cost in the 19th year of its 25 years of useful life and generating 12596.62 euros of profit. However, it has been possible to verify that with the current technology without substantial subsidies this type of installation is not economically viable.
- All the elements of the system could be installed in the building without any space problems and they complied with the current dimensioning regulations.

Our installation is summarized in the following scheme (figure42):

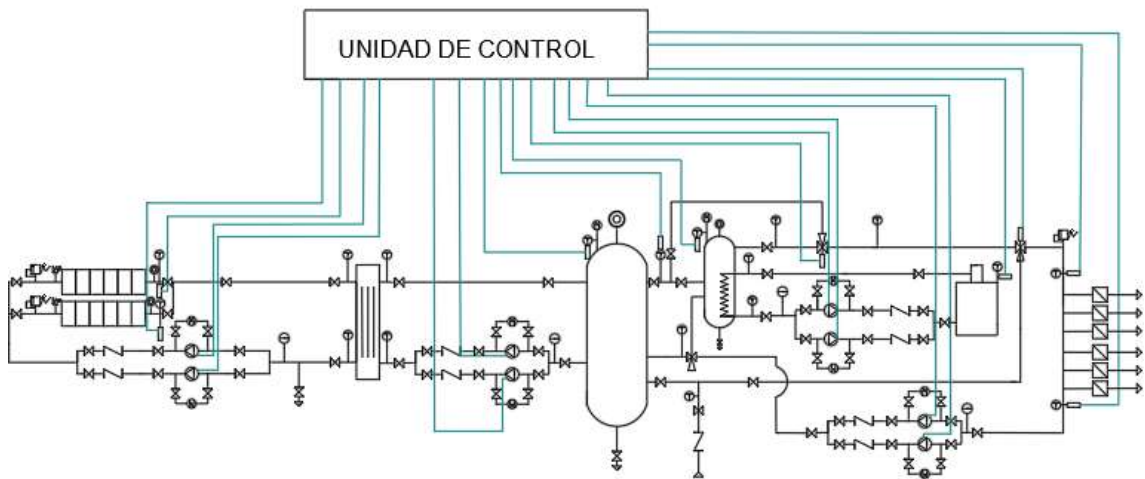


Figure 40 General diagram of the process. Own elaboration.

16. Appendixes

FICHA TÉCNICA DEL CAPTADOR SOLAR ESCOSOL SOL 2300 SELECTIVO TITAN



1. CARACTERÍSTICAS TÉCNICAS

DIMENSIONES DEL COLECTOR		SOL 2300 Selectivo Titan
Largo	mm	1.900
Ancho	mm	1.213
Altura	mm	106
SUPERFICIES DE REFERENCIA		
Área del absorbedor	m ²	2,07
Área de apertura	m ²	2,16
Área total	m ²	2,30
ESPECIFICACIONES GENERALES		
Tipo de colector		Plano
Peso vacío	Kg	41,2
Peso lleno	Kg	43,7
Fluido calor - portante		Propilén-glicol-agua
Caudal mínimo	l/h	75
Caudal máximo aconsejable	l/h/m ²	120
Caída de presión		140 Pa a 4,9 Kg/mín y ((20±2)°C
Presión máxima de servicio	bar	10
Temperatura máxima de trabajo	°C	200
Contenido de fluido	litros	2,5
Material de la estructura		Perfil de aluminio pintado
Juntas de sellado		Caucho EPDM
Al aislamiento térmico	Material	Poliuretano libre de CFC 25 mm espesor Lana de vidrio 25 mm espesor
	Conductividad W/m °C	Poliuretano: 0,030; Lana de vidrio: 0,036
Vidrio	características	Vidrio templado prismático bajo contenido férrico
	Espesor mm	4
ABSORBEDOR		
Material		Cobre
Recubrimiento		Altamente selectivo
Construcción		Cobre, 10 tubos de 12 mm verticales 2 Colectores de Ø22mm
RENDIMIENTO TÉRMICO		
Rendimiento óptico	η_0	0,775
Pérdidas lineales	a_1 W/m ² K	3,67
Pérdidas cuadráticas	a_2 W/m ² K ²	0,020

• Accesorios de conexión

Código	Artículo	€
SO 05 421	Racor doble recto unión colectores	5,81
SO 05 422	Racor recto macho salida colector	4,48
SO 05 423	Racor recto hembra salida colector	4,38
SO 05 451	Manguito tipo cruz + vaina + racor	28,00
AA 25 032	Tapón rosca hembra latón 3/4"	1,18

▶ VASOS DE EXPANSIÓN PARA INSTALACIONES A.C.S.

Diseñados para Aplicación de Sistemas de Energía Solar Térmica.
Declaración de Conformidad con los Requisitos esenciales de Seguridad, según lo previsto en la Normativa 97/23/CE (PED). Homologación CE.
Presión de Precarga 3 bar. Temperatura de Trabajo: -10 °C a 99 °C.



Código VASO	Detalles litros	Detalles código	Rosca	Diametro	Altura	Embalaje	P.V.P.
GD-5	5	A402L47	3/4"	205	225	-	40 €
GD-8	8	A402L51	3/4"	205	300	-	44 €
GD-11	11	A402L55	3/4"	300	270	-	51 €
GD-18	18	A432J47	3/4"	270	410	-	58 €
GD-24	24	A432J51	1"	320	355	-	67 €
GD-35	35	A432J55	1"	400	390	-	107 €
GDV-50	50	A432J59	1"	400	570	-	147 €
GDV-80	80	A402L51	1"	400	825	-	225 €
GDV-100	100	A402L55	1 1/4"	500	779	-	319 €
GDV-150	150	A432J47	1 1/4"	500	1007	-	431 €
GDV-200	200	A432J51	1 1/4"	600	1076	-	519 €
GDV-300	300	A432J55	1 1/4"	650	1251	-	673 €
GDV-500	500	A432J51	1 1/4"	775	1410	-	1.038 €



VÁLVULA DE BOLA INOX - 2 PIEZAS

2 PIECES - STAINLESS STEEL BALL VALVE

Cuerpo: **INOX AISI-316** - Bola: **INOX AISI 316** - Eje: **INOX AISI 316** - Anillos de cierre: **Teflón (PTFE)** - Palanca: **INOX AISI 304** - Presión máx: **65 bar** - Temp máx: **150°C** - Cierre de seguridad incorporado
Body:SS316 - Ball:SS316 - Seats: PTFE - Lever: SS304 - Working press:65 bar - Max temp: 150°C - Locking device



Código Code	Medida Size	Uds. caja pcs. box	Precio C/ud. Price €/pc.
AA 03 261	1/4"	-	13,17
AA 03 262	3/8"	-	13,17
AA 03 263	1/2"	-	14,25
AA 03 264	3/4"	-	18,58
AA 03 265	1"	-	28,37
AA 03 266	1-1/4"	-	41,83
AA 03 267	1-1/2"	-	58,85
AA 03 268	2"	-	99,65
AA 03 269	2-1/2"	-	190,51
AA 03 270	3"	-	295,32

VÁLVULA DE RETENCIÓN CLAPETA CIERRE METAL

SWING CHECK VALVE METAL SEAT

Cuerpo: **Latón** - Clapeta: **Latón** - Temperatura máx.: **90°C** - Presión máx: **16 bar (1/2" a 1")**, **10 bar (1-1/4" a 2")**, **8 bar (2-1/2 a 4")**

Body: Brass - Disc: Brass - Max temperature: 90°C - Max pressure: 16 bar (1/2" to 1"), 10 bar (1-1/4" to 2"), 8 bar (2-1/2" to 4")



Código Code	Medida Size	Uds. caja pcs. box	Precio C/ud. Price €/pc.
AA 05 251	1/2"	18	8,87
AA 05 252	3/4"	10	12,48
AA 05 253	1"	8	17,82
AA 05 254	1-1/4"	6	28,23
AA 05 255	1-1/2"	4	36,40
AA 05 256	2"	3	62,18
AA 05 257	2-1/2"	-	96,71
AA 05 258	3"	-	146,29
AA 05 259	4"	-	254,15

VÁLVULA DE SEGURIDAD REGULABLE ADJUSTABLE SAFETY VALVE



Cuerpo: Latón - Campana: Latón - Junta cierre: Teflón (PTFE) - Campo regulación: 2 a 8 bar - Temp. máx: 130°C
Body: Brass - Seat: PTFE - Adjustable pressures 2 to 8 bar - Max. temperature: 130°C

Código Code	Medida Size	Uds. caja pca. box	Precio €/ud. Price €/pc.
AA 11 121	3/8"	-	28,06
AA 11 122	1/2"	-	31,25
AA 11 123	3/4"	-	45,19
AA 11 124	1"	-	58,01
AA 11 125	1-1/4"	-	95,05
AA 11 126	1-1/2"	-	120,74
AA 11 127	2"	-	168,01

Hoja técnica / data sheet: pag. 70

Reguladores de caudal TACOSSETTER by-pass 100

TACOSSETTER BY-PASS 100 – Características técnicas

VÁLVULA DE EQUILIBRADO CON ROSCA INTERIOR



Latón, Temp. máx.: 100 °C, Presión máx.: 10 bar, versión exenta de silicona bajo demanda.



Código	DN	Conexión H-H	Kv (m³/h)	Caudal (l/min.)	PVP €
223.2262.000	15	1/2" x 1/2"	1,95	2 – 8	182,10
223.2361.000	20	3/4" x 3/4"	1,95	2 – 8	182,10
223.2360.000	20	3/4" x 3/4"	3,3	4 – 15	182,10
223.2362.000	20	3/4" x 3/4"	5	8 – 30	182,10
223.2460.000	25	1" x 1"	5,1	6 – 20	189,40
223.2461.000	25	1" x 1"	8,1	10 – 40	189,40
223.2561.000	32	1 1/4" x 1 1/4"	17	20 – 70	234,40
223.2661.000	40	1 1/2" x 1 1/2"	30	30 – 120	310,20
223.2861.000	50	2" x 2"	54	50 – 200	347,98



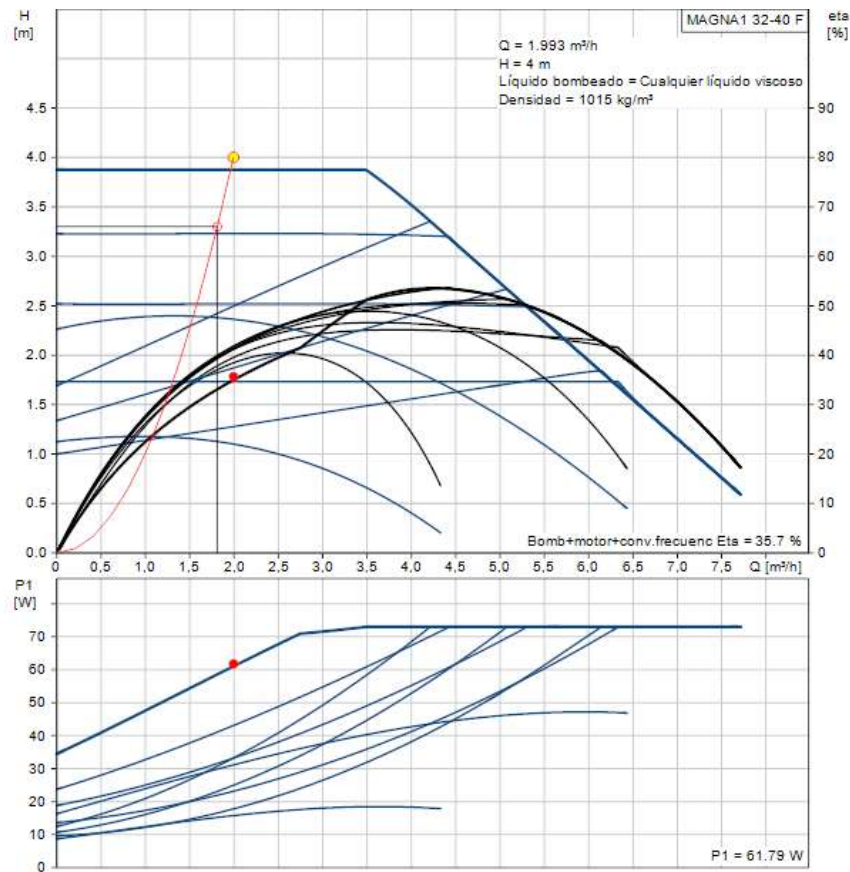
ANTIFROST SOLAR ECO

Propilenglicol 100 atóxico para solar térmica y geotermia. (*)

Código	Bidón (l)	Palet	PVP €
502512	2	320	18,30
502505	5	120	41,96
502510	10	60	83,60
502520	20	24	165,60

Temperatura congelación	Volumen Antifrost	Volumen agua
-11 °C	25 %	75 %
-15 °C	30 %	70 %
-19 °C	35 %	65 %
-24 °C	40 %	60 %
-30 °C	45 %	55 %
-38 °C	50 %	50 %

Primary circuit pump



Specifications

Product:	MAGNA1 32-40 F
Code:	99221263
EAN number:	5712608942365
Price	955,00 EUR

Technical

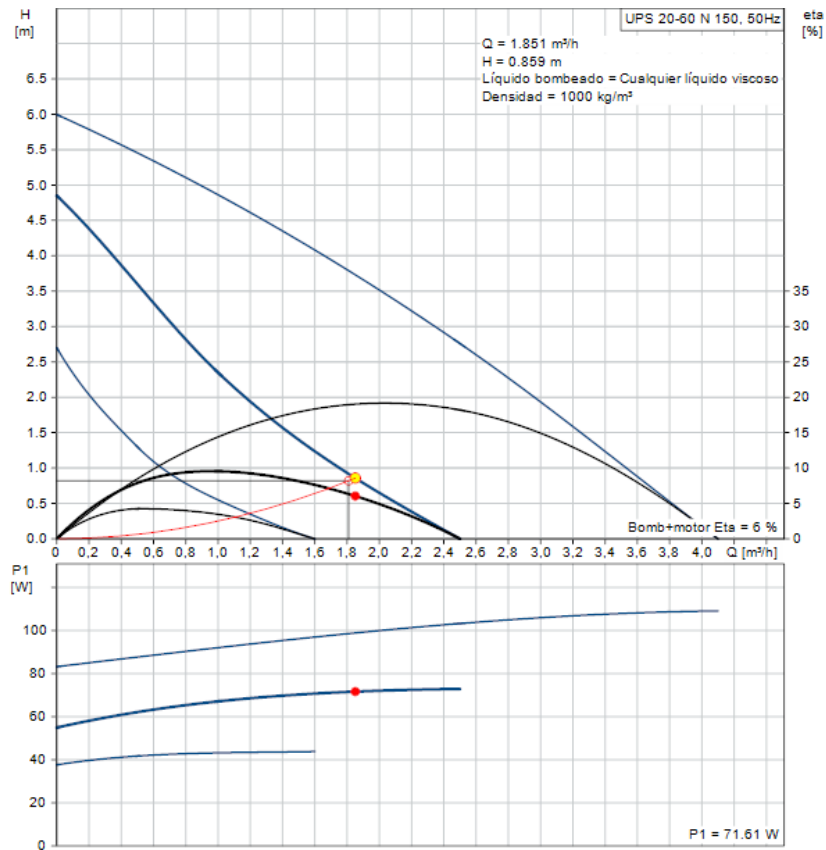
Calculated actual flow	1,993 m³/h
Resulting pump head	4 m
Max. height	40 dm
TF Class	110
Approvals on the nameplate	CE, VDE, EAC, CN ROHS, WEEE
Model	C

Materials

Pump housing	Cast Iron
--------------	-----------

Pump housing	EN-GJL-200
Pump housing	ASTM A48-200B
Driving force	WEIGHT 30 % GLASS FIBRE
Installation	
Ambient temperature range	0 .. 40 °C
Maximum working pressure	10 bar
Flange regulations	DIN
Pipe connection	DN 32
Nominal pressure	PN6/10
Length port to port	220 mm
Liquid	
Pumped liquid	Any viscous liquid
Liquid temperature range	-10 .. 110 °C
Density	1015 kg/m ³
Electrical data	
Power - P1	9 .. 73 W
Grid frequency	50 / 60 Hz
Nominal voltage	1 x 230 V
Maximum intensity consumption	0.09 .. 0.59 A
Degree of protection (IEC 34-5)	X4D
Insulation class (IEC 85)	F
Others	
Energy (IEE)	0.20
Net weight	7.5 kg
Gross weight	8.5 kg
Transport volume	0.016 m ³
Finnish	4615313
Country of origin.	DE
Personalized rate no.	84137030

Secondary circuit pump



Specifications

Product:	UPS 20-60 N 150
Code:	96913106
EAN number:	5700313544523
Price	728,00 EUR

Technical

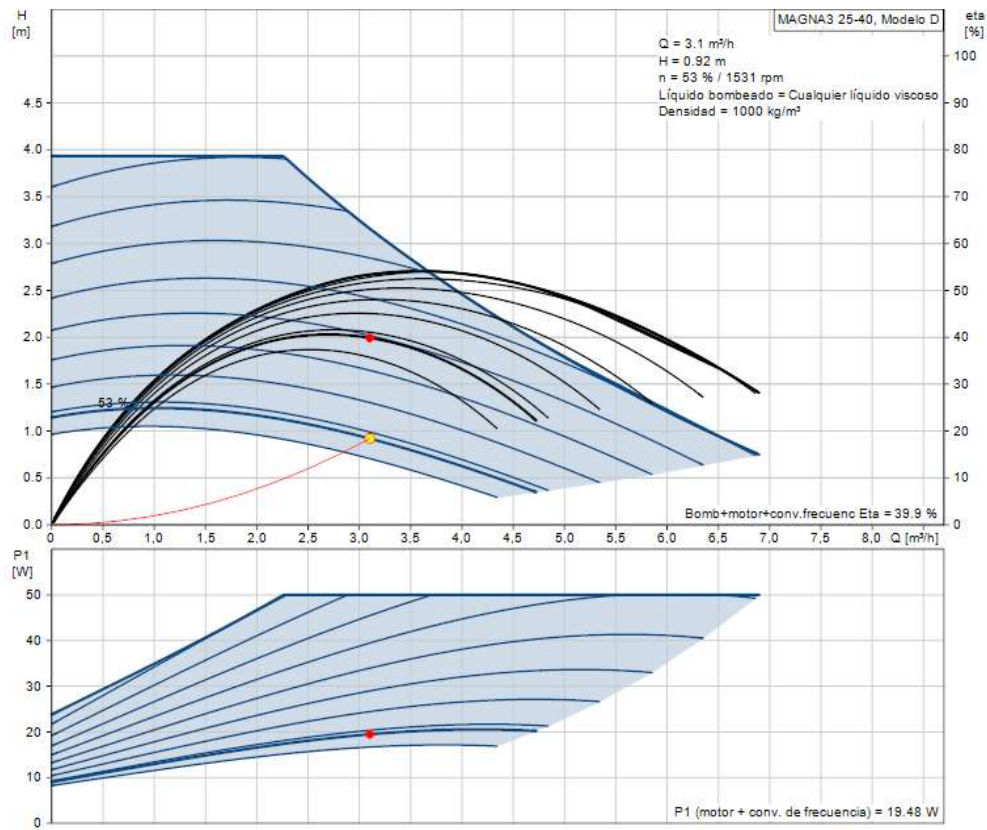
Calculated actual flow	1,851 m ³ /h
Resulting pump head	0.859 m
Max. height	60 dm
TF Class	110
Approvals on the nameplate	CE, VDE, EAC, WEEE

Materials

Pump housing	Stainless steel
--------------	-----------------

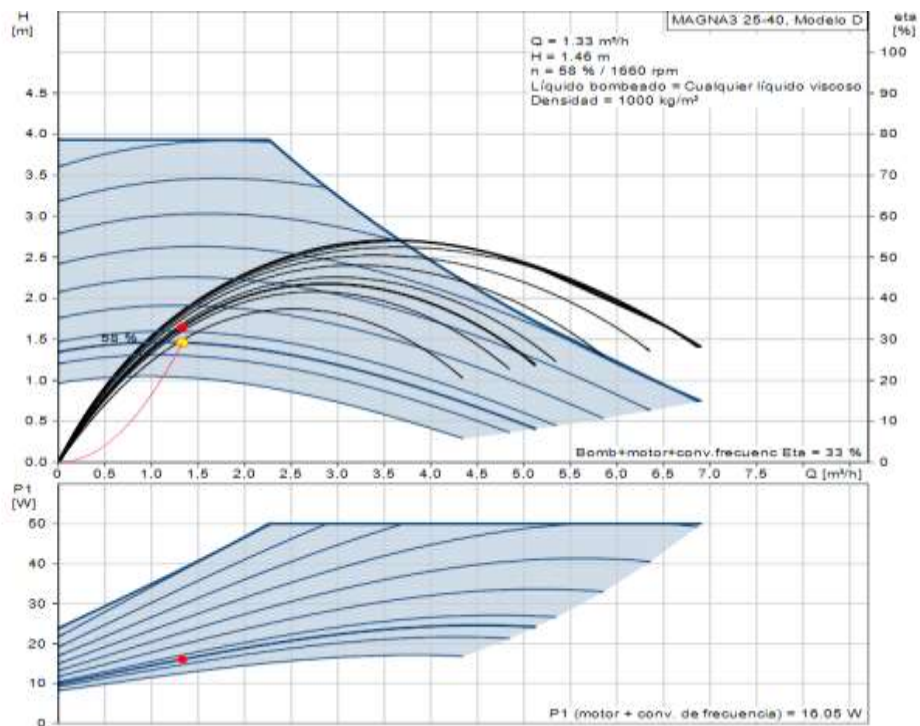
Pump housing	DIN W.-Nr. 1.4301
Driving force	Composite, PES/PP
Installation	
Amb. max. with liquid at 80°C	40 °C
Maximum working pressure	10 bar
Pipe connection	G 1 1/4
Nominal pressure	PN 10
Length port to port	150 mm
Amb. max. with liquid at 80°C	40 °C
Liquid	
Pumped liquid	Any viscous liquid
Liquid temperature range	2 .. 110 °C
Density	1000 kg/m ³
Electrical data	
Power input at speed 1	50 W
Power input at speed 2	60 W
Max. input power	70 W
Grid frequency	50 Hz
Nominal voltage	1 x 230 V
Intensity at speed 1	0.22 A
Intensity at speed 2	0.27 A
Current at speed 3	0.3 A
Capacitor size - Operation	2.5 µF
Degree of protection (IEC 34-5)	IP44
Insulation class (IEC 85)	F
Motor protection	NONE
Thermal protection	Impedance protection
Others	
Net weight	2.8 kg
Gross weight	3Kg
Transport volume	0,004 m ³
Country of origin	RS

Support circuit pump



Recirculation circuit pump

It is the same as the support circuit, but operating at a different point in the curve.



Specifications

Product:	MAGNA3 25-40
Code:	97924244
EAN number:	5710626493197
Price	857,00 EUR

Technical

Calculated actual flow	3.1 m ³ /h
Resulting pump head	0.92 m
Max. height	40 dm
TF Class	110
Approvals on the nameplate	CE, VDE, EAC, CN ROHS, WEEE
Model	D

Materials

Pump housing	Cast Iron
Pump housing	EN-GJL-200
Pump housing	ASTM A48-200B
Driving force	WEIGHT 30 % GLASS FIBRE

Installation

Ambient temperature range	0 .. 40 °C
Maximum working pressure	10 bar
Pipe connection	G 1 1/2"
Nominal pressure	PN10
Length port to port	180 mm
Ambient temperature range	0 .. 40 °C

Liquid

Pumped liquid	Any viscous liquid
Liquid temperature range	-10 .. 110 °C
Density	1000 kg/m ³

Electrical data

Power - P1	9 .. 50 W
------------	-----------

Grid frequency	50 / 60 Hz
Nominal voltage	1 x 230 V
Maximum intensity consumption	0.09 .. 0.46 A
Degree of protection (IEC 34-5)	X4D
Insulation class (IEC 85)	F

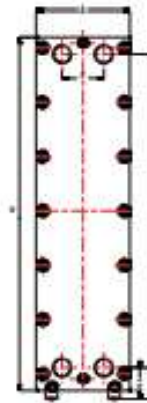
Others	
Energy (IEE)	0.18
Net weight	4.81 kg
Gross weight	5.27 kg
Transport volume	0.015 m ³
Danish VVS No.	380790040
Swedish RSK No.	5732571
Finnish	4615540

IP 3705 / INTERCAMBIADOR DE PLACAS DESMONTABLES



CARACTERÍSTICAS

- Intercambiador de calor de placas desmontables
- Placas en acero inoxidable o titanio
- Juntas en nitrilo NBR o en EPDM-PRX
- Juntas pegadas a placas
- Placas de alta eficiencia A o baja eficiencia B
- Conexiones en rosca Gas macho 2"
- Flujo paralelo



- 1 Entrada primario
- 2 Salida primario
- 3 Entrada secundario
- 4 Salida secundario

En el código de un intercambiador mod. 3705 es importante indicar correctamente el tipo de placa y el material de la junta:

CONDICIONES DE DISEÑO

Presión diseño	Temperatura diseño	
	NBR	EPDM
10 bar	95 °C	140 °C

Tipo de placa (eficiencia):

- A** Alta eficiencia térmica
Alta pérdida de carga
- B** Baja eficiencia térmica
Baja pérdida de carga
- M** Mezcla de placas tipos A y B

Material de junta:

- N** Junta en nitrilo NBR
(95°C - Temperatura diseño)
- P** Junta en EPDM-PRX
(140°C - Temperatura diseño)

DIMENSIONES

Nº placas	Área placa (m²)	Dimensiones (mm)							Conexiones Rosca gas MACHO
		H	E	A	F	S	L	L1	
0 - 39	0,25	1183	1050	314	140	210	nº placas x 3,5	403	2"
40 - 67		1183	1050	314	140	210	nº placas x 3,5	503	2"
68 - 81		1183	1050	314	140	210	nº placas x 3,5	603	2"

Área total intercambio (m²)	Peso (kg)
A = (Nº placas - 2) * Área de placa	159 + Nº placas * 1,23

TARIFA DE PRECIOS

PLACAS EN ACERO INOXIDABLE

INTERCAMBIADOR CON JUNTAS NBR

Código	Nº placas	PVP (€)	Código	Nº placas	PVP (€)
IP3705*09NX10	9	1.815	IP3705*39NX10	39	3.248
IP3705*11NX10	11	1.910	IP3705*41NX10	41	3.352
IP3705*13NX10	13	2.006	IP3705*43NX10	43	3.447
IP3705*15NX10	15	2.101	IP3705*45NX10	45	3.542
IP3705*17NX10	17	2.196	IP3705*47NX10	47	3.637
IP3705*19NX10	19	2.291	IP3705*49NX10	49	3.733
IP3705*21NX10	21	2.382	IP3705*51NX10	51	3.828
IP3705*23NX10	23	2.487	IP3705*53NX10	53	3.923
IP3705*25NX10	25	2.582	IP3705*55NX10	55	4.018
IP3705*27NX10	27	2.677	IP3705*57NX10	57	4.113

INTERCAMBIADOR CON JUNTAS EPDM

Código	Nº placas	PVP (€)	Código	Nº placas	PVP (€)
IP3705*09PX10	9	1.840	IP3705*39PX10	39	3.355
IP3705*11PX10	11	1.940	IP3705*41PX10	41	3.463
IP3705*13PX10	13	2.041	IP3705*43PX10	43	3.564
IP3705*15PX10	15	2.142	IP3705*45PX10	45	3.665
IP3705*17PX10	17	2.242	IP3705*47PX10	47	3.765
IP3705*19PX10	19	2.343	IP3705*49PX10	49	3.866
IP3705*21PX10	21	2.449	IP3705*51PX10	51	3.966
IP3705*23PX10	23	2.550	IP3705*53PX10	53	4.067
IP3705*25PX10	25	2.650	IP3705*55PX10	55	4.168
IP3705*27PX10	27	2.751	IP3705*57PX10	57	4.268

**AISLAMIENTO TUBULAR FLEXIBLE
Clase M1**

Procell

Características:

- Grueso: ≤ 25 mm.
- Elastómero estruido de célula cerrada NBR - PVC
- Conductividad térmica λ :
0,033 W/m.k a 0°C
0,034 W/m.k a 10°C
0,037 W/m.k a 40°C
- Temperatura de trabajo tubos:
-40 a +110°C
- Coef. permeabilidad (UNI 9233):
 ≥ 10.000
- Clasificación al fuego: B1 B2 d0
- Resistencia al ozono*: Excelente
- Resist. agentes atmosféricos*: Excelente
- Longitud estándar: 2 metros

*Consulte dato técnico.



Características:

- Grueso: > 25 mm.
- Conductividad térmica λ :
0,036 W/m.k a 0°C
0,037 W/m.k a 10°C
0,040 W/m.k a 40°C
- Escala de temperatura tubo: -45 a +110°C
manta: -45 a 85°C
- Factor de fusión al vapor de agua:
 ≥ 7.000
- Flexibilidad: Excelente
- Clasificación al fuego: B1 B3 d0
- Reducción al ruido: 32 dB (A)
- Densidad: 85 ± 10 Kg/m³
- Longitud estándar: 2 metros

Código	Artículo					Metro lineal €
	Ref.	Ø nominal	Ø Cobro	Ø Huevo	Cont. caps	
ESPESOR 25 mm (M)						
AI 04 143	6 x 25	6	1/4"	—	64	4,68
AI 04 144	10 x 25	10	3/8"	1/8"	60	4,76
AI 04 240	12 x 25	12	1/2"	—	54	4,81
AI 04 311	15 x 25	15	5/8"	—	52	4,94
AI 04 317	18 x 25	18	3/4"	3/8"	50	5,23
AI 04 318	22 x 25	22	7/8"	1/2"	42	5,63
AI 04 319	25 x 25	25	1"	—	40	5,39
AI 04 320	28 x 25	28	1-1/8"	3/4"	40	6,95
AI 04 321	35 x 25	35	1-3/8"	1"	28	7,47
AI 04 109	42 x 25	42	1-5/8"	1-1/4"	22	8,22
AI 04 110	48 x 25	48	—	1-1/2"	18	8,96
AI 04 118	54 x 25	54	2-1/8"	—	16	9,62
AI 04 119	60 x 25	60	2-3/8"	2"	12	10,48
AI 04 120	64 x 25	64	2-5/8"	—	12	11,06
AI 04 140	76 x 25	76	3"	2-1/2"	10	12,54
AI 04 150	80 x 25	80	3-1/2"	3"	8	14,56
AI 04 151	102 x 25	102	3-5/8"	3-1/2"	6	17,98
AI 04 185	114 x 25	114	4-1/2"	4"	6	19,92
AI 04 213	140 x 25	140	—	5"	4	22,39
AI 04 214	160 x 25	160	—	—	4	29,99
ESPESOR 32 mm						
AI 04 191	15 x 32	15	5/8"	1/4"	36	5,39
AI 04 192	18 x 32	18	3/4"	3/8"	32	7,20
AI 04 193	22 x 32	22	7/8"	1/2"	32	7,30
AI 04 194	25 x 32	25	1"	—	24	8,09
AI 04 195	28 x 32	28	1-1/8"	3/4"	24	8,61
AI 04 196	35 x 32	35	1-3/8"	1"	22	9,75
AI 04 258	42 x 32	42	1-5/8"	1-1/4"	16	10,75
AI 04 259	48 x 32	48	—	1-1/2"	14	11,41
AI 04 260	54 x 32	54	2-1/8"	—	12	12,30
AI 04 261	60 x 32	60	2-3/8"	2"	10	13,08
AI 04 262	64 x 32	64	2-5/8"	—	10	13,96
AI 04 263	76 x 32	76	3"	2-1/2"	8	15,38
AI 04 264	80 x 32	80	3-1/2"	3"	8	17,79
AI 04 265	102 x 32	102	3-5/8"	3-1/2"	6	23,20
AI 04 266	108 x 32	108	4"	—	6	23,24
AI 04 267	114 x 32	114	4-1/2"	4"	6	23,28
AI 04 268	140 x 32	140	—	5"	4	28,06
AI 04 269	160 x 32	160	—	—	4	36,95
AI 04 270	168 x 32	168	—	6"	4	42,40
ESPESOR 40 mm						
AI 04 217	6 x 40	6	1/4"	—	24	10,92
AI 04 218	10 x 40	10	3/8"	—	24	11,81
AI 04 219	12 x 40	12	1/2"	—	24	12,71
AI 04 220	15 x 40	15	5/8"	—	22	13,32
AI 04 332	18 x 40	18	3/4"	3/8"	22	13,39
AI 04 333	22 x 40	22	7/8"	1/2"	22	13,68
AI 04 334	25 x 40	25	1"	—	16	14,72
AI 04 335	28 x 40	28	1-1/8"	3/4"	16	15,73
AI 04 336	35 x 40	35	1-3/8"	1"	16	17,27
AI 04 337	42 x 40	42	1-5/8"	1-1/4"	16	18,60
AI 04 338	48 x 40	48	—	1-1/2"	12	20,24
AI 04 339	54 x 40	54	2-1/8"	—	10	20,34
AI 04 340	60 x 40	60	2-3/8"	2"	10	20,53
AI 04 340	64 x 40	64	2-5/8"	—	10	20,93
AI 04 350	76 x 40	76	3"	2-1/2"	10	22,13
AI 04 354	80 x 40	80	—	—	10	22,76
AI 04 358	80 x 40	80	3-1/2"	3"	10	23,41
AI 04 312	102 x 40	102	3-5/8"	3-1/2"	8	25,32
AI 04 313	114 x 40	114	4-1/2"	4"	8	25,66
AI 04 314	140 x 40	140	—	5"	6	29,38
AI 04 315	160 x 40	160	—	—	4	36,43
AI 04 316	168 x 40	168	—	6"	4	41,51

INFORMATION

Storage tank made of stainless steel AISI 316L, suitable for contact with drinking water, in accordance with Regulation 1935/2004. AISI-316L (1.4404) stainless steel belongs to the austenitic steel family (18-8 with 2% molybdenum and carbon content less than 0.035%), which is characterized by its high resistance to corrosion. In the case of drinking water, corrosion can be zero.

APPLICATION

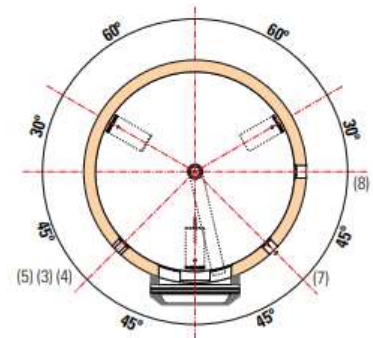
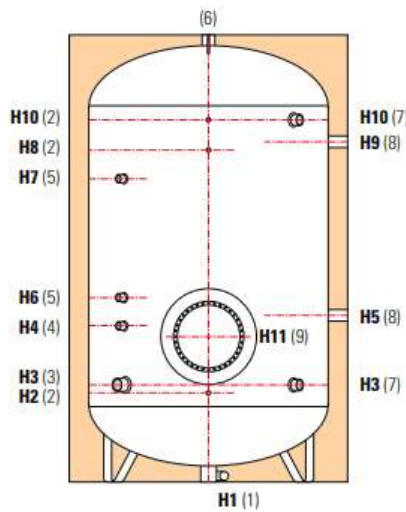
Domestic hot water (DHW) storage for domestic or industrial use. Suitable for installation in installations with solar panels, as it is equipped with a manhole with an internal diameter of DN400 for capacities greater than 750 lts. as indicated in section HE4 - Minimum solar contribution to domestic hot water of the Technical Building Code. Smaller manholes are also available for 750 lts and lower volumes, as well as for other types of installations. The use of sacrificial magnesium anodes as cathodic protection is recommended (see section on ACCESSORIES on page 89).

ISOLATION

The standard insulation consists of flexible polyurethane foam with a thermal conductivity coefficient of 0.038 W/m²K. The exterior finish is a red sky cover of 0.28 mm. It can also be supplied WITHOUT INSULATION or with another type of insulation and exterior finish (weatherproof cover, aluminium sheet, armaflex, rock wool ...). See options in INSULATION. The accumulators meet the criteria of ecological design according to Regulation 814/2013 and energy labelling according to Regulation 812/2013.



- 1 Vaciado
- 2 Instrumentación
- 3 Entrada agua fría
- 4 Recirculación
- 5 Ánodo de protección catódica
- 6 Salida agua caliente
- 7 Salida a intercambiadores de placas externos
- 8 Resistencia eléctrica
- 9 Boca de inspección
- H Altura total
- De Diámetro acumulador con aislamiento
- Df Diámetro acumulador sin aislamiento



CONDICIONES DE DISEÑO

Presión diseño	Temperatura diseño
8 bar	95 °C

Bajo petición se pueden suministrar acumuladores para otras presiones de diseño (6 y 10bar), así como otras capacidades y dimensiones.

DIMENSIONES



Volumen (litros)	Dimensiones (mm)													
	Df	De	H	H1	H2	H3	H4	H5	H6	H7	H8	H9	H10	H11
750	750	950	2086	103	386	436	836	936	1036	1636	1536	1461	1736	686
1000	850	1050	2125	53	399	449	949	849	1099	1649	1549	1474	1749	749
1500	1000	1200	2211	58	446	496	896	971	1096	1696	1596	1521	1796	796
2050	1150	1250	2282	42	468	518	918	993	1118	1718	1618	1543	1818	818
2500	1250	1350	2378	81	535	585	985	1060	1185	1785	1685	1610	1785	885
3000	1250	1350	2878	81	535	585	985	1060	1185	1985	2185	2235	2385	910
4000	1400	1500	2934	61	554	604	1004	1079	1204	2004	2204	2254	2404	929
5000	1600	1700	3022	35	584	634	1034	1109	1234	2034	2234	2284	2434	959

Posibilidad de fabricación en otras medidas. Consultar precios.

Volumen (litros)	Rosca G macho (1)	Conexiones Rosca G hembra								(9) Ø int.	Peso (Kg.)
		(2)	(3)	(4)	(5)	(6)	(7)	(8)			
750	1"	1/2"	2"	1"1/2	1"1/4	2"	1"1/4	1"1/4	212	122	
1000	1"1/2	1/2"	2"	1"1/2	1"1/4	2"	2"	2"	402	184	
1500	1"1/2	1/2"	2"	1"1/2	1"1/4	2"	2"	2"	402	211	
2050	1"1/2	1/2"	2"1/2	1"1/2	1"1/4	2"1/2	2"	2"	402	291	
2500	1"1/2	1/2"	2"1/2	1"1/2	1"1/4	2"1/2	2"	2"	402	318	
3000	1"1/2	1/2"	2"1/2	1"1/2	1"1/4	2"1/2	2"	2"	402	397	
4000	1"1/2	1/2"	2"1/2	1"1/2	1"1/4	2"1/2	2"	2"	402	444	
5000	1"1/2	1/2"	2"1/2	1"1/2	1"1/4	2"1/2	2"	2"	402	616	

PRICE LIST

UNINSULATED

Code	Vol. (Its)	PVP (euro)
DV0756L08B2	.617	750
DV1006L08B1000		3,628
DV1506L08B1500		4.270
DV2006L08B2050		5,255

Code	Volume (Its)	PRICE (EUROS)
DV2506L08B	2500	5.838
DV3006L08B	3000	6.834
DV4006L08B	4000	8.555
DV5006L08B	5000	11.155

WITH STANDARD INSULATION

Code	Volume (Its)	PRICE (EUROS)
DV0756L08BRFP	750	3.181
DV1006L08BRFP	1000	4.215
DV1506L08BRFP	1500	5.124
DV2006L08BRFP	2050	5.883

Code	Volume (Its)	PRICE (EUROS)
DV2506L08BRFP	2500	6.499
DV3006L08BRFP	3000	7.613
DV4006L08BRFP	4000	9.400
DV5006L08BRFP	5000	12.151

IV / AISI 316 STAINLESS STEEL INTERACCUMULATOR

TECHNICAL INFORMATION

Inter-accumulator tank built in AISI 316L stainless steel, suitable for contact with drinking water, according to Regulation 1935/2004. The AISI-316L stainless steel is characterized by its high resistance to corrosion. In the case of drinking water, it can reach zero.

APPLICATION

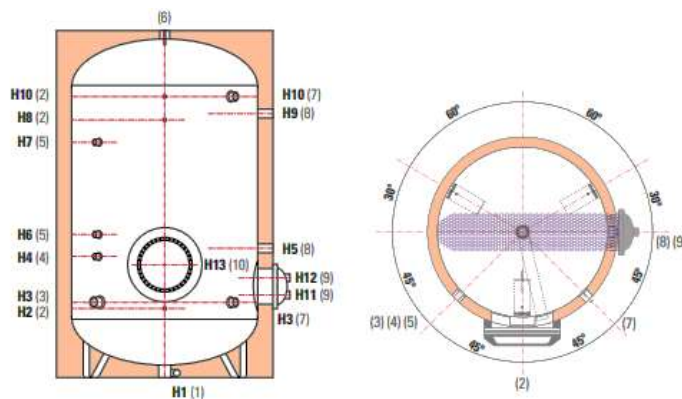
Production and accumulation of domestic hot water (DHW) for domestic or industrial use Suitable for installation in installations with solar panels, as it is equipped with a manhole with an internal diameter of DN400 for capacities of more than 750 lts. This manhole is additional to the manhole where the heating coil is mounted. For volumes of 750 lts and below, the size of the manhole is DN 200. The use of sacrificial magnesium anodes for cathodic protection is recommended (see section on ACCESSORIES on page 89).

Different types of coils are supplied depending on the required heating time:

- TC1 Warm-up time in 1 hour.
- TC2 Heating time in 2 hours.
- TC1/2 Heating time in 1/2 hour (high production).

ISOLATION

The standard insulation consists of flexible polyurethane foam with a thermal conductivity coefficient of 0.038 W/m²K. The exterior finish is a red sky cover of 0.28 mm. It can also be supplied WITHOUT INSULATION or with another type of insulation and exterior finish (weatherproof cover, aluminium sheet, armaflex, rock wool ...). See options in INSULATION. Interaccumulators comply with the criteria of ecological design according to Regulation 814/2013 and energy labelling according to Regulation 812/2013



- | | | |
|--------------------------------|--|--|
| 1 Vaciado | 7 Salida a intercambiadores de placas externos | H Altura total |
| 2 Instrumentación | 8 Resistencia eléctrica | De Diámetro acumulador con aislamiento |
| 3 Entrada agua fría | 9 Conexión a serpentín | Df Diámetro acumulador sin aislamiento |
| 4 Recirculación | 10 Boca de inspección | |
| 5 Ánodo de protección catódica | | |
| 6 Salida agua caliente | | |

	Pressure temperature	Design design
Deposit	8 bar	95 C°
Coil	8 bar	95 C°

DIMENSIONS For all models TC1, TC2 and TC1/2

Volume (litres)	Dimensions (mm)															
	Df	From	H	H1	H2	H3	H4	H5	H6	H7	H8	H9	H10	H11	H12	H13
750	750	950	2086	103	386	436	836	936	1036	1636	1536	1461	1736	551	651	686
1000	850	1050	2125	53	399	449	949	849	1099	1649	1549	1474	1749	564	664	749
1500	1000	1200	2211	58	446	496	896	971	1096	1696	1596	1521	1796	586	736	796
2050	1150	1250	2282	42	468	518	918	993	1118	1718	1618	1543	1818	608	758	818
2500	1250	1350	2378	81	535	585	985	1060	1185	1785	1685	1610	1785	675	825	885
3000	1250	1350	2878	81	535	585	985	1060	1185	1985	2185	2235	2385	675	825	910
4000	1400	1500	2934	61	554	604	1004	1079	1204	2004	2204	2254	2404	694	844	929
5000	1600	1700	3022	35	584	634	1034	1109	1234	2034	2234	2284	2434	724	874	959

Possibility of manufacturing in other sizes. Consult prices.

Volume (litres)	Male G-thread (1)	Connections Female G-thread								(10) Ø int
		(2)	(3)	(4)	(5)	(6)	(7)	(8)	(9)	
750	1"	1/2"	2"	"1"1/2	"1"1/4	2"	"1"1/4	"1"1/4	"1"1/4	212
1000	"1"1/2	1/2"	2"	"1"1/2	"1"1/4	2"	2"	2"	2"	402
1500	"1"1/2	1/2"	2"	"1"1/2	"1"1/4	2"	2"	2"	2"	402
2050	"1"1/2	1/2"	"2"1/2	"1"1/2	"1"1/4	"2"1/2	2"	2"	2"	402
2500	"1"1/2	1/2"	"2"1/2	"1"1/2	"1"1/4	"2"1/2	2"	2"	2"	402
3000	"1"1/2	1/2"	"2"1/2	"1"1/2	"1"1/4	"2"1/2	2"	2"	2"	402
4000	"1"1/2	1/2"	"2"1/2	"1"1/2	"1"1/4	"2"1/2	2"	2"	2"	402
5000	"1"1/2	1/2"	"2"1/2	"1"1/2	"1"1/4	"2"1/2	2"	2"	2"	402

TECHNICAL AND OPERATIONAL DATA

PRICE LIST

DHW production and boiler heating

TC1 / warm-up time: 1 hour

Vol. (litres)	Code	Surface area interchange(m ²)	Vol. serp. (litres)	Pot. (kW)	Prod. (lts/hour)	Weight (Kg.)
750	IV075TC16LB08	1,41	4,3	35	851	160
1000	IV100TC16LB08	1,87	5,7	46	1128	226
1500	IV150TC16LB08	2,81	8,6	69	1696	275
2050	IV200TC16LB08	3,75	11,5	92	2263	361
2500	IV250TC16LB08	4,69	14,4	115	2830	396
3000	IV300TC16LB08	5,62	17,2	138	3391	482
4000	IV400TC16LB08	7,50	23,0	184	4526	543
5000	IV500TC16LB08	9,37	28,7	230	5654	728

UNINSULATED

INSULATED

Code	Vol. (lts)	PVP (€)	Code	PVP (€)
IV075TC16LB08B	750	3.846	IV075TC16LB08BRFP	4.382
IV100TC16LB08B	1000	4.771	IV100TC16LB08BRFP	5.416
IV150TC16LB08B	1500	6.158	IV150TC16LB08BRFP	7.040
IV200TC16LB08B	2050	7.238	IV200TC16LB08BRFP	7.894
IV250TC16LB08B	2500	8.033	IV250TC16LB08BRFP	8.727
IV300TC16LB08B	3000	9.333	IV300TC16LB08BRFP	10.140
IV400TC16LB08B	4000	11.223	IV400TC16LB08BRFP	12.099
IV500TC16LB08B	5000	14.133	IV500TC16LB08BRFP	15.199



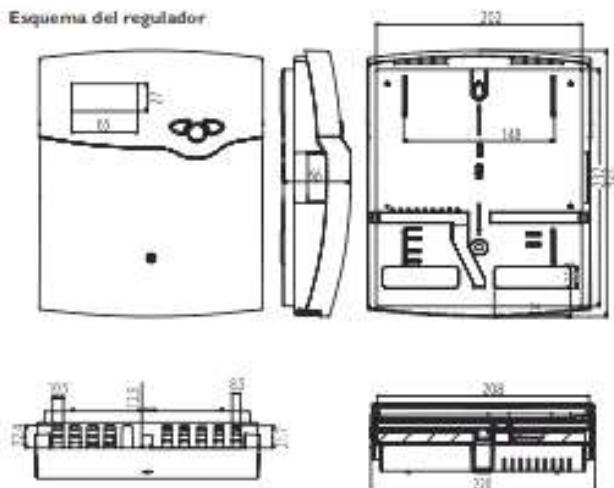
CPA-BTH

Monobloc boilers made of special steel plate to guarantee a long life. Overpressure firebox with combustion chamber and totally refrigerated smoke circuit. Easy installation and maintenance: wide front door that facilitates the cleaning of the tubular bundle and the combustion chamber. Reversible door, easily adaptable to open to the right or left according to the needs of the installation. Versatility of regulation: boiler control by means of electronic regulation KSF or analogical regulation.



		55	70	100	130
Useful power	kW	55	70	100	130
Payload performance (1) at 100% load	%	94,0%	94,1%	94,3%	94,5%
Payback time (1) with 30% load	%	94,8%	94,7%	95,2%	95,5%
Combustion chamber overpressure	mm.c.a	3	5	6	9
Water circuit pressure loss $\Delta t=15^{\circ}\text{C}$	mm.c.a	50	50	53	82
Approximate net weight	kg	285	320	385	425
A: Width dimension	mm	810	810	880	880
B: Height	mm	870	870	940	940
D: Depth	mm	1.254	1.394	1.394	1.494
Diameter of smoke evacuation level	mm	175	175	195	195
G					
Ida is at	"	2"	2"	DN 65	DN 65
Return level b	"	2"	2"	DN 65	DN 65
Water capacity	l	130	150	170	180
Maximum working pressure	bar	5	5	5	5
Boiler with basic control panel 1 stage					
Reference		7503869	7503872	7503875	7503878
PVP		2.219 €	2.453 €	2.856 €	3.234 €

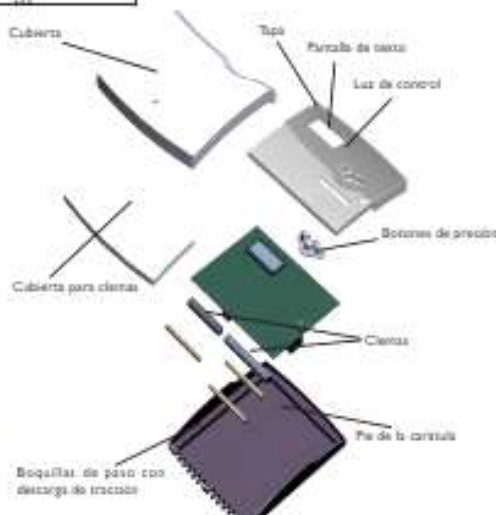
Esquema del regulador



- Pantalla digital multifuncional.
- Entrada para 15 sondas.
- Salida para 9 relés.
- 7 sistemas básicos.
- Posibilidad de añadir opciones y funciones nuevas.
- Asignación libre para las funciones de temperatura y termostato.
- BUS e interfaz RS232.

Datos técnicos:

Carátula:	Plástico, PC-ABS y PMMA
Protección:	IP 20 / DIN 40 050
Temp. ambiente:	0 ... 40 °C
Tamaño:	260 x 216 x 64 mm.
Montaje:	En pared o en cuadro
Pantalla:	Texto LC de 4 dígitos (iluminada), menú bilingüe y led luminoso de 2 colores
Manejo:	Mediante 3 pulsadores frontales.
Funciones:	Regulador solar para el control de sistemas solares y de calefacción. Uno calorímetro integrados y control de un circuito de calefacción. Parámetros ajustables, opciones programables y funciones de diagnóstico
Entradas:	Entradas para 12 sondas de temperatura Pt1000 o para 11 sondas Pt1000, 1 control a distancia RTA11, 1 caudalímetro V40 y una célula solar CS10.
Salidas:	9 salidas para relés, 4 estándar; 4 semiconductores y 1 libre de potencial
Bus:	Bus, RS232
Suministro:	220 ... 240 V~
Consumo:	6.3 (1) A, 220 ... 240 V~
Grado de contaminación:	2
Voltaje de impulso:	2.5 kW



Modo de funcionamiento:

Typ 1.c

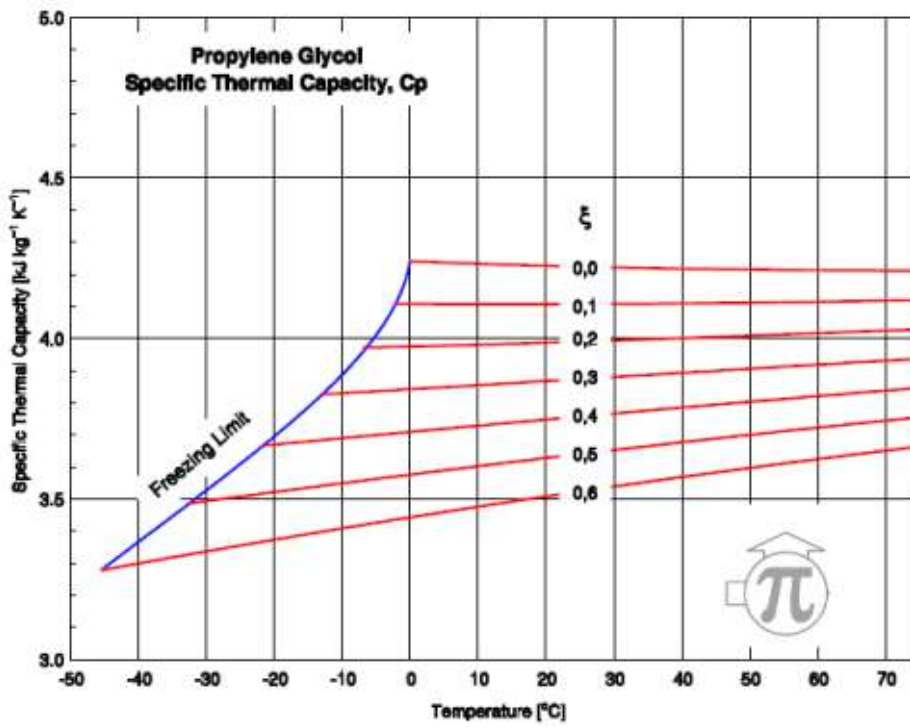
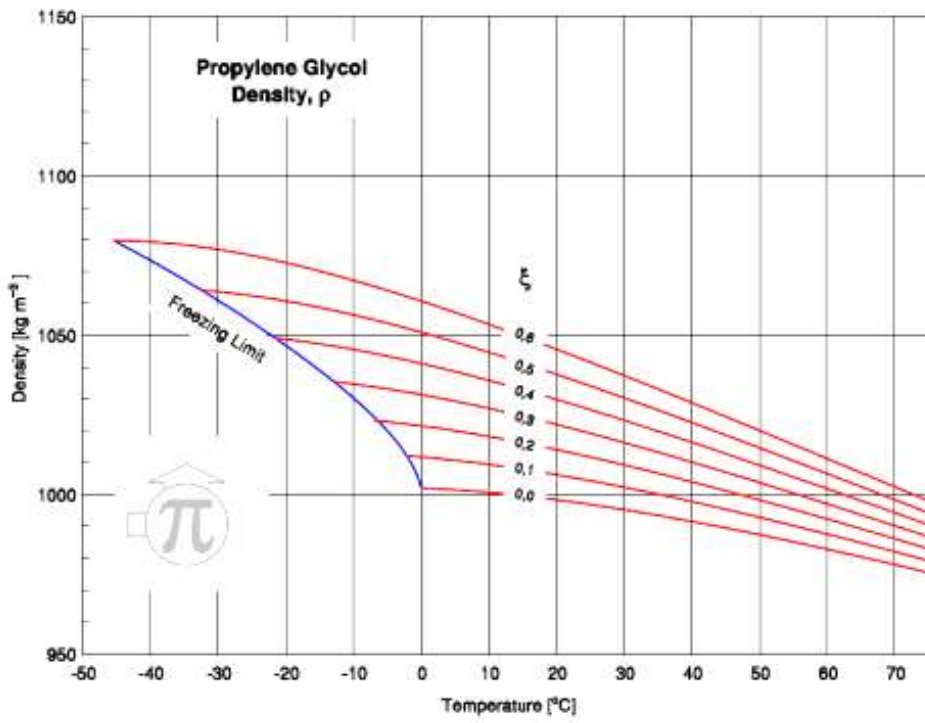
Test de dureza a la penetración de una bola: 75 °C.

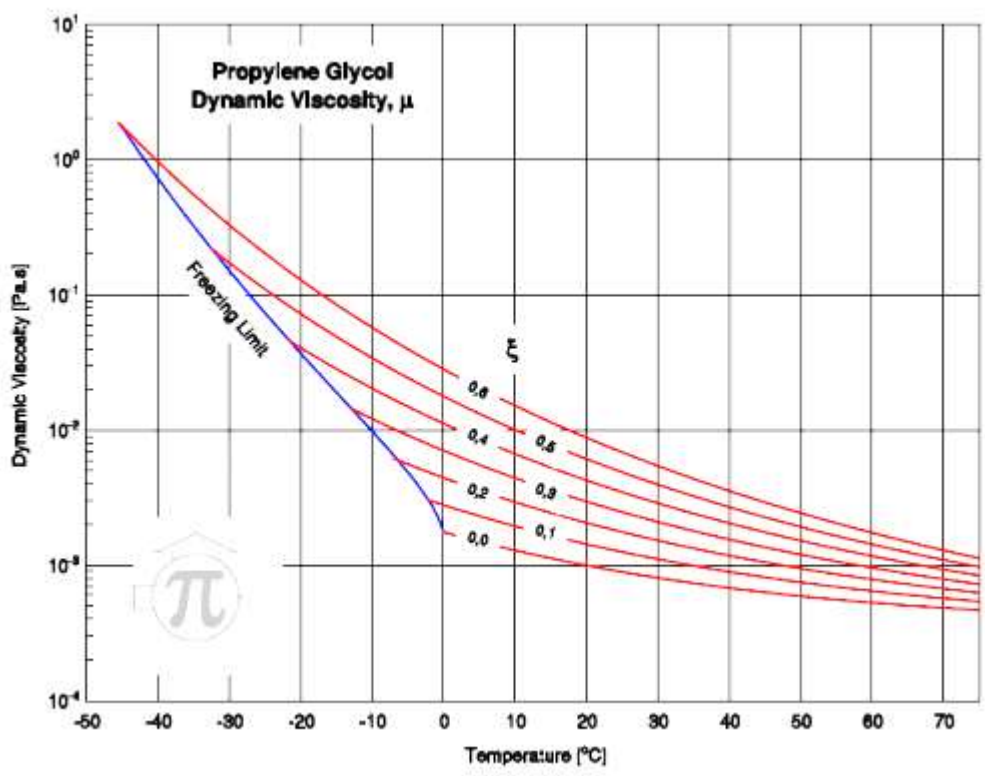
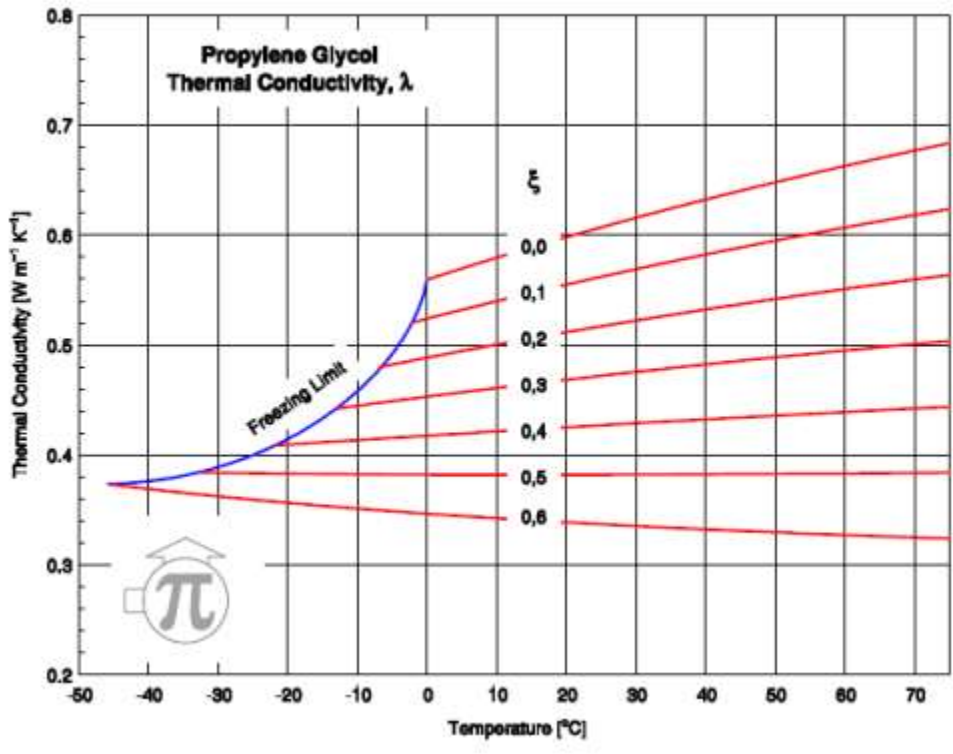


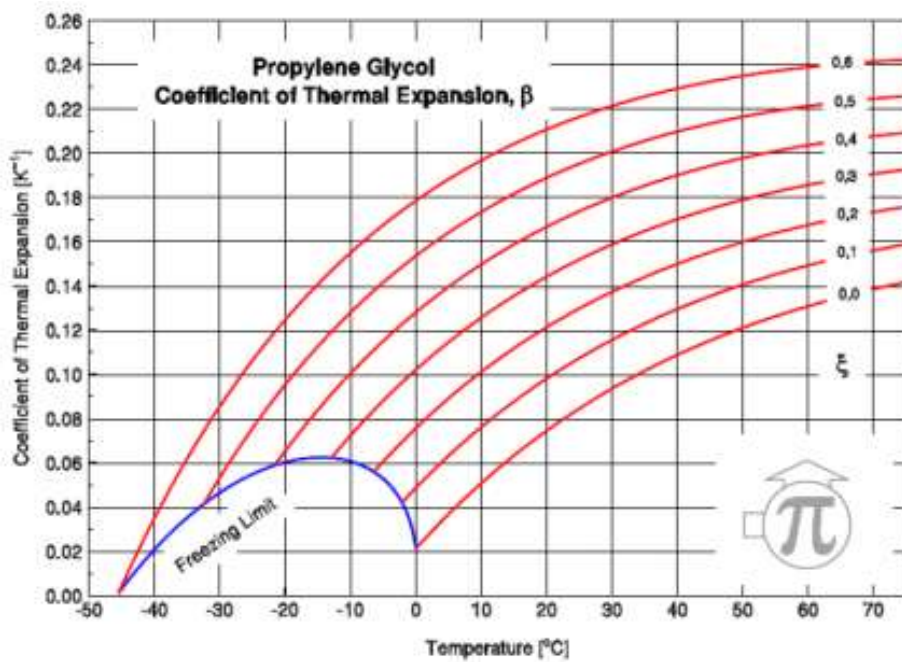
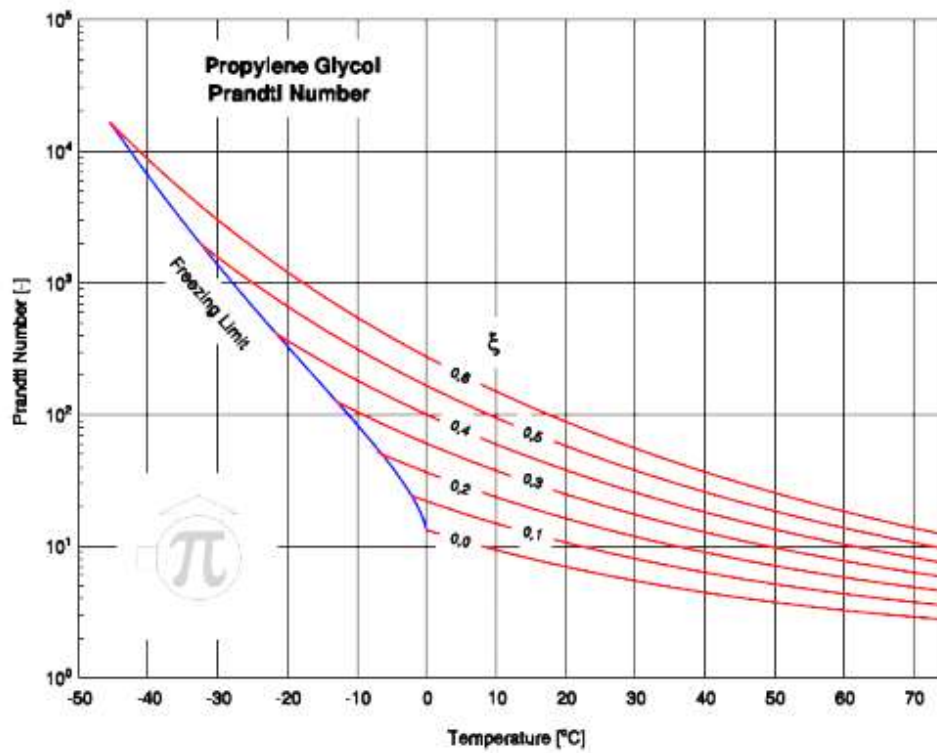
¡Atención, riesgo de contacto con componentes de alta tensión!



Las descargas electrostáticas pueden dañar los componentes electrónicos del regulador.







Propiedades del aire a 1 atm de presión

Temp. $T, ^\circ\text{C}$	Densidad $\rho, \text{kg/m}^3$	Calor específico c_p $\text{J/kg} \cdot \text{K}$	Conductividad térmica $k, \text{W/m} \cdot \text{K}$	Difusividad térmica $\alpha, \text{m}^2/\text{s}$	Viscosidad dinámica $\mu, \text{kg/m} \cdot \text{s}$	Viscosidad cinemática $\nu, \text{m}^2/\text{s}$	Número de Prandtl Pr
-150	2.866	983	0.01171	4.158×10^{-5}	8.636×10^{-5}	3.013×10^{-5}	0.7246
-100	2.038	966	0.01582	8.036×10^{-5}	1.189×10^{-4}	5.837×10^{-5}	0.7263
-50	1.582	999	0.01979	1.252×10^{-4}	1.474×10^{-4}	9.319×10^{-5}	0.7440
-40	1.514	1002	0.02057	1.356×10^{-4}	1.527×10^{-4}	1.008×10^{-4}	0.7436
-30	1.451	1004	0.02134	1.465×10^{-4}	1.579×10^{-4}	1.087×10^{-4}	0.7425
-20	1.394	1005	0.02211	1.578×10^{-4}	1.630×10^{-4}	1.169×10^{-4}	0.7408
-10	1.341	1006	0.02288	1.696×10^{-4}	1.680×10^{-4}	1.252×10^{-4}	0.7387
0	1.292	1006	0.02364	1.818×10^{-4}	1.729×10^{-4}	1.338×10^{-4}	0.7362
5	1.269	1006	0.02401	1.880×10^{-4}	1.754×10^{-4}	1.382×10^{-4}	0.7350
10	1.246	1006	0.02439	1.944×10^{-4}	1.778×10^{-4}	1.426×10^{-4}	0.7336
15	1.225	1007	0.02476	2.009×10^{-4}	1.802×10^{-4}	1.470×10^{-4}	0.7323
20	1.204	1007	0.02514	2.074×10^{-4}	1.825×10^{-4}	1.516×10^{-4}	0.7309
25	1.184	1007	0.02551	2.141×10^{-4}	1.849×10^{-4}	1.562×10^{-4}	0.7296
30	1.164	1007	0.02588	2.208×10^{-4}	1.872×10^{-4}	1.608×10^{-4}	0.7282
35	1.145	1007	0.02625	2.277×10^{-4}	1.895×10^{-4}	1.655×10^{-4}	0.7268
40	1.127	1007	0.02662	2.346×10^{-4}	1.918×10^{-4}	1.702×10^{-4}	0.7255
45	1.109	1007	0.02699	2.416×10^{-4}	1.941×10^{-4}	1.750×10^{-4}	0.7241
50	1.092	1007	0.02735	2.487×10^{-4}	1.963×10^{-4}	1.798×10^{-4}	0.7228
60	1.059	1007	0.02808	2.632×10^{-4}	2.008×10^{-4}	1.896×10^{-4}	0.7202
70	1.028	1007	0.02881	2.780×10^{-4}	2.052×10^{-4}	1.995×10^{-4}	0.7177
80	0.9994	1008	0.02953	2.931×10^{-4}	2.096×10^{-4}	2.097×10^{-4}	0.7154
90	0.9718	1008	0.03024	3.086×10^{-4}	2.139×10^{-4}	2.201×10^{-4}	0.7132
100	0.9458	1009	0.03095	3.243×10^{-4}	2.181×10^{-4}	2.306×10^{-4}	0.7111
120	0.8977	1011	0.03235	3.565×10^{-4}	2.264×10^{-4}	2.527×10^{-4}	0.7073
140	0.8542	1013	0.03374	3.898×10^{-4}	2.345×10^{-4}	2.745×10^{-4}	0.7041
160	0.8148	1016	0.03511	4.241×10^{-4}	2.420×10^{-4}	2.975×10^{-4}	0.7014
180	0.7788	1019	0.03646	4.593×10^{-4}	2.504×10^{-4}	3.212×10^{-4}	0.6992
200	0.7459	1023	0.03779	4.954×10^{-4}	2.577×10^{-4}	3.455×10^{-4}	0.6974
250	0.6746	1033	0.04104	5.890×10^{-4}	2.760×10^{-4}	4.091×10^{-4}	0.6946
300	0.6158	1044	0.04418	6.871×10^{-4}	2.934×10^{-4}	4.765×10^{-4}	0.6935
350	0.5664	1056	0.04721	7.892×10^{-4}	3.101×10^{-4}	5.475×10^{-4}	0.6937
400	0.5243	1069	0.05015	8.951×10^{-4}	3.261×10^{-4}	6.219×10^{-4}	0.6948
450	0.4880	1081	0.05298	1.004×10^{-3}	3.415×10^{-4}	6.997×10^{-4}	0.6965
500	0.4565	1093	0.05572	1.117×10^{-3}	3.563×10^{-4}	7.806×10^{-4}	0.6986
600	0.4042	1115	0.06093	1.352×10^{-3}	3.846×10^{-4}	9.515×10^{-4}	0.7037
700	0.3627	1135	0.06581	1.598×10^{-3}	4.111×10^{-4}	1.133×10^{-3}	0.7092
800	0.3289	1153	0.07037	1.855×10^{-3}	4.362×10^{-4}	1.326×10^{-3}	0.7149
900	0.3008	1169	0.07465	2.122×10^{-3}	4.600×10^{-4}	1.529×10^{-3}	0.7206
1000	0.2772	1184	0.07868	2.398×10^{-3}	4.826×10^{-4}	1.741×10^{-3}	0.7260
1500	0.1990	1234	0.09599	3.908×10^{-3}	5.817×10^{-4}	2.922×10^{-3}	0.7478
2000	0.1553	1264	0.11113	5.664×10^{-3}	6.630×10^{-4}	4.270×10^{-3}	0.7539

We calculate the monthly air properties for the ambient conditions at the installation site:

Month	T.amb. hours of sunshi ne (°C)	Density (Kg/m3)	Dynamic Viscosity (N-s/m2)	Thermal conductivity (W/m-K)	Specific heat (J/Kg-K)	Cinematic viscosity (m2/s)	Pr
January	10,76	1,24	1,78E-05	0,02	1007	1,44E-05	0,73
February	11,76	1,24	1,79E-05	0,02	1007	1,44E-05	0,73
March	13,76	1,23	1,80E-05	0,02	1007	1,46E-05	0,73
April	16,88	1,22	1,81E-05	0,02	1007	1,53E-05	0,73
May	19,88	1,20	1,83E-05	0,03	1007	1,52E-05	0,73
June	23,88	1,19	1,84E-05	0,03	1007	1,60E-05	0,73
July	25,88	1,18	1,85E-05	0,03	1007	1,57E-05	0,74
August	25,88	1,18	1,85E-05	0,03	1007	1,57E-05	0,74
September	23,88	1,19	1,84E-05	0,03	1007	1,60E-05	0,73
October	19,76	1,20	1,83E-05	0,03	1007	1,52E-05	0,73
November	15,76	1,22	1,81E-05	0,02	1007	1,53E-05	0,73
December	11,76	1,24	1,79E-05	0,02	1007	1,44E-05	0,73

Maintenance

The CTE guidelines a series of measures to be taken to ensure the operation of the installation:

- Monitoring plan: This is a simple observation plan of the main functional parameters, to verify the correct operation of the installation.

Elemento de la instalación	Operación	Frecuencia (meses)	Descripción
CAPTADORES	Limpieza de cristales	A determinar	Con agua y productos adecuados
	Cristales	3	IV condensaciones en las horas centrales del día.
	Juntas	3	IV Agrietamientos y deformaciones.
	Absorbedor	3	IV Corrosión, deformación, fugas, etc.
	Conexiones	3	IV fugas.
CIRCUITO PRIMARIO	Estructura	3	IV degradación, indicios de corrosión.
	Tubería, aislamiento y sistema de llenado	6	IV Ausencia de humedad y fugas.
	Purgador manual	3	Vaciado el aire del botellín.
CIRCUITO SECUNDARIO	Termómetro	Diaria	IV temperatura
	Tubería y aislamiento	6	IV ausencia de humedad y fugas.
	Acumulador solar	3	Purgado de la acumulación de lodos de la parte inferior del depósito.

- Preventive maintenance plan: Visual inspection and verification of actions that must allow the operating conditions, performance, protection and durability of the installation to be kept within acceptable limits.

Equipo	Frecuencia (meses)	Descripción
Captadores	6	IV diferencias sobre original. IV diferencias entre captadores.
Cristales	6	IV condensaciones y suciedad
Juntas	6	IV agrietamientos, deformaciones
Absorbedor	6	IV corrosión, deformaciones
Carcasa	6	IV deformación, oscilaciones, ventanas de respiración
Conexiones	6	IV aparición de fugas
Estructura	6	IV degradación, indicios de corrosión, y apriete de tornillos
Captadores*	12	Tapado parcial del campo de captadores
Captadores*	12	Destapado parcial del campo de captadores
Captadores*	12	Vaciado parcial del campo de captadores
Captadores*	12	Llenado parcial del campo de captadores

Equipo	Frecuencia (meses)	Descripción
Depósito	12	Presencia de lodos en fondo
Ánodos sacrificio	12	Comprobación del desgaste
Ánodos de corriente impresa	12	Comprobación del buen funcionamiento
Aislamiento	12	Comprobar que no hay humedad

Equipo	Frecuencia (meses)	Descripción
Intercambiador de placas	12	CF eficiencia y prestaciones
	12	Limpieza
Intercambiador de serpentín	12	CF eficiencia y prestaciones
	12	Limpieza

Equipo	Frecuencia (meses)	Descripción
Fluido refrigerante	12	Comprobar su densidad y pH
Estanqueidad	24	Efectuar prueba de presión
Aislamiento al exterior	6	IV degradación protección uniones y ausencia de humedad
Aislamiento al interior	12	IV uniones y ausencia de humedad
Purgador automático	12	CF y limpieza
Purgador manual	6	Vaciar el aire del botellín
Bomba	12	Estanqueidad
Vaso de expansión cerrado	6	Comprobación de la presión
Vaso de expansión abierto	6	Comprobación del nivel
Sistema de llenado	6	CF actuación
Válvula de corte	12	CF actuaciones (abrir y cerrar) para evitar agarrotamiento
Válvula de seguridad	12	CF actuación

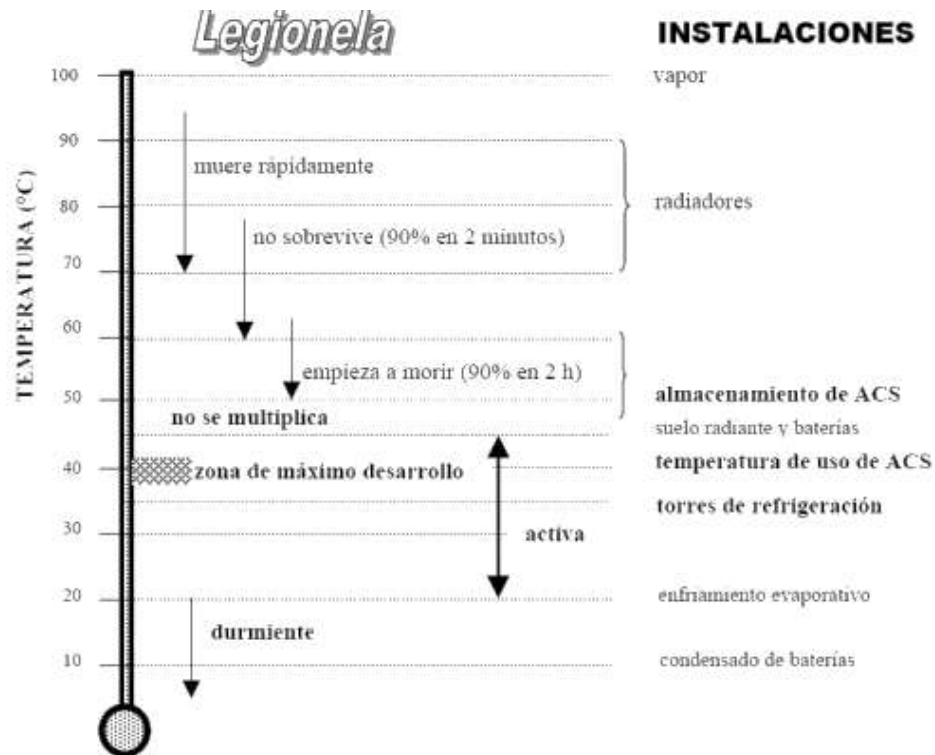
Equipo	Frecuencia (meses)	Descripción
Cuadro eléctrico	12	Comprobar que está siempre bien cerrado para que no entre polvo
Control diferencial	12	CF actuación
Termostato	12	CF actuación
Verificación del sistema de medida	12	CF actuación

Equipo	Frecuencia (meses)	Descripción
Sistema auxiliar	12	CF actuación
Sondas de temperatura	12	CF actuación

- Corrective maintenance: These are operations carried out as a result of the detection of any anomaly in the operation of the installation, in the surveillance plan or in the preventive maintenance plan. (CTE)

Proper maintenance of the installation prevents the proliferation of the Legionella Pneumophila bacteria, which causes legionnaire's disease, through water. The risk of contracting the disease

increases as the amount of bacteria inhaled and the time of exposure increases. Of all the parameters influencing the development of the bacteria, temperature has been found to be the most significant. Centralized preparation systems for H.S.W. with accumulation are the most risky, so you will need to maintain them properly. Below we can see the behavior of the bacteria for different temperature ranges:



From 50°C he starts to die. To avoid possible sources of infection, cleaning and disinfection should be carried out every three months, raising the temperature of the distribution circuit to 70°C for 1 hour. (Legionella, 2017)

Bibliography

- Energía térmica solar a baja temperatura. (2007). Retrieved April 11, 2020, from <http://bibing.us.es/proyectos/abreproy/5194/fichero/2.ENERG%C3%8DA+T%C3%89RICA+SOLAR+A+BAJA+TEMPERATURA.pdf>
- Cleanergysolar. (2015). Retrieved April 15, 2020, from <https://renovablesconsaburum.files.wordpress.com/2015/12/tablas-factor-correccion-k.pdf>
- GasFríoCalor. (2015). Retrieved Agosto 17, 2020, from <https://www.gasfriocalor.com/blog/ayudas-y-subvenciones/como-instalar-un-sistema-solar-por-termosifon/>
- Desarrollo de proyectos de instalaciones termicas y fluidos. (2017). Retrieved Marzo 27, 2020, from <https://coolproyect.es/website/wp-content/uploads/2017/02/Energia-solar-1.pdf>

- Legionella. (2017). Retrieved Agosto 28, 2020, from <https://www.gesplasur.es/legionella/ecologia-y-biologia-de-la-legionella/>
- BOE-A-2019-4677. (2019). Retrieved Julio 24, 2020, from https://www.boe.es/diario_boe/txt.php?id=BOE-A-2019-4677
- Arnabat, I. (2020, Mayo). Frío y Calor. Retrieved Agosto 28, 2020, from https://www.google.es/search?q=interacumulador+tipos&tbm=isch&ved=2ahUKEwiS25OH7sDrAhUGAmMBHVoiDQUQ2-cCegQIABAA&oeq=interacumulador+tipos&gs_lcp=CgNpbWcQAzoECCMQJzoECAAQzoFCAAQsQM6AggAOggIABCxAXCDAToHCAAQsQMQQzoECAAQGFDniwJY_qYCYN6oAmgAcAB4AIABkAGIAfAPkgE
- Barcelona, A. d. (2019). Ayudas a la rehabilitación energética. Retrieved Julio 6, 2020, from <https://habitatge.barcelona/es/servicios-ayudas/rehabilitacion/ayudas/eficiencia-energetica>
- Baxi. (n.d.). Retrieved Agosto 7, 2020, from <https://mediacdn.baxi.es/-/media/inriver-media/baxi-iberia-media/2020/5/26/a00b04c22e25catalog5es01pdf.pdf?v=1&d=20200526T191054Z>
- Besa, Y. G. (2014). Retrieved Abril 17, 2019, from <http://bibing.us.es/proyectos/abreproy/90163/fichero/TFG+-+Yolanda+Gonz%C3%A1lez+Besa.pdf>
- Calculo de la demanda de DHW para un edificio. (n.d.). Retrieved Abril 17, 2020, from <https://certificacionenergetica.info/calculo-de-la-demanda-de-DHW-para-un-edificio/>
- Cantero, D. F. (n.d.). Retrieved Mayo 7, 2020, from <https://core.ac.uk/download/pdf/29401052.pdf>
- Catalunya, G. d. (2009, Dicimembre). Retrieved Abril 27, 2020, from http://icaen.gencat.cat/web/.content/10_ICAEN/17_publicacions_informes/04_coleccio_QuadernPractic/quadern_practic/arxiu/03_energia_solar_termica.pdf
- Ceen. (2018). Conexiones en paralelo, serie y mixto. Retrieved Marzo 28, 2020, from <https://certificacionenergetica.info/conexiones-en-paralelo-serie-y-mixto/>
- CTE. (n.d.). Retrieved Agosto 27, 2020, from <http://www.terra.org/data/cteseccionhe4.pdf>
- CYPE ingenieros. (n.d.). Retrieved Agosto 8, 2020, from <http://www.generadordeprecios.info/#gsc.tab=0>
- Díaz, R. F. (2018, Julio). Retrieved Julio 13, 2020, from file:///C:/Users/roger/Downloads/FeijooDiaz_Rocio_TFG_2018.pdf
- Domínguez, J. G. (2009, Marzo). Retrieved Agosto 28, 2020, from <https://core.ac.uk/download/pdf/30042423.pdf>
- Eficiencia energética. (n.d.). Retrieved Agosto 2020, from <https://certificacionenergetica.info/materiales-mas-usados-para-DHW/>

Factor energía. (n.d.). Retrieved Marzo 15, 2020, from <https://www.factorenergia.com/es/blog/autoconsumo/energia-solar/>

Grundfos. (n.d.). Retrieved Julio 27, 2020, from <https://www.grundfos.com/>

Hamzat, A. (2020, Junio). Enhancing the thermal performance of solar collectors using nanofluids. Retrieved Agosto 13, 2020, from https://www.researchgate.net/publication/341881166_Enhancing_the_thermal_performance_of_solar_collectors_using_nanofluids

HE 4. (n.d.). Retrieved Junio 27, 2020, from <http://fic-grup.com/wp-content/uploads/2016/10/CTE-DBH4-2013-11-08.pdf>

Ingeniería mecánica. (n.d.). Retrieved Agosto 2020, from <https://ingemecanica.com/tutorialsemanal/tutorialn188.html>

Ingenierio marino. (n.d.). Retrieved Agosto 28, 2020, from <https://ingenieromarino.com/intercambiadores-de-calor/>

José, R. G. (n.d.). Aislamiento térmico de tuberías. Retrieved Agosto 21, 2020, from <https://eficiencia.com/aislamiento-termico-de-tuberias/>

Landa, M. (2005). Energía solar en España. Retrieved Agosto 28, 2020, from <https://www.consumer.es/medio-ambiente/energia-solar-en-espana.html>

Miralles, M. L. (2013). Instalaciones de energía solar térmica. Retrieved Mayo 13, 2020, from <http://umh0715.edu.umh.es/wp-content/uploads/sites/495/2013/02/Tema-1-IST-Energ%C3%A9tica-Solar.pdf>

Miranda, B. d. (2004). Cálculo caudal simultáneo en un edificio viviendas. Retrieved Mayo 22, 2020, from <https://www.ingenierosindustriales.com/como-calcular-el-caudal-simultaneo-de-agua-en-un-edificio-de-viviendas/>

Miranda, B. d. (2019). Cálculo de vasos de expansión cerrados. Retrieved Julio 27, 2020, from <https://www.ingenierosindustriales.com/calculo-de-vasos-de-expansion-cerrados/>

Ponce, J. (2013, Dicimebre). Cálculo de tuberías de agua fría y DHW. Retrieved Junio 4, 2020, from <http://javiponce-formatec.blogspot.com/2013/12/calculo-de-tuberias-de-agua-fria-afs-y.html>

Quiles, P. V. (2019). Retrieved Abril 22, 2020, from <https://www.atecyr.org/blog/2020/03/17/el-nuevo-documento-basico-de-ahorro-de-energia-del-cte-2019-por-pedro-vicente-quiles/>

Rivas, P. (2016, Noviembre 15). Paneles solares térmicos. Retrieved Abril 24, 2020, from <https://instalacionesyeficienciaenergetica.com/paneles-solares-termicos-cual-elegimos/>

Robles, G. (2014). Que es un vaso de expansion? Retrieved Abril 7, 2020, from <https://gerardorobles.es/vaso-expansion/>

Roth. (n.d.). Retrieved Agosto 22, 2020, from

<https://www.yumpu.com/en/document/view/15702727/solar-control-units-bw-h-comfort-installation-instructions-roth-uk>

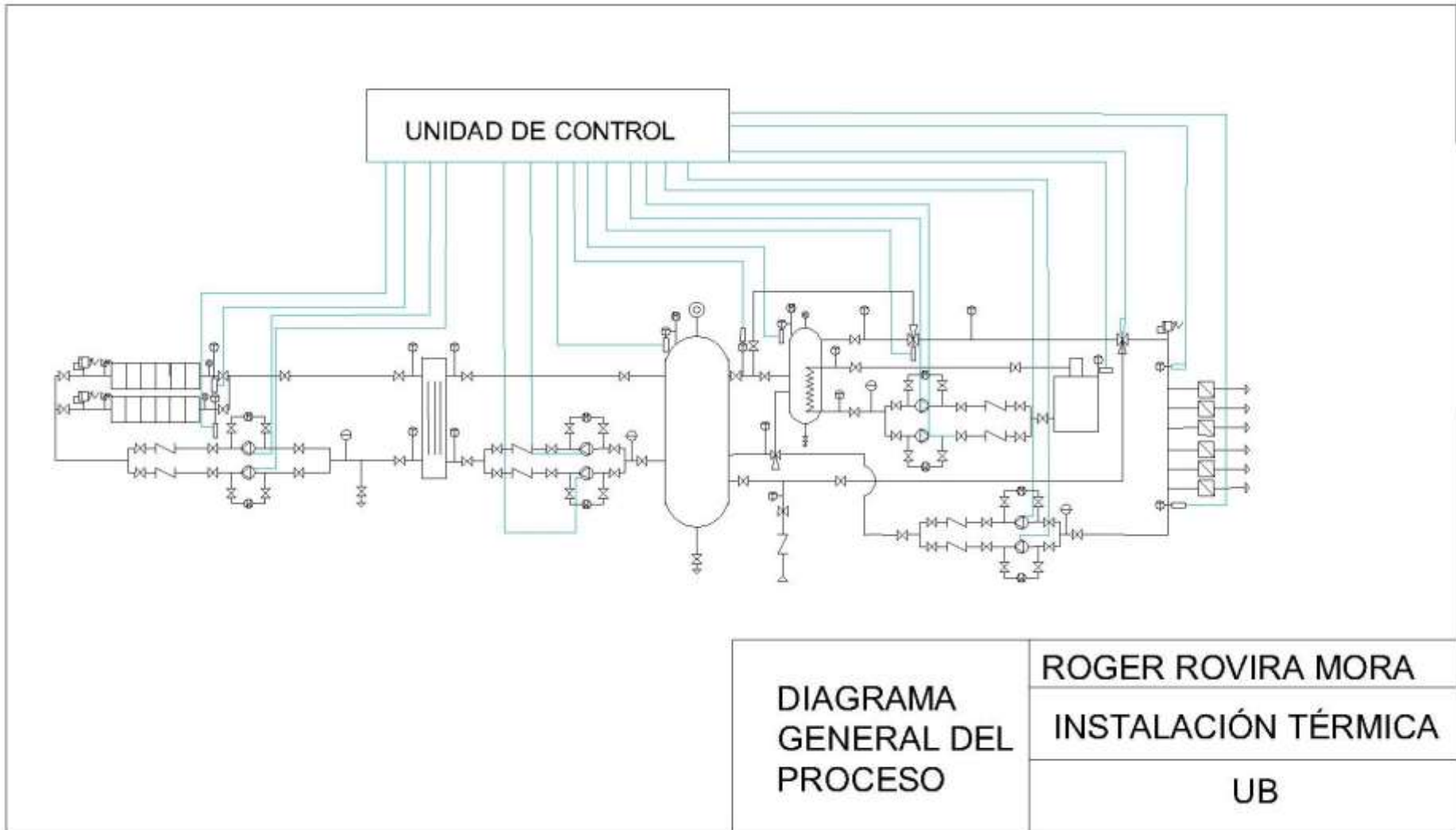
Salvador Escoda. (n.d.). Retrieved Julio 27, 2020, from <https://www.salvadorescoda.com/>

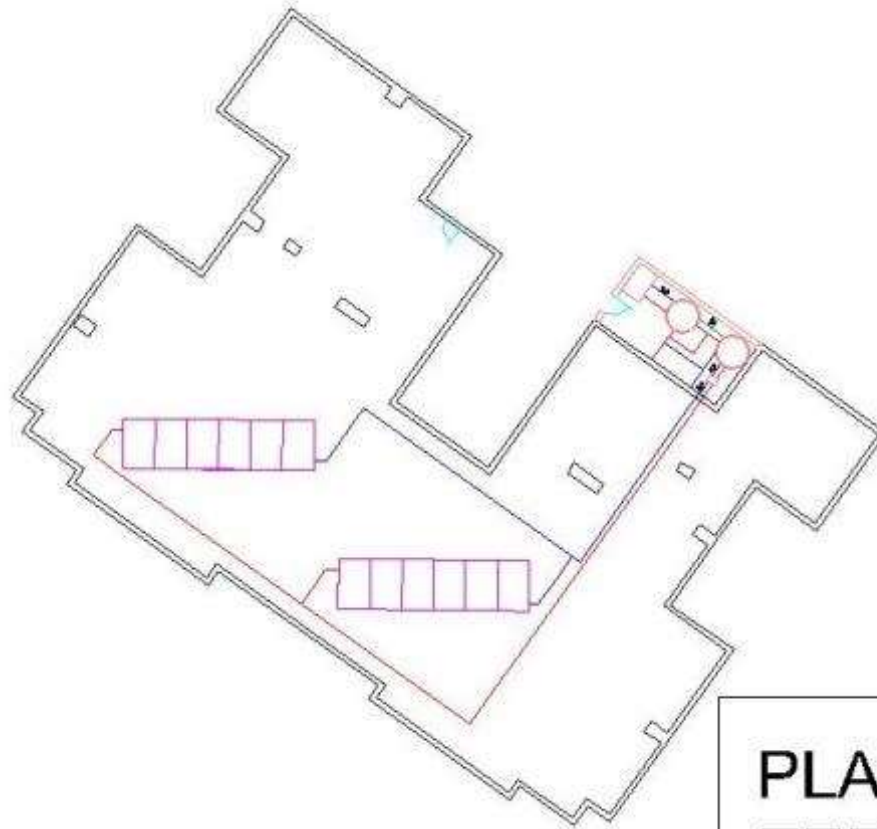
Simon. (2015, Diciembre). Glenergy. Retrieved Agosto 13, 2020, from

<http://glenergysolar.ie/solar-panels/solar-panels-efficiency/>

Suicalsa. (n.d.). Retrieved Agosto 4, 2020, from <https://suicalsa.com/>

Weiss, W. (2019). Solar heat worldwide. Retrieved Marzo 24, 2020, from <https://www.iea-shc.org/Data/Sites/1/publications/Solar-Heat-Worldwide-2019.pdf>





**PLANO
TERRAZA**

ROGER ROVIRA MORA

INSTALACIÓN TÉRMICA

UB

